04015-3-P

Progress Report No. 3

SMOKE PLUME PHOTOGRAPHY STUDY

BIG ROCK POINT NUCLEAR PLANT

CHARLEVOIX, MICHIGAN

Prepared for

Consumers Power Company
Jackson, Michigan

by

E. Wendell Hewson
Gerald C. Gill
Gerald J. Walke

Department of Meteorology and Oceanography
The University of Michigan

December 1963

ACKNOWLEDGMENTS

The writers wish to express their sincere appreciation of the work of several persons in the execution of the study. The following members in our Meteorology Group have contributed significant and diverse assistance in the analysis: D. Leavengood, P. Kaufman, J. Harrington and E. Bierly. Worthy of special mention are the contributions of W. Moroz, who contributed a number of studies to the project, most of the excellent photography of the smoke plume study and much valuable advice. The service organization of the University of Michigan Office of Research Administration is also to be commended. The contributions of G. Prosser, H. Willsher and G. Davenport made the successful completion of this report possible.

The writers wish to express their appreciation to a number of people in the Consumers Power Company for their contributions to the study. R. E. Kettner provided vital support and understanding throughout the study. J. Hills diligently participated in the editing and preparing of the report. Dorothea Zuver and the Parnell Road Stenographic Department carefully prepared the manuscript.

TABLE OF CONTENTS

I. GENERAL DISCUSSION

Earlier work in this investigation is described in Progress Report No. 1, 04015-1-P, November 1961 [1] and Progress Report No. 2, 04015-2-P, March 1962 [2]. These early reports set forth the background of the study, describe the installation of the meteorological instruments on the Big Rock Point Nuclear Plant site, the methods used in the analysis of the climatological data and include an analysis of the diffusion climatology of the area based on observational data available at the time. This report deals with the atmospheric diffusion experiments conducted at the site using a smoke plume released from the meteorological tower and from the plant stack as a visible tracer. It is assumed that the reader is familiar with the previously mentioned progress reports.

A. Statement of the Problem

The details of the Big Rock Point site are displayed in Figure 1. This map shows, in addition to wind directions in 36 points around the compass, wind directions grouped in Categories 1 through 5 according to the nature of the underlying surface. The nature of this surface over which the air flows is the prime factor in determining the atmospheric diffusion characteristics of airborne material released at the plant site. These atmospheric diffusion characteristics are governed by turbulence generated at the surface.

1. Turbulence and Diffusion Regimes

Atmospheric diffusion processes are governed by turbulence generated in either of two ways: by mechanical action as the airflow is made irregular as the air moves over a rough surface; by thermal buoyancy forces which either stimulate or inhibit vertical turbulence and mixing.

The critical vertical temperature gradient, or vertical temperature lapse rate, is 10 C per km or 5-1/2 F per 1000 feet. This critical lapse rate is known as the dry adiabatic lapse rate. When the temperature decreases or lapses with height at a rate greater than 10 C km^{-1}, the air is unstable, and active vertical churning known as thermal turbulence occurs. Under such conditions plume looping is observed. If the lapse rate is less than 10 C km^{-1}, the air is stable and vertical mixing is inhibited. When an inversion occurs in which the temperature increases with height, the air is very stable and mixing

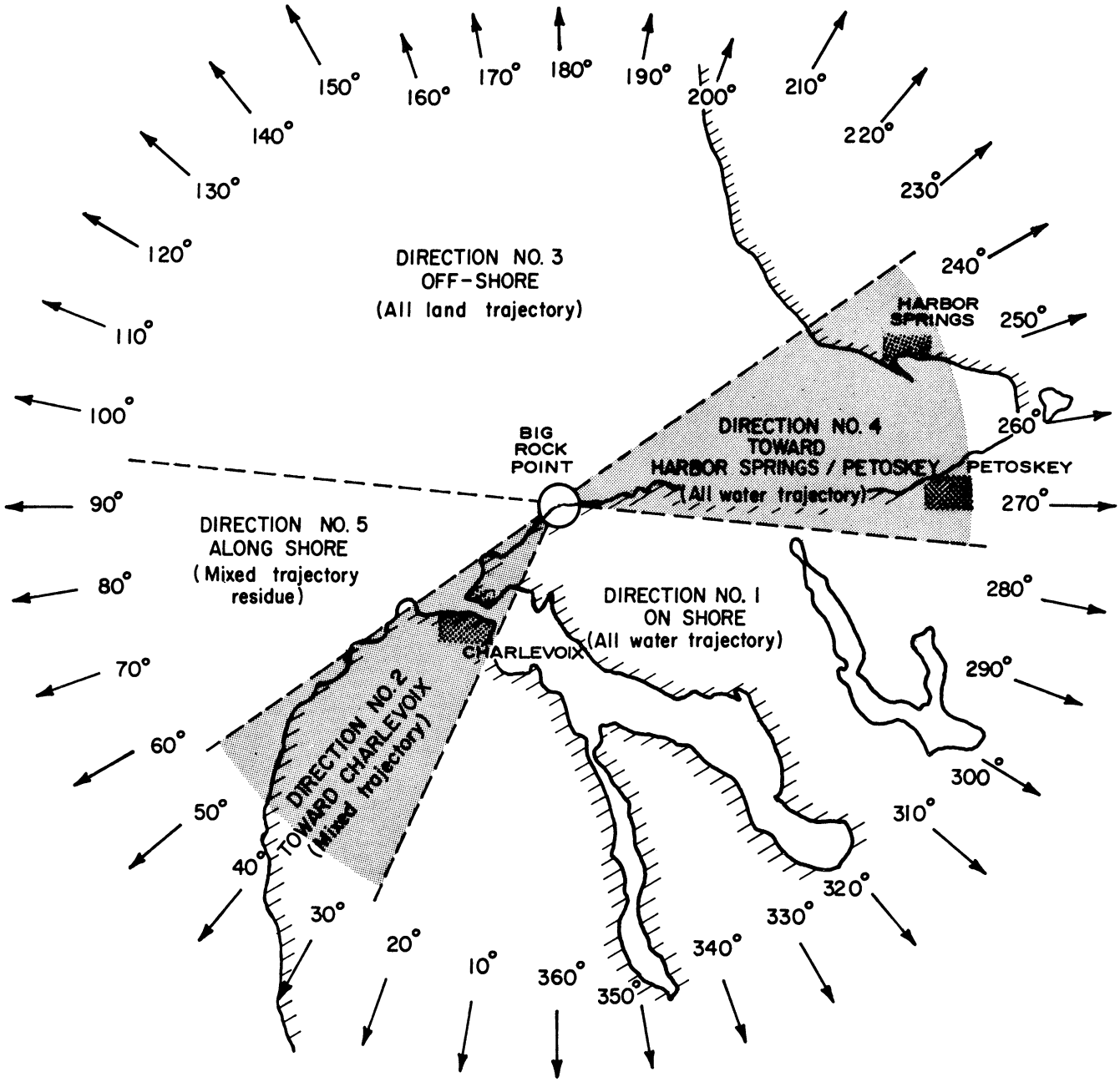

Fig. 1. Wind direction categories of special interest at the Big Rock Point Site.

NOTE: Arrows and numbers around periphery indicate direction from which wind is blowing.

is very slight. A fanning plume with pronounced horizontal dispersion but minimal vertical dispersion occurs with an inversion.

With brisk winds blowing over rough terrain, mechanical turbulence develops. The vertical mixing induced tends to maintain the lapse rate at a value close to 10 C km^{-1}, in which the air is neither stable nor unstable but neutral. Mechanical turbulence of this type leads to plume coning, which is characterized by nearly equal horizontal and vertical dispersion.

Both types of turbulence and various plume formations are readily observed in the Big Rock Point area. As the wind blows across the shoreline, pronounced changes in mechanical turbulence and in thermal turbulence often occur. Thermal effects are maximal in the late spring and late fall when the temperature differences between water and land are greatest.

2. Shoreline Influences Near Big Rock Point

Winds coming off the water are generally less turbulent than winds coming off the land, given the same meteorological conditions. This is especially the case in the late spring and early summer months when the surface lake temperature is lower than the average air temperature. This difference in the air-water temperature gives rise to an inversion condition over the water and, consequently, a reduction in the turbulence. Figure 2 shows the typical annual variation of water and air temperature. Onshore winds reaching the plant site (Directions No. 1, 2 and 4, Figure 1) during the months of May, June and July generally have very low turbulence. Winds, as they move inland, gain somewhat in turbulence in the lower layers due to the surface roughness of the trees and the thermal heating of the land. This turbulence does not in many instances, however, extend upward as high as 200-300 feet for some distance from the site. One would anticipate that winds toward Harbor Springs-Petoskey (Direction No. 4) would remain quite stable while crossing Little Traverse Bay; as it turned out, this generally was not the case. Winds from offshore and alongshore (Directions No. 3 and 5) generally arrive at the tower with marked turbulence but this turbulence is damped out over the lake at some distance from the site.

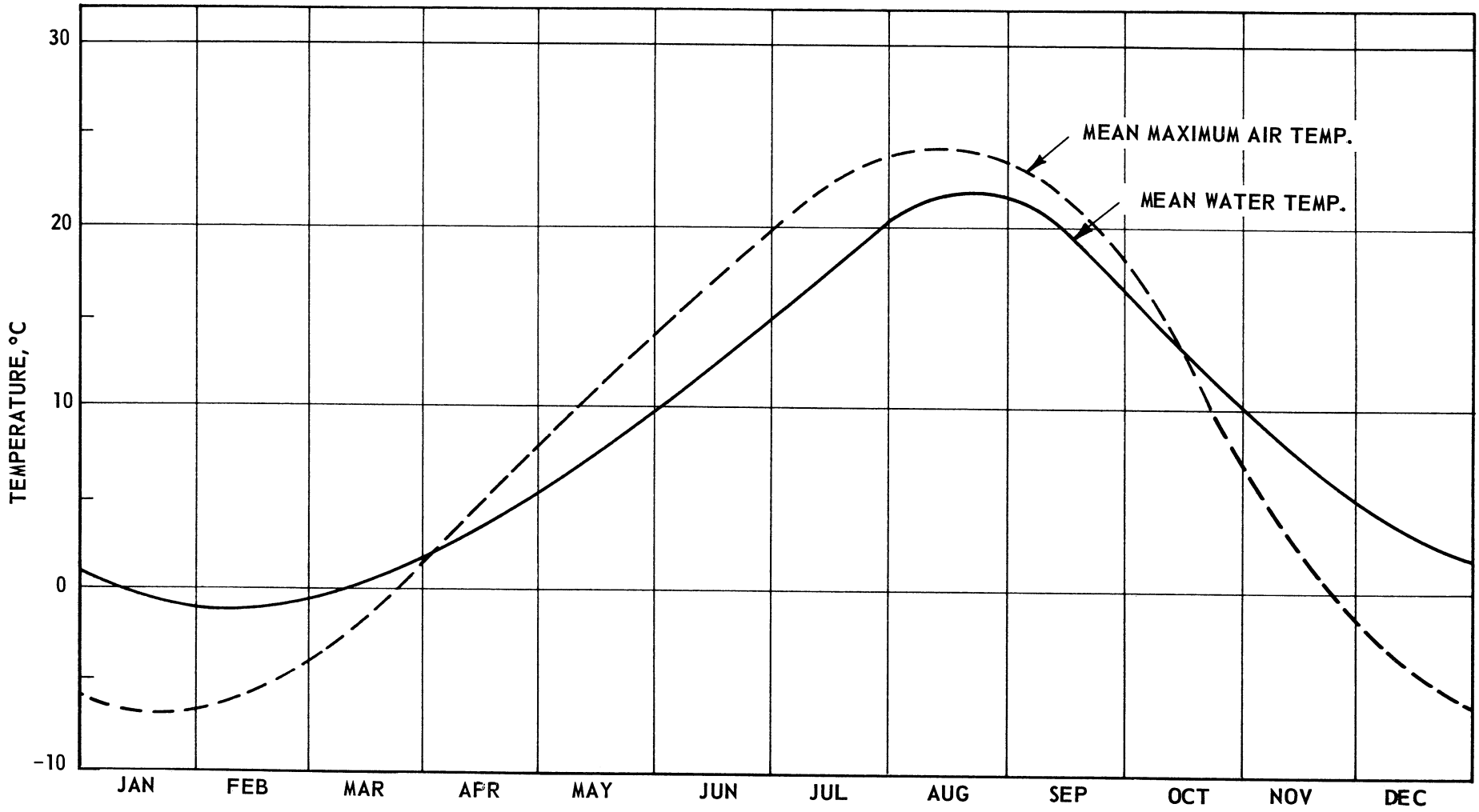

Figure 2. Typical annual variation of the mean daily water temperature at a depth of 3 feet in Little Traverse Bay and the mean daily maximum air temperature at a height of 10 feet. Based on data collected from February 1961 through January 1963.

The wind speed and wind direction instruments at the tower provide very reliable data on the average airflow past the tower and on the turbulence at the tower location and, hence, on the natural ventilation rate. The mean flow data have been used to determine the climatology of the site. The turbulence data provide reliable information on the dilution potential of the air as it passes the site. The shoreline location of the site, however, makes it apparent that diffusion patterns will vary substantially in the horizontal. It was thus obvious that the tower data must be supplemented by additional diffusion information in order to reveal these horizontal variations. The method employed is that involving plume photography as recommended by Gifford [3]. Smoke was released from the tower and photographed from above and from the side. From the photographs the horizontal and vertical diffusion coefficients were then estimated. By checking the diffusion coefficients as determined from the photographs against the diffusion coefficients as found from the tower data, the range of applicability of the tower data for various meteorological conditions was determined. Since maximum inversion development is expected over the lake in late spring and early summer, the months of June and July should have minimum diffusion and thus were given close study.

B. Objectives of the Diffusion Study

The objectives of the diffusion study during the late spring and early summer were as follows:

1. To correlate tower data with the dispersion of a visible tracer.

2. To determine if, with offshore winds, strong turbulence as measured at the tower at a given height quickly degenerates into weak turbulence over the water.

3. To determine if, with onshore winds, weak turbulence as measured at the tower at a given height quickly develops into strong turbulence over the land.

4. To measure the horizontal and vertical growth of the smoke plumes with stable westerly flow of air past the tower over Little Traverse Bay.

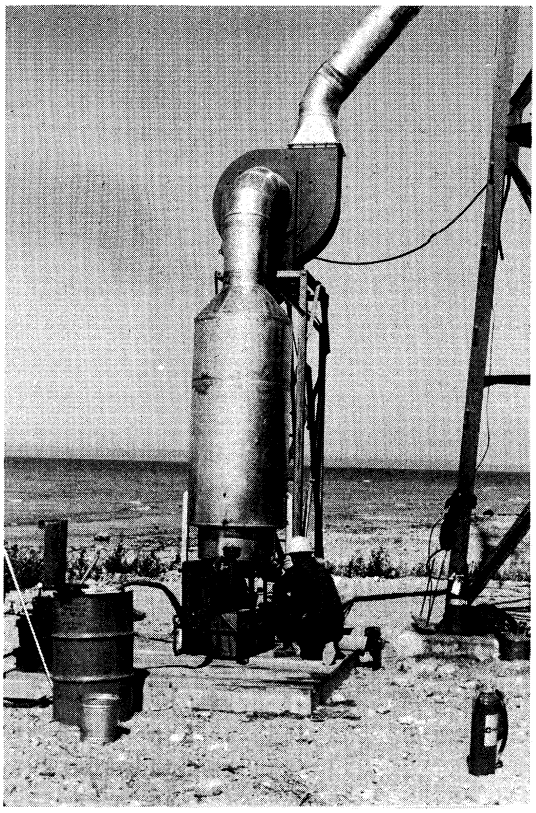

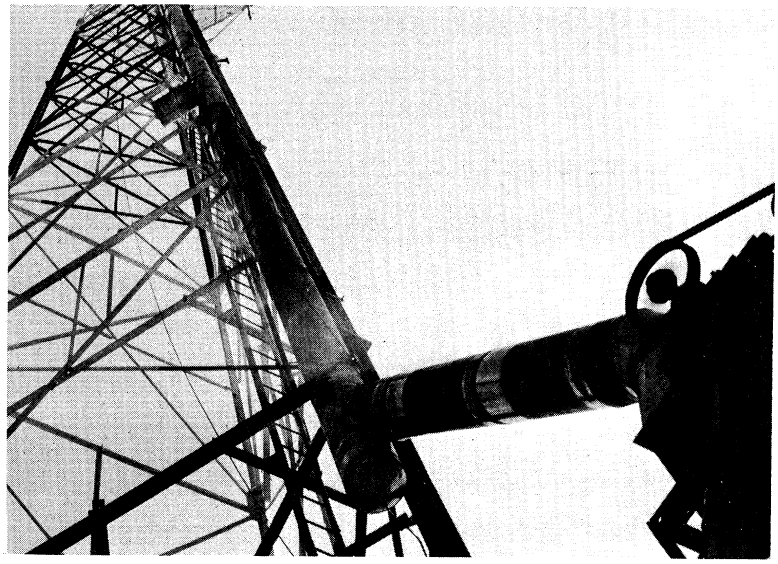

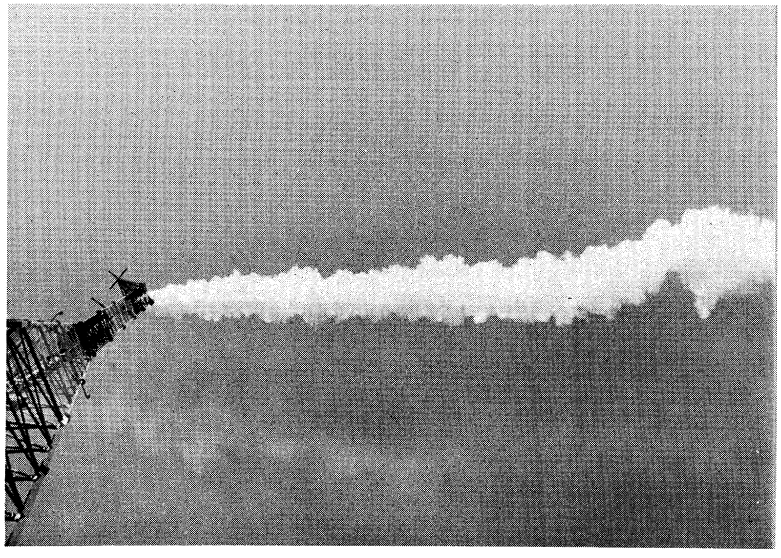

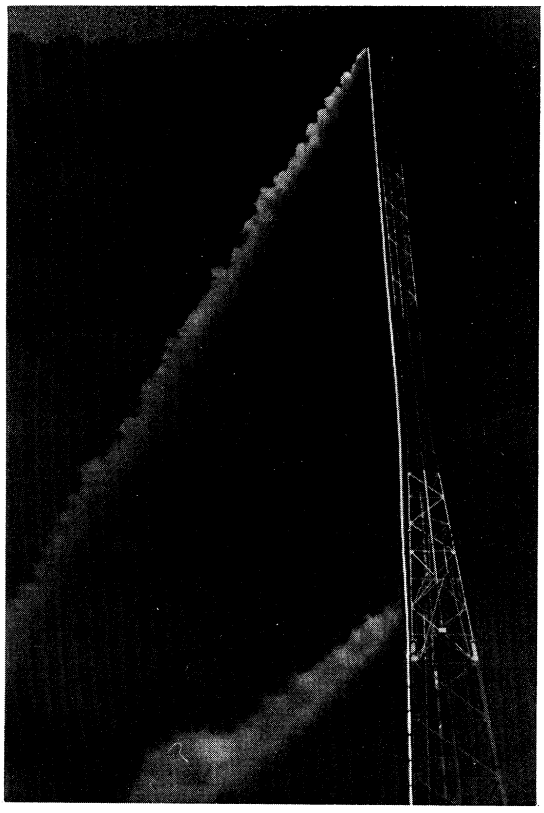

Figure 3. (a) View of fan, manifold and smoke generator at base of tower.

(b) View up duct. Note smoke outlet at the 64 foot level and the oil collector and drain at the bottom of the duct.

(c) Oil fog smoke plume released at the 256 foot level, at a generator output of 20 gal./hr (17 g/s).

(d) Smoke plumes at the 256 and 128 foot levels.

If the above objectives are fully realized, the dilution potential of the air passing the tower will be readily determined from the tower data alone.

II. THE DIFFUSION STUDY

A. Technique

1. General

An oil-fog generator supplied the volume and density of smoke needed to determine plume dispersion up to 5 miles from the tower under moderate to very poor dispersion conditions. A vertical pipe attached to the tower conveyed the smoke from the ground-based generator to the desired level for release. Outlets for the smoke were provided at the 60, 128 and 256 foot levels. See Figure 3 for details.

Most of the photographs of plumes were taken from an airplane. A ground-based camera on occasion supplemented the airplane photography. The ground-based camera was variously stationed on the top of the reactor containment vessel, on a high point of land or in a boat on the water. The ground-based camera, although occasionally supplying needed information, was generally superfluous. Time-lapse photography was tried but background difficulties eliminated this technique from further consideration.

2. Data Collected

During the time the smoke plumes were being photographed, a Gelman-Gill bivane was in operation at the height of release of the smoke plume. The bivane measured the horizontal and vertical fluctuations in the wind direction. In addition, the wet-bulb and dry-bulb temperatures at various heights were measured by instrumentation on the airplane. These data combined with the routine wind speed, wind direction and temperature lapse rate data collected on the tower gave a complete summary of the meteorological conditions in the immediate area.

3. Diffusion Experiments

The diffusion experiments were initiated in July 1961. During the shakedown period while getting the equipment operational, a fire destroyed the fan and forced postponement of the experiments to the following summer. During the period June 10 through July 20, 1962, experiments were conducted whenever inversion conditions persisted for a

number of hours prior to or during daylight hours. During this period, such conditions occurred nearly every fair-weather morning and late evening. In all, about 25 full-scale diffusion experiments were made. The results of these experiments are presented in later sections of this report.

B. Photographic Data Analysis

1. Mathematical Derivation

In analyzing the plume photographs Gifford's method [3] was used to determine diffusion coefficients. This method is derived from the idea that smoke particles act to obscure the background, and when enough of them are along a line of sight, the background disappears. This observation limit is called the "edge" of the smoke.

The steady state concentration from a continuously emitting point source at the origin of the x, y and z-axes is usually expressed mathematically by the familiar Gaussian diffusion equation:

$$X_{(x,y,z)} = \frac{Q}{2\pi \bar{u} \left(\sigma_y^2 \sigma_z^2\right)^{\frac{1}{2}}} \exp - \frac{y^2}{2\sigma_y^2} \exp - \frac{z^2}{2\sigma_z^2} \quad \ldots\ldots\ldots (1)$$

where, X = concentration of material at point (x,y,z), (M/L^3)

Q = emission rate of the source, (M/T)

$\bar{u}$ = mean wind speed along x-axis, (L/T)

σ_y^2, σ_z^2 = horizontal and vertical variances of the plume concentration distribution, (L^2), which are a function of the dispersion time T, where $T = x/\bar{u}$.

If the plume is viewed from a fairly great vertical distance, the total density of smoke particles along a line of sight is:

$$\int_{-\infty}^{\infty} X \, dz = \frac{Q \exp\left(-y^2/2\sigma_y^2\right)}{2\pi \bar{u} \left(\sigma_y^2 \sigma_z^2\right)^{\frac{1}{2}}} \int_{-\infty}^{\infty} \exp\left(\frac{-z^2}{2\sigma_z^2}\right) dz \quad \ldots\ldots\ldots (2)$$

If there is a fixed value of this integrated concentration, say X_e, corresponding to the visible edge of the plume, and if this value occurs at distance Y from the x-axis, then

$$\frac{X_e}{Q} = \frac{\exp\ (-Y^2/2\ \sigma_y^2)}{(2\pi\ \sigma_y^2)^{\frac{1}{2}}\ \bar{u}} \qquad \ldots \ldots \ldots \ldots \ldots \ldots \ldots \ldots \ldots \ldots \ldots \ (3)$$

At $Y = 0$ (i.e., at the end of the plume)

$$\frac{X_e}{Q} = 2\ \sigma_y^2(T)\ \bar{u}^{2\ -\frac{1}{2}} \qquad \ldots \ldots \ldots \ldots \ldots \ldots \ldots \ldots \ldots \ldots \ldots \ (4)$$

where $\sigma_y^2(T)$ in this case is the constant value of σ_y^2 that applies at the end of the plume. Equating equations (3) and (4), and differentiating logarithmically with respect to $x/\bar{u}$, it follows that:

$$\frac{d(Y^2)}{dx} = \frac{d\sigma_y^2}{dx}\ \left(\frac{Y^2 - \sigma_y^2}{\sigma_y^2}\right)$$

Now when $Y^2 = \sigma_y^2$, $\frac{d(Y^2)}{dx} = 0$. This of course occurs at the widest dimension of the plume, say at the point where the half-width is Y_m. It then follows from (3) and (4) that the constant, $\sigma_y^2\ (T)$, is

$$\sigma_y^2(T) = eY_m^2 \qquad \ldots \ldots \ldots \ldots \ldots \ldots \ldots \ldots \ldots \ldots \ldots \ldots \ldots \ (5)$$

where e is the base of natural logarithms.

The distribution of smoke in space is completely characterized by equation (1). The only unknown quantities in equation (1) are σ_y^2 and σ_z^2. Practically speaking, X may also not be known. In terms of the visible plume this means that X_e may not be known; but X_e may be determined, if necessary by combining equations (4) and (5). If one assumes, as has been done in most smoke dispersion studies, some particular form for σ_y^2, i.e., Sutton's form:

$$\sigma_y^2 = 1/2\ C^2\ x^{2-n},\ 0<n<1 \qquad \ldots \ldots \ldots \ldots \ldots \ldots \ldots \ldots \ldots \ldots \ (6)$$

where, C = a generalized diffusion coefficient, $(L^{n/2})$
(often called the Sutton diffusion coefficient)

x = distance downwind, (L)

n = a dimensionless parameter which depends upon atmospheric stability.

Then the plume geometry is firmly fixed so far as the mathematics is concerned. Consequently, it is reasonable that some simple geometrical

measurements of the plume are all that is needed in order to determine the diffusion coefficient, C.

Combining equation (5) with equation (6), it is found that

$$C_y^2 = 2 x_t^n e (Y_m/x_t)^2 \quad \ldots\ldots\ldots\ldots\ldots\ldots\ldots\ldots\ldots\ldots (7)$$

where C_y = diffusion coefficient in the lateral direction, $(L^{n/2})$.

x_t = distance from the stack to the end of the visible plume, (L).

The corresponding result for C_z, the vertical diffusion coefficient is:

$$C_z^2 = 2 x_t^n e (Z_m/x_t)^2 \quad \ldots\ldots\ldots\ldots\ldots\ldots\ldots\ldots\ldots\ldots (8)$$

where Z_m = the vertical half-width of the plume at its maximum dimension.

When the end of the visible plume cannot be determined or if there is a preference not to use it, another means of determining the variances is available. By combining equations (3) and (4) and (5), it can be shown that

$$Y_m^2 = \sigma_y^2 (x_m/\bar{u})$$

where, x_m is the distance from the stack where Y_m occurs. Using equation (6), equations similar to (7) and (8) can be derived:

$$C_y^2 = 2 x_m^n (Y_m/x_m)^2 \quad \ldots\ldots\ldots\ldots\ldots\ldots\ldots\ldots\ldots\ldots (9)$$

$$C_z^2 = 2 x_m^n (Z_m/x_m)^2 \quad \ldots\ldots\ldots\ldots\ldots\ldots\ldots\ldots\ldots\ldots (10)$$

In this study, because of the difficulties in determining x_m, the distance downwind at which the maximum plume height Z_m occurred, equation (8) was used in preference to equation (10) in determining C_z.

The most serious restrictions on the use of visually or photographically determined dimensions of plumes as dispersion indices are inherent in the nature of turbulent diffusion. At any instant, the visual or photographic appearance of a plume suggests that it is a dispersion of particles about a center line which is itself deformed by the air turbulence. This type of diffusion is distinctly different from the phenomenon described by equation (1). Various studies have shown that formulae such as equation (1), relating dispersion to a fixed axis, can

only apply to averaged conditions, i.e., only to the mean concentration distribution. It would be expected then, that the opacity theory would apply to long time exposure photographs of plumes. To successfully use instantaneous photographs of plumes taken from an airplane, one would, therefore, need to use an averaging technique which involved the use of a number of photographs taken over an extended period. In the experiments described in this report, photographs of plumes taken over a half-hour period were averaged to yield the average plume dimensions for the calculation of the diffusion coefficients.

Gifford [3] and others have pointed out various shortcomings of the opacity method. For example, the ability to detect the edge of the visible plume depends to some extent on the nonuniformity of background illumination and the dependence of visual contour perception on luminosity gradients. These limitations have not been studied quantitatively and little is known about how serious they may be. In view of quantitative results produced by Gifford [3] and Frenkiel [4], it appears that the opacity method provides at least a useful, practical tool. It is felt that this conjecture is confirmed by the results in this report.

2. Analysis of Photographs

Smoke emission from the stack was started at least a half-hour before any photographs of plumes were taken. For very low wind speeds, it was started earlier. This practice gave assurance that the smoke plume would be close to an equilibrium condition when the photography from the airplane was started. In some instances, atmospheric conditions did not persist unchanged during the experiment. For example, on more than one occasion, a plume flowing along the shore would suddenly be acted on by a lake breeze and would rapidly change direction, width, length and shape. Gifford's technique could not be used for those runs. Only those runs which had constant atmospheric conditions over at least one and a half hours are analyzed in this report. The averaging techniques for arriving at the half-hour plume dimensions assumed constant atmospheric conditions over the whole period of the experiment - including the time before the run necessary for the plume to reach equilibrium.

The analysis of the photographs consisted basically of averaging the visible plume dimensions over a half-hour. The following technique was used: Each smoke plume photography run lasted one hour. Photographs of the smoke plume were taken in three distinct time segments. The first 15 minutes of each run were spent at the level of the plume taking side view photographs of the vertical development. Then the airplane would climb to 3000 feet and photographs of the horizontal and longitudinal development of the plume would be taken over a one-half hour period. The airplane would then descend to the level of the plume and side view photographs of the vertical development of the plume would be taken over the remaining 15 minutes of the experimental run. During most runs, the meteorological conditions did not change enough to cause any difficulty in averaging plume behavior over the one-hour period. Those runs which did have variable meteorological conditions during the one-hour period must be treated in a different manner. See Appendix II for complete details on the photographic techniques used during these experiments.

The plume widths and the plume lengths were determined from the photographs. For this, use was made of landmarks in the photographs (roads, topographic features, etc) and also perspective grid overlays to determine the plume dimensions. See Appendix III for details on construction and use of the grids. In addition, the observer's notes made at the time of the experiments were used to check plume dimensions determined from the photographs. The stability parameter, n, was estimated from the air temperature profile as measured by the instrumentation on the tower and in the airplane. The values used for n for the various lapse conditions are listed in Table I:

Table I

Temperature Difference $T_{256} - T_{50} \equiv \Delta T$ (°C)	Lapse Condition	Stability Parameter n
$\Delta T > 3.0$	Very Stable	0.50
$3.0 \geq \Delta T > 0$	Stable	0.33
$0 \leqq \Delta T \leqq -0.6$	Near Neutral	0.25
$\Delta T < -0.6$	Unstable	0.20

The problems of determining the values of n are such that it has been the practice to assign values to n depending on the temperature profile [5]. It happens that n and C_y and C_z are so related that errors in estimating n are compensated for in the values obtained for C_y and C_z.

C. Turbulence Data Analysis

The estimation of σ_y and σ_z from the bivane data (see equations (1) and (6)) was accomplished using the relationships recommended by Pasquill [10]. Briefly, Pasquill states that: "... the practical problem reduces to making appropriate estimates of σ_d, from wind directions averaged over a time interval equal to one-quarter of the time of downwind travel involved. ...this method should only be applied for release-times at least as long as the time of travel." In the above, σ_d is either the vertical or the horizontal standard deviation of the wind direction in degrees. Further, Pasquill states that the proper estimate of the standard deviation "... will be given by the square root of the differences of the squares of the standard deviations recorded for sampling durations of τ and T/4." Expressed mathematically,

$$\sigma_{\tau,T/4} = (\sigma^2_{\tau,s} - \sigma^2_{T/4,s})^{\frac{1}{2}} \quad \ldots\ldots\ldots\ldots\ldots\ldots\ldots\ldots \quad (11)$$

where τ = the sampling duration (usually 30 minutes for the smoke plume photography experiments).

T = $x/\bar{u}$ = the travel time ($x = x_t$, the visible plume length in the smoke plume photography experiments).

4 = the ratio of the Lagrangian and Eulerian time scales.

s = the effective averaging time which is inherent in the wind instruments.

The above means that the low-frequency cutoff is equivalent to the sampling duration τ (30 minutes) and the high-frequency cutoff is $T/4=(x_t/4\bar{u})$.

The outputs of the bivane were recorded on standard milliampere chart recorders. The mechanics of analyzing the strip charts consisted simply of calculating the visible plume travel time, T/4, then going to the strip chart and marking off intervals of T/4 for the appropriate sampling interval (usually 30 minutes). σ_d was calculated directly from these values. A nomogram for converting σ_d to Sutton's C is presented in Appendix V. The basic relationship used is equation (6). C_y and C_z calculated for each run in the above manner are included in Columns 10 and 11 of Table II.

A standard Esterline-Angus wind direction recorder was also in operation during the experiments. In an effort to calibrate this record, a C_y was calculated for each run using the wind direction trace. The range of the trace over T/4 was used to estimate the value of σ_d. The wind direction fluctuations were assumed to be distributed normally and the range divided by 4.3 was assumed to be equal to σ_d. The nomogram in Appendix V was also used in this calculation. Column 9 in Table II shows C_y calculated for each run in this manner.

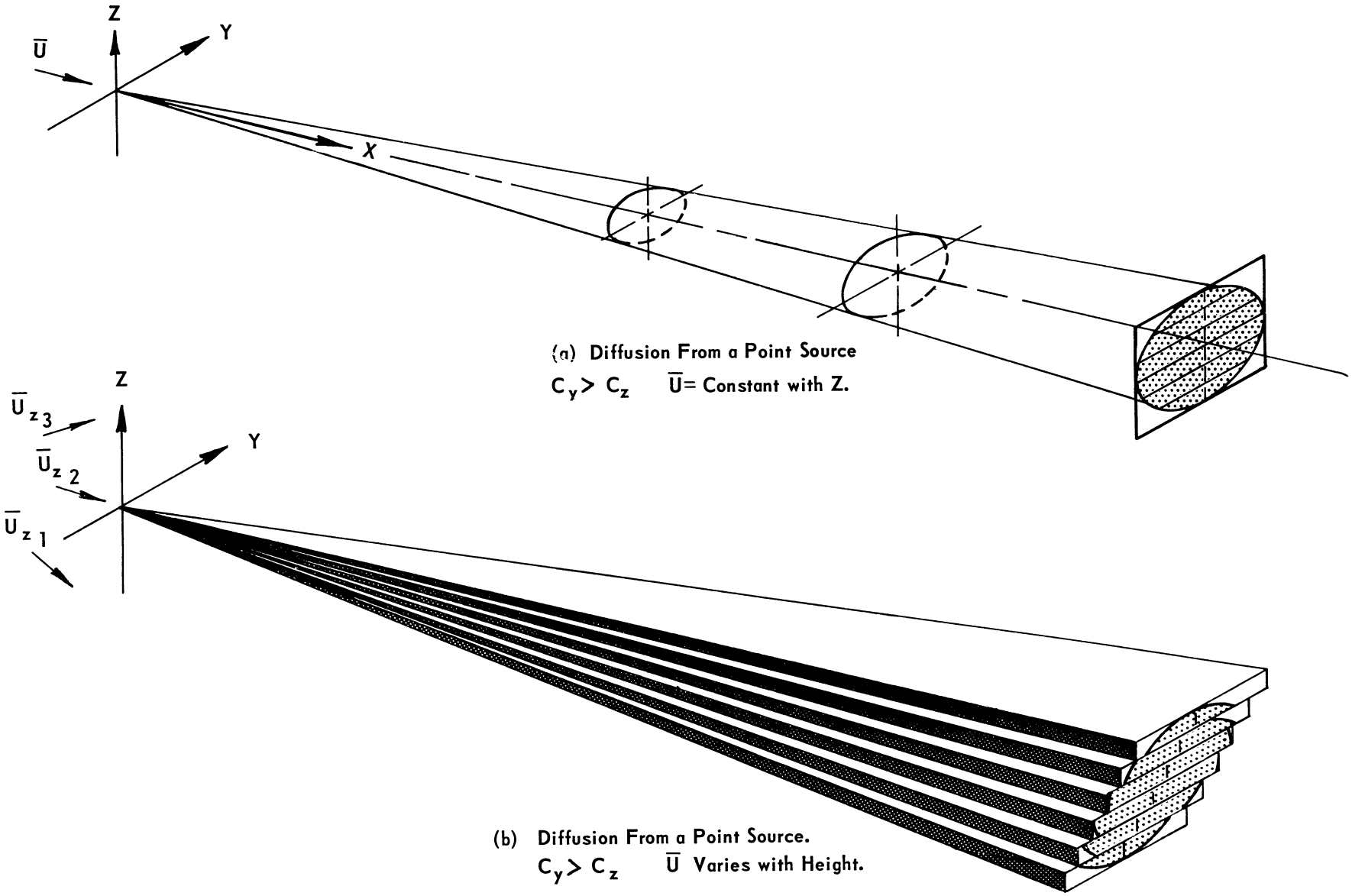

Figure 4. Effect of Crosswind Shear on Diffusion From a Point Source. Cross-Sectional Areas Equal.

III. RESULTS OF THE DIFFUSION STUDY

A. Discussion of Numerical Data

1. General

Table II summarizes most of the major parameters derived from the diffusion studies. Column 1 lists the experimental run number for identification purposes. Column 2 shows the temperature difference between the 256-foot and 50-foot levels on the tower. These levels were chosen to represent the lapse conditions during the experiments because they indicate the type of stability of the atmosphere in the region of greatest interest, i.e., in the region from the top of the stack to near the ground. For example, if the temperature difference between these two levels is positive, the lapse condition in this layer is stable and downward movement of stack effluents will be restricted. Column 3 lists the average wind speed at 256 feet at the time the photographs analyzed were taken. Column 4 shows the average wind direction at 256 feet at the same time.

Column 5 shows the difference in the wind direction at the 256-foot and the 128-foot levels on the tower. This term is often called wind direction shear or crosswind shear. Consider a plume, as in Figure 4, whose cross section is being deformed by crosswind shear compared to a normal plume. In the illustration, the cross-sectional areas are equal. However, the perimeter of the plume affected by crosswind shear is greater than that of the plume not affected by shear. Since the mixing of the plume with the surrounding air occurs around the perimeter of the plume, diffusion of a plume would thus be enhanced by shear. An analysis by Brock and Hewson [9] giving the results of an analog solution of the Fickian diffusion equation indicates that crosswind shear will enhance diffusion. The results of the smoke plume photography experiments support this conclusion and also suggest that shear may be an important diffusion parameter at shoreline sites.

Columns 6, 7 and 8 list the one-half hour, averaged plume dimensions from which the Sutton diffusion coefficients were calculated. These three columns show the total continuous plume widths, heights and lengths for each experimental run. It was necessary to specify the continuous portion of the plume because, under certain conditions,

TABLE II

SUMMARY OF DATA DERIVED FROM EXPERIMENTAL RUNS

Column Number	Run Number 1	ΔT °C 2	$\bar{u}$ mph 3	A deg 4	S deg/128' 5	$2Y_m$ ft 6	$2Z_m$ ft 7	x_t mi 8	Diffusion Coefficients - $m^{n/2}$ Std C_y 9	Bivane C_y 10	Bivane C_z 11	Visual C_y 12	Visual C_z 13	Photos C_y 14	Photos C_z 15	X_o/Q x10^{-12} sec/cc 16	N_o x10^{-3} g/m^2 17
Lapse Condition																	
	13	+0.2	11	182	8	2600	400	8.0	0.42	0.50	0.50	-	-	0.35	0.06	0.4	2.0
	6	+1.6	12	355	5	1500	260	5.0	0.13	0.14	0.07	0.07	0.04	0.30	0.05	1.3	3.3
	8	+1.8	13	255	25	1500	260	5.0	0.13	0.10	0.03	-	0.03	0.31	0.05	1.1	3.0
Stable Conditions	15	+0.2	9	212	17	5280	160	3.5	0.90	-	0.20	0.70	0.08	1.40	0.05	0.6	1.3
	18	+1.4	14	335	15	1300	230	3.0	0.13	0.15	0.07	0.30	-	0.40	0.07	1.3	3.2
n = .33	19	+0.1	4	90	30	2600	160	3.0	0.16	0.20	0.10	0.50	0.02	0.80	0.05	3.2	5.6
	11	+1.3	1	355	25	3100	430	2.6	0.30	0.60	0.10	0.60	-	1.07	0.15	4.0	20.0
	14	+0.2	9	270	3	1600	130	2.6	0.40	0.20	0.10	-	-	0.51	0.05	2.8	4.5
	25	+0.3	3	245	45	3700	160	2.0	0.36	0.25	0.09	0.40	0.10	1.60	0.07	3.1	5.4
	16	-0.5	10	250	12	2100	230	3.5	0.60	0.20	0.15	0.25	0.05	0.40	0.05	1.0	2.9
Near Neutral Conditions	22	-0.5	8	262	16	1600	330	2.4	0.32	0.20	0.16	0.30	0.30	0.40	0.09	1.3	5.0
	20	-0.5	7	322	13	2600	720	2.0	0.16	0.25	0.18	0.50	0.20	0.80	0.22	0.4	2.8
n = .25	21	-0.6	4	265	5	1000	260	2.0	0.32	0.20	0.10	-	-	0.32	0.08	4.3	14.3
	12	-0.6	6	215	3	1600	430	1.4	0.45	0.40	0.20	0.30	0.30	0.50	0.20	1.6	8.4
	24	-0.7	12	245	17	1000	600	2.5	0.20	0.20	0.10	0.15	0.10	0.21	0.12	0.9	4.9
Unstable Conditions	17	-0.8	13	360	15	1600	1100	2.5	0.20	0.18	0.18	0.25	0.25	0.34	0.23	0.2	2.8
n = .20	23	-0.7	8	325	20	1600	1100	2.0	0.30	0.25	0.25	0.40	0.25	0.40	0.28	0.4	4.8
	9	-0.8	11	140	12	1800	430	1.3	0.60	0.60	0.20	0.20	0.20	0.65	0.15	0.4	3.0
																Avg	5.4

especially over water, bits and disjointed pieces of plume could be seen miles away from the continuous plume. A total plume dimension based on these fragments would be unrealistic.

Columns 9 through 15 list the familiar Sutton diffusion coefficients calculated for the same period using different data and various techniques. By comparing the diffusion coefficients in this manner, it was hoped that the relationship between the various techniques could be ascertained.

Column 16 shows what could be called a "dispersion factor." It was calculated in the following way for each run using Sutton's diffusion equation and the various parameters derived from the diffusion study:

$$\frac{X_o}{Q} = \frac{10^{-6}}{\pi C_y C_z \bar{u} (x_t)^{2-n}}$$

where, X_o = the plume center line concentration at x_t where the continuous plume is no longer visible, (μg/cc)

Q = mass of oil fog leaving stack, (ug/sec)

C_y = diffusion parameter in the horizontal direction, ($m^{n/2}$)

C_z = diffusion parameter in the vertical direction, ($m^{n/2}$)

n = a dimensionless parameter associated with stability

$\bar{u}$ = wind speed, (m/sec)

x_t = distance from stack to end of continuous, visible plume (m)

10^{-6} = This factor appears in the numerator to convert the units of the right-hand side of the equation from (μg/m^3) to (μg/cc)

The $\frac{X_o}{Q}$ term indicates the maximum amount of diffusion occurring on the visible plume center line.

Column 17 shows the minimum density of oil fog for the detection of the edge of the smoke plume. This term will now be derived. It can be shown that smokes become opaque when the mass of suspended matter per unit of projected area reaches or exceeds some minimum value. This minimum value will be represented by N_o, g/m^2. Its numerical value varies

with the nature of the smoke, background and illumination. Sutton's equation gives the concentration per unit volume, but the quantity of importance in smoke plume studies is the density, or mass per unit of horizontal area. The density N_o can be obtained by evaluating the definite integral of concentration with height, as follows:

$$N_o = \int_o^\infty X_o dz = \frac{Q}{\sqrt{\pi}\ \bar{u}\ C_y\ x_t^{\frac{2-n}{2}}}$$

If light conditions and analysis techniques were constant through all the experimental runs, N_o would be the same for each run. N_o is calculated using the values of C_y and x_t derived from the analysis of plume photographs. For these experimental runs the smoke generator output was 20 gal/hr or 17 g/s.

2. Results

Table II summarizes the experimental runs made under the various lapse conditions. In many of the runs listed it will be noted that the wind direction shear, S (Column 5), is greater than 15^o. For these runs, the large value of S is reflected in the large values of C_y derived from the visual and photographic data. If the diffusion were not enhanced by the wind shear, one would expect that the N_o terms calculated for the runs with large C_y due to a large value of S, would be quite small. Consider the defining equation for N_o. The quantities x_t and C_y are related variables. Any inconsistencies in the experimental sets of x_t and C_y would show up immediately in the calculation of N_o. Inspection of Column 17 shows the values of N_o range from 1.3×10^{-3} g/m^2 to 20.0×10^{-3} g/m^2 with an average value of 5.4×10^{-3} g/m^2, (3.7×10^{-3} g/m^2 if the three high values are omitted). Most of the extreme variations can be explained by unusual lighting or background conditions during the runs. For example, the maximum N_o's occurred on very hazy days when the plume edge could be easily lost in the haze. This was the case for Runs 11, 12 and 21. The minimum value of N_o for Run 15 occurred on a day when the plume was over a very dark, lake water background. The values of N_o are within an order of magnitude and this must be considered good agreement. This compares to a minimum value of $N_o = 10 \times 10^{-3}$ g/m^2 found by Frenkiel [4]

for smoke puffs made by black powder explosions against the sky. Gifford [3] states that Holland found $N_o = 15 \times 10^{-3}$ g/m^2 for oil fog. The fact that the N_o value derived in these experiments is lower than either Holland's or Frenkiel's value might be attributed to the manner in which the smoke plumes were illuminated. In all cases the smoke plume photographs were taken in early morning or in late afternoon when the sun was low in the sky. It appears that the camera is more sensitive to low concentrations of the oil fog under these lighting conditions. It is also suspected that some of the difference may be attributed to the type of averaging used to determine the plume outlines over the half-hour period.

If it were assumed that the average N_o was correct and that all the errors were in C_y, the C_y's would never be off by more than a factor of about 3 and most of the time would be within a factor of 2. Considering the very large values of a number of C_y's, this indicates rather strongly that crosswind shear has a great influence on the diffusion.

Runs 6 and 18 provide an opportunity to compare the effects of crosswind shear on plume center line concentrations. It will be noted from Table II that the turbulence parameters for both these runs are strikingly similar. Columns 9, 10 and 11 for each run are for all practical purposes, identical. In addition, the wind speeds, wind direction and lapse condition are very close. The major difference is in the value of S, the crosswind shear; for Run 6, $S = 5^o/128'$ and for Run 18, $S = 15^o/128'$. These differences are reflected in the visible plume widths and lengths for each run; for Run 6, $C_y = 0.30$ and $x_t = 5.0$ miles and for Run 18, $C_y = 0.40$ and $x_t = 3.0$ miles. If it can be assumed that both experimental runs were identical except for shear, and all the data indicates they were, an inference as to the effect of shear on diffusion coefficients can be made.

Considering just the end of the visible plume, the following expression must hold true:

$$(N_o)_{\text{Run 6}} = (N_o)_{\text{Run 18}}$$

therefore

$$\frac{Q_6}{\bar{u}_6 \, C_{y_6} \, x_{t_6}^{\frac{2-n}{n}}} = \frac{Q_{18}}{\bar{u}_{18} \, C_{y_{18}} \, x_{t_{18}}^{\frac{2-n}{n}}}$$

Substituting the various parameters from Table II and letting n = 0.33,

$$\frac{1}{(12)(0.30)(5)^{.835}} = \frac{1}{(14)(0.40)(3)^{.835}}$$

$$0.072 \doteq 0.071$$

This calculation, although far from conclusive, suggests that the diffusion coefficients as calculated from the photographic data may, indeed, be realistic at least for intermediate distances from the tower. Since crosswind shear is often prominent under stable conditions, the above would suggest that, at shoreline sites, the stable and very stable atmospheric conditions may not be the most restrictive meteorological condition for the annual dose calculations. By this, it is meant that, in general, atmospheric diffusion is quite good at the site, even under stable conditions. Because the annual dose would be so low, it would be quite likely that the short-term, transient atmospheric conditions, i.e., looping, fumigation, etc, would be the largest contributors to the annual dose.

Further study of Table II shows that, under stable conditions, a dispersion factor, $\frac{X_o}{Q}$ (Column 14) of at least 10^{-12} sec/cc would be realized within 5 miles of the stack at the plume center line. The only exception is a plume which was visible for 8 miles over water. Since the nearest land after an overwater trajectory is 9 miles away, an $\frac{X_o}{Q}$ of at least 10^{-13} sec/cc would be expected at any point overland after all water plume travel. It must be remembered that the dispersion factor is for the plume center line. Under stable lapse conditions, the plume travels long distances without significant vertical diffusion. Hence, the dispersion factor at the ground would have a much lower value.

A study of the diffusion coefficients in Table II suggests that,with stable atmospheric conditions and when a large value of S is not evident, $C_y = 0.4$ should be used. When a large value of S is evident, $C_y = 0.8$ should be used. In both cases, $C_z = 0.05$ should be used. It is also interesting to note that the diffusion coefficients calculated from tower turbulence data, Columns 9, 10 and 11, are in fair agreement with the diffusion coefficients derived from the photographs for the near neutral and unstable conditions. It is obvious from Table II that under stable atmospheric conditions the tower data seriously underestimate the atmospheric diffusion potential at the Big Rock Point site. This most certainly can be attributed to the local effects at the shoreline.

Columns 12 and 14, which list the visually determined C_y's and the photographically determined C_y's, point out an interesting problem. For the stable lapse conditions, the visual C_y's are significantly smaller than the photo C_y's. This is attributed to the fact that the observer during the experimental run is so busy taking photographs that he does not have time to continually plot the visible outline of the smoke plume. The visual C_y's then represent 3 to 10 minute (estimated) diffusion coefficients as compared to the 30 minute diffusion coefficients as represented by the photo C_y's. It is interesting to note that this problem is not quite as marked for the runs with near neutral or unstable lapse conditions. Apparently the 3 to 10 minute diffusion coefficients do not differ greatly from the 30 minute diffusion coefficients for these conditions. This would suggest that the low frequency, meander producing eddies are quite important to the diffusion under stable lapse conditions. It might be said that these low frequency eddies "contribute" about 30 to 50 percent of the spread to the horizontal plume diffusion.

3. Conclusions From Numerical Data

a. The following average values of diffusion coefficients for various lapse conditions at the Big Rock Point site should be:

Lapse Condition	n	C_y	C_z
Stable	0.33	0.40	0.05
Stable - With S $\geqq 15^{o}$	0.33	0.80	0.05
Near Neutral	0.25	0.40	0.10
Unstable	0.20	0.40	0.20

b. Diffusion coefficients derived from the tower turbulence data generally underestimate the atmospheric diffusion potential at the site. This is especially true under stable atmospheric conditions.

c. Wind direction shear significantly enhances diffusion at the site, especially under stable lapse conditions.

d. Overland, a minimum dispersion factor of $\frac{X_o}{Q} = 10^{-12}$ sec/cc is attained within 5 miles of the stack at plume center line for a continuous plume under even the most stable atmospheric conditions.

e. Average diffusion is generally good, hence, transient meteorological conditions, e.g., looping, fumigation, downwash, may be controlling factors in the annual dose calculations.

f. The average value of the density of oil fog per unit area for the threshold of visibility, under the lighting and background conditions at Big Rock Point is:

$$N_o = 5.4 \times 10^{-3} \text{ g/m}^2.$$

B. Discussion of Photographic Data

1. General

Figures 5, 6 and 7 show diagrams of typical visible plume contours for stable, near neutral and unstable lapse conditions. A study of these figures shows the effects of lapse condition, wind speed, and wind direction shear on the visible plume contours. In general, wind speeds greater than 10 mph produce long, narrow plumes. When these high wind speeds are combined with stable atmospheric conditions, the plumes are even longer. Under stable atmospheric conditions, large values of crosswind shear, S, produce short, fat plumes, except when the vertical diffusion is not sufficient to permit the plume to reach the shear layer. Under near neutral and unstable lapse conditions, crosswind shear doesn't appear to appreciably improve the horizontal diffusion. Generally, plumes diffusing under near neutral or unstable atmospheric conditions have a visible length of less than 3 miles.

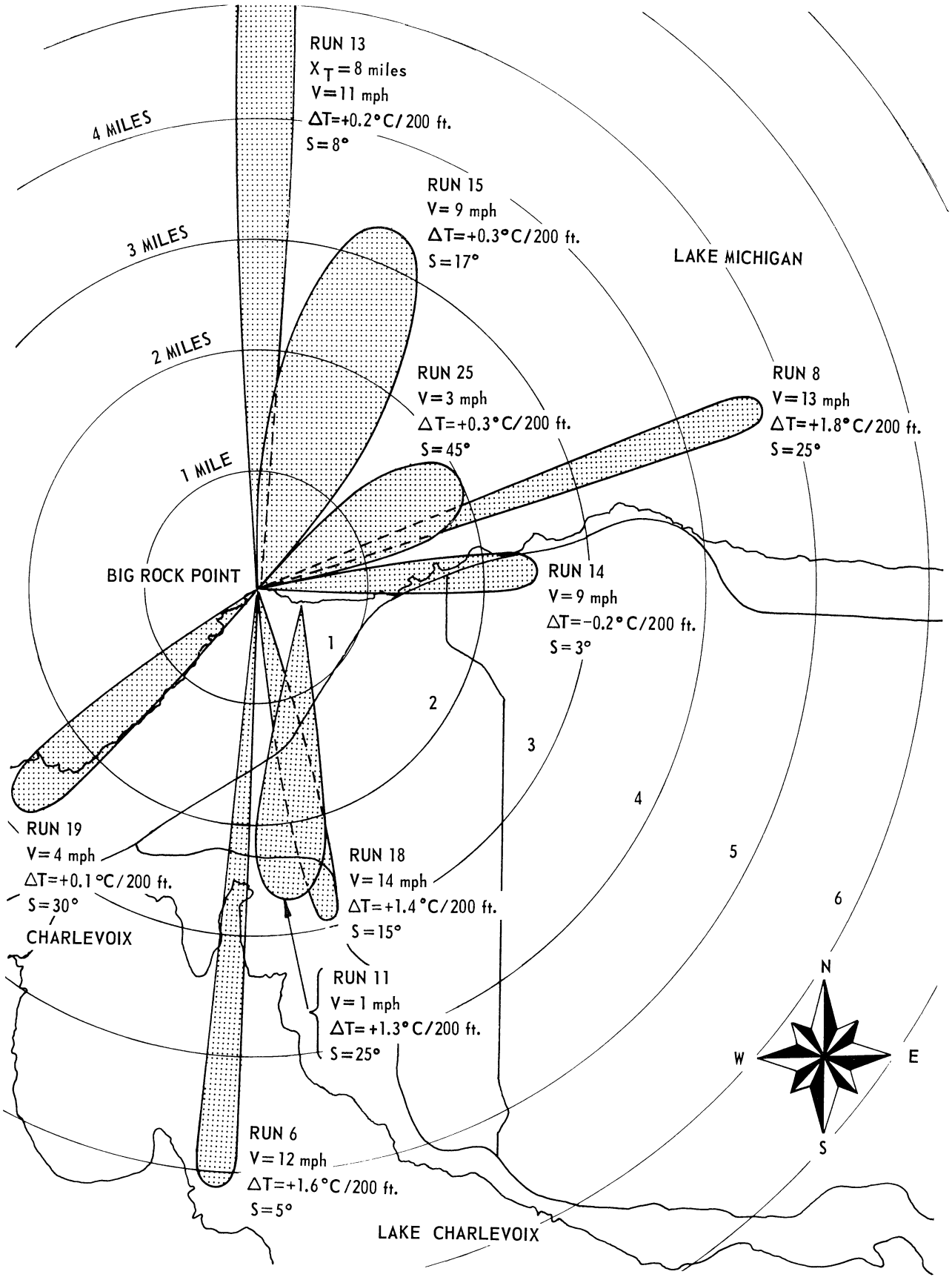

Figure 5. Smoke plume trajectories for stable (inversion) atmospheric conditions.

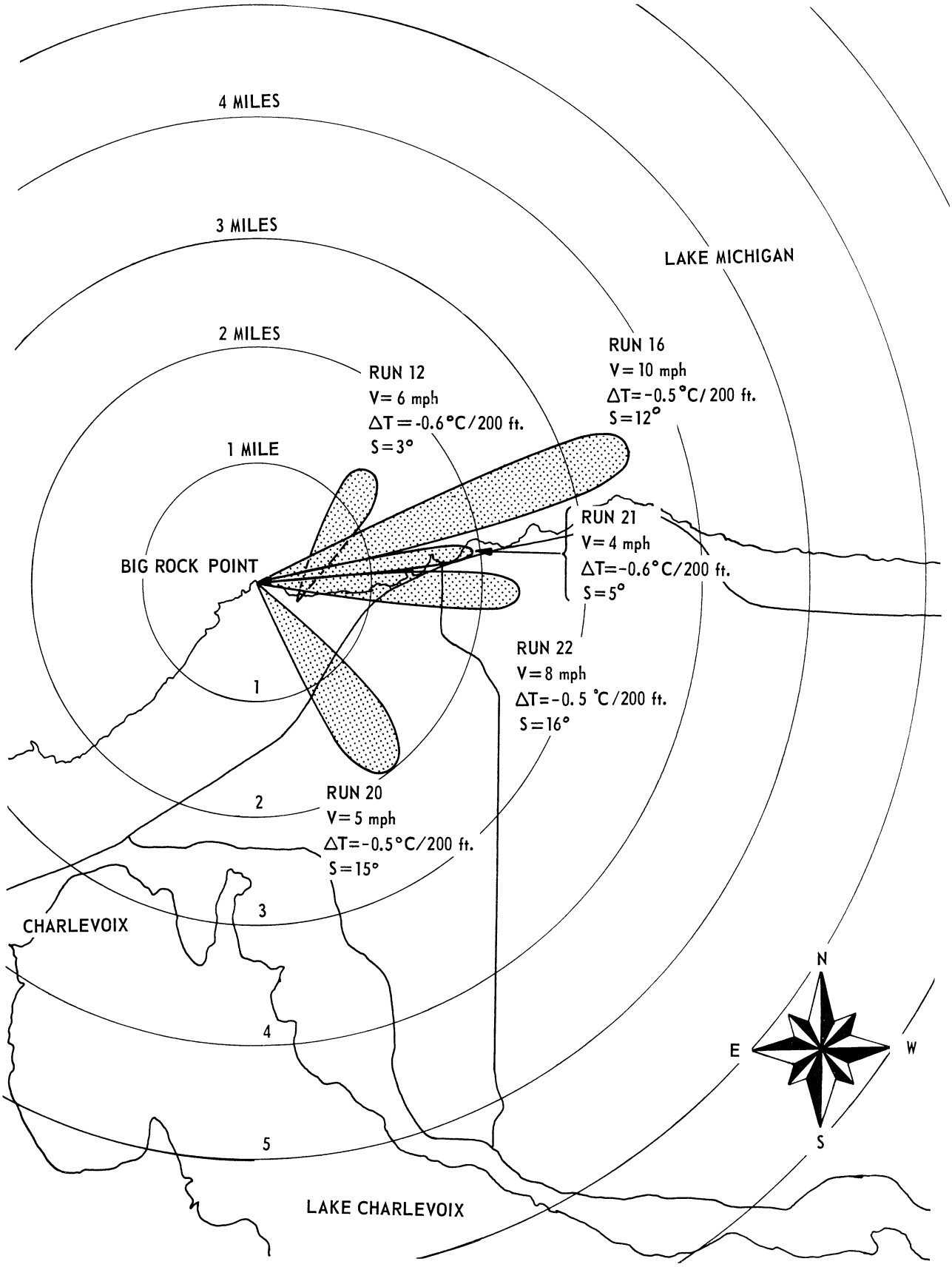

Figure 6. Smoke plume trajectories for near neutral (weak lapse) atmospheric conditions.

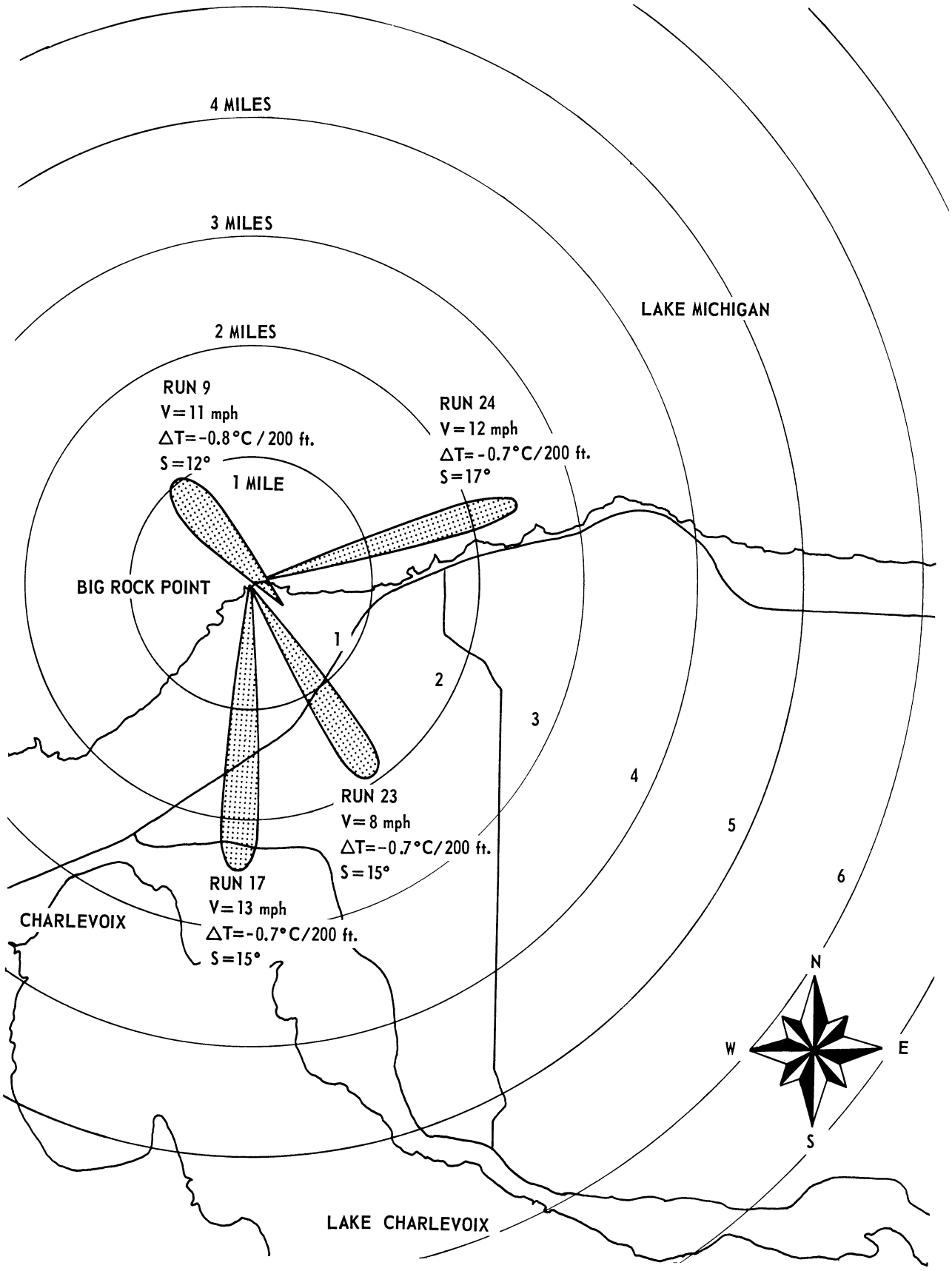

Figure 7. Smoke plume trajectories for slightly unstable (moderate lapse) atmospheric conditions.

(a)

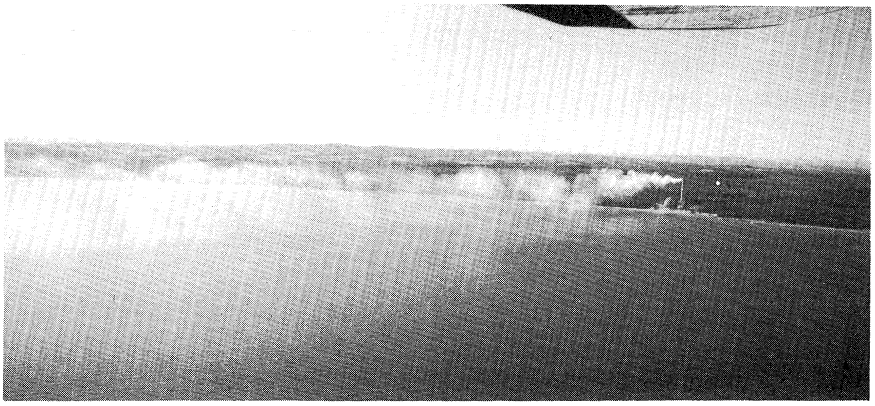

(b)

(c)

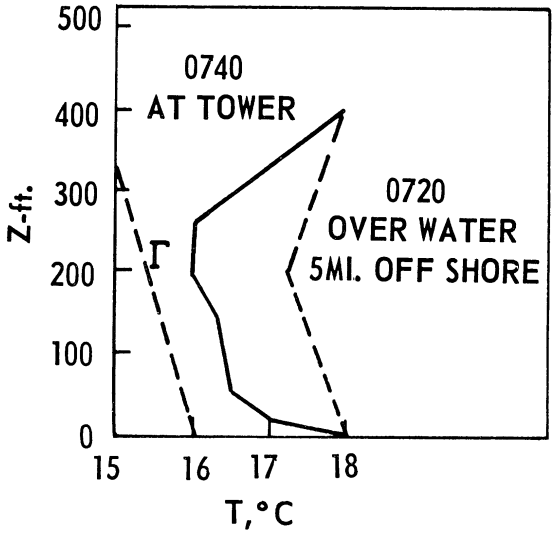

(d)

Figure 8: Representative Smoke Plume Photographs, Run 13.

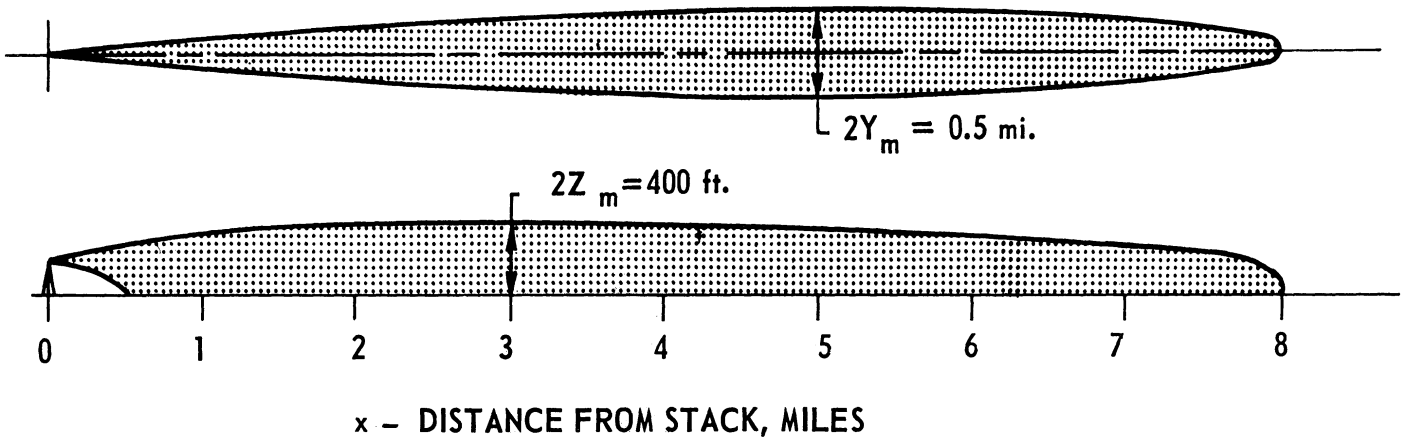

2. Stable Lapse Conditions

Run 13. Figure 8e shows horizontal and vertical contours of the visible plume as derived from photographs taken over a period of one hour. Figures 8a, 8b and 8c are representative photographs taken during this period.

This run is especially noteworthy because it produced the longest visible plume of the 1962 series. The temperature profiles over land and water are shown in Figure 8d. The photographs show the plume to be well mixed in the lower 200 feet of the atmosphere, as one would expect from a consideration of the temperature profile. The plume, in fact, appears to be completely trapped within the lower 400 feet. The lateral diffusion appears to be moderate. The unusually long plume can, then, be partially attributed to the inversion layer from 200 feet to 400 feet. Wind speed also has a great effect on visible plume length. In this case, the wind speed measured over land as 11 mph is, undoubtedly, less than over water because of the effect of surface roughness on wind speed profiles. The high wind speed, plume trapping and the smooth flow over water, then, may be said to account for the unusually long visible plume.

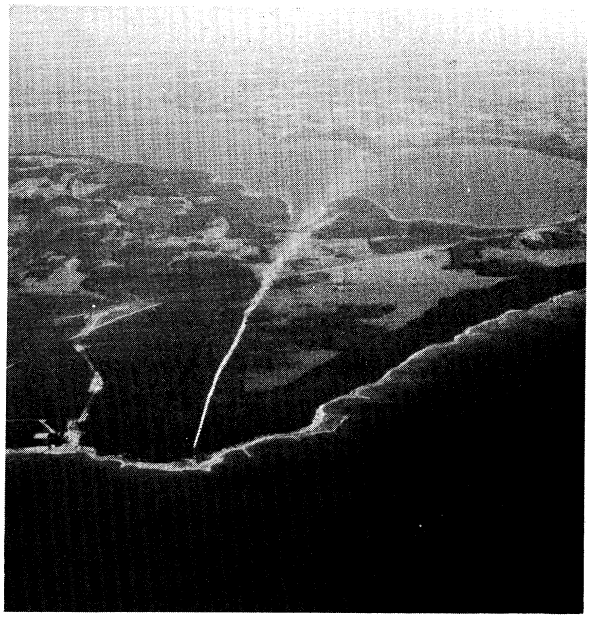

(a)

(b)

(c)

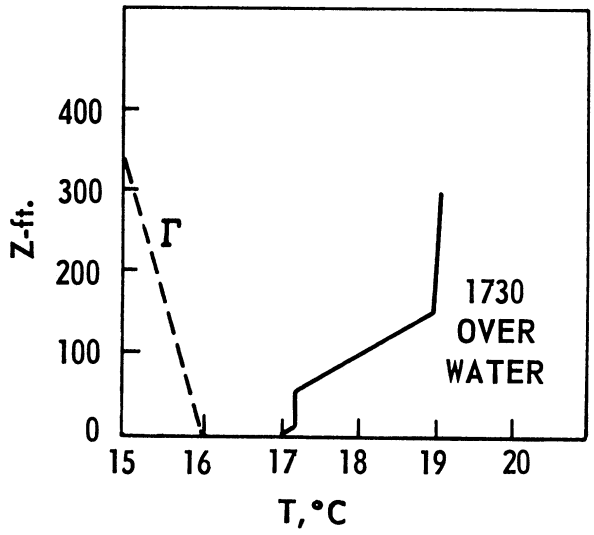

(d)

Figure 9: Representative Smoke Plume Photographs, Run 6.

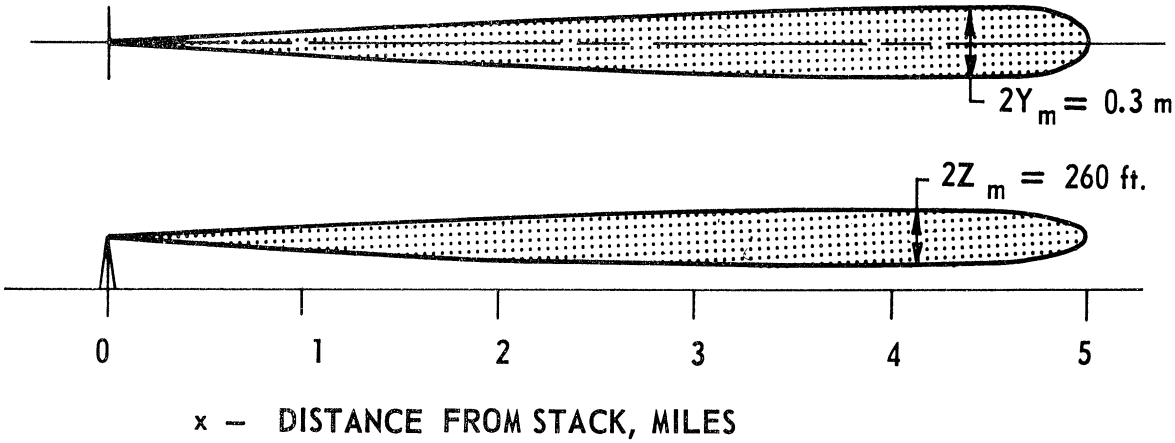

Run 6. The photographs (Figures 9 and 10) show the plume to be quite long, with little vertical or horizontal spreading. The temperature profile shows a fairly strong inversion in the layer from the ground up to 150 feet. From 150 feet up to an undetermined height, there appears to be a slight inversion. The wind speed was 12 mph. The initial slow vertical and horizontal spreading indicates that the inversion caused by the lower layers of air being cooled over the lake persists inland to about 1-1/2 miles. A study of Figure 10, which is a mosaic of the whole visible plume, shows that there are very few thermal eddies acting on the plume even though the time was late afternoon (1800) and the sky was clear. From this composite photo the fine structure of the turbulence acting on the plume can be readily seen. The structure of the visible smoke eddies strongly suggests mechanical turbulence only, acting on the plume. It is interesting to note that the turbulent sheath above the trees just extends up to the height of the plume at about 1-1/2 miles. Diffusion from this point on is considerably better than would be expected from the inversion present at the tower. Figures 9b and 9c showing the end of the visible plume indicate that the overland diffusion regime was established well within 4 miles of the shoreline.

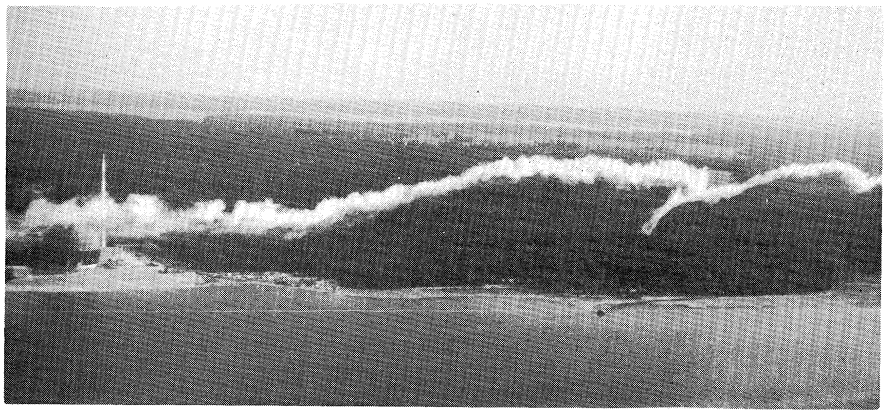

(a)

(b)

(c)

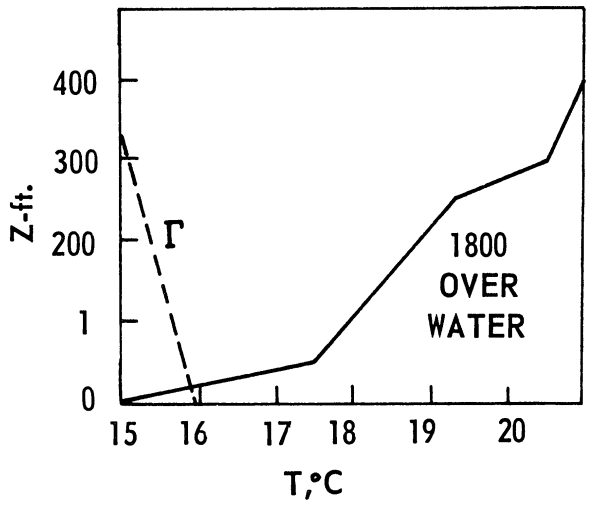

(d)

Figure 12: Representative Smoke Plume Photographs, Run 8.

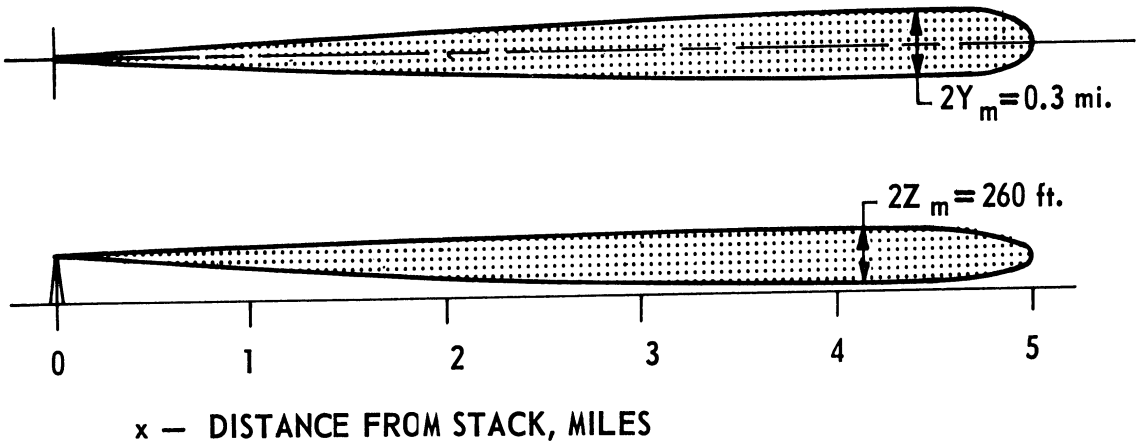

Run 8. Figures 11 and 12 are rather remarkable photos of a very narrow, long smoke plume. From the photos, it can be seen that, for the first 4 miles, the plume is extremely narrow. At about 4 miles, the plume suddenly begins to fan. The tower wind data show that there is a crosswind shear of 25° between the 256 and 128 foot levels on the tower, and that the wind speed was 13 mph. The former suggests an explanation for the sudden display of fanning. The rather strong inversion (as shown by the temperature profile Figure 12d) had inhibited the vertical diffusion of the plume. There was, however, some vertical diffusion and at about 4 miles the edge of the visible plume finally reached the layer which exhibited crosswind shear. Once in this layer, the plume rapidly diffused horizontally to give the appearance of the fanning plume. It is this fanning action which so enhanced the diffusion in the plume that its visible length was restricted to about 5 miles. (See Figure 12b which shows the end of the plume.) Considering the manner in which the plume diffused in the first 4 miles, the rather severe inversion, and the extremely smooth flow over water, one might expect a visible plume of much greater length.

Figure 11 is a composite photo showing the vertical development of the plume. At no time in this picture does the vertical extent of the plume appear to exceed 50 feet in depth. Especially noteworthy in this composite are the "scalloped" portions of the plume. This would suggest intermediate size eddies which do not reach up to the height of the plume. These eddies may be standing waves caused by the air flowing up over the land at the tower.

(a)

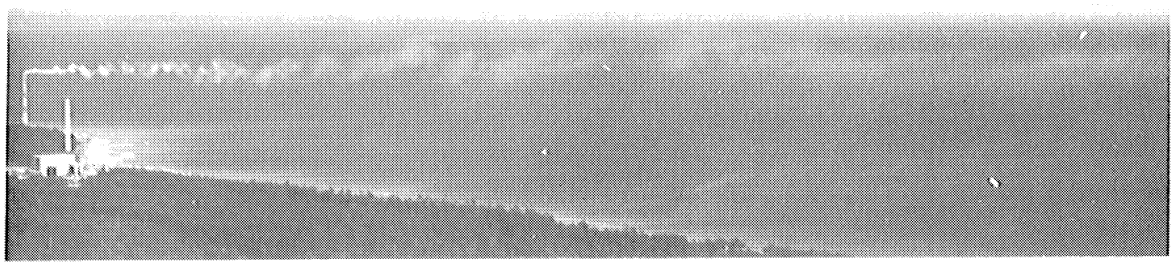

(b)

(c)

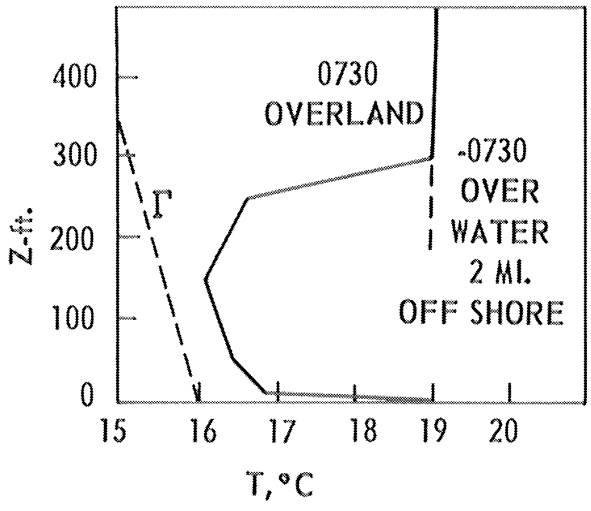

(d)

Figure 13: Representative Smoke Plume Photographs, Run 15.

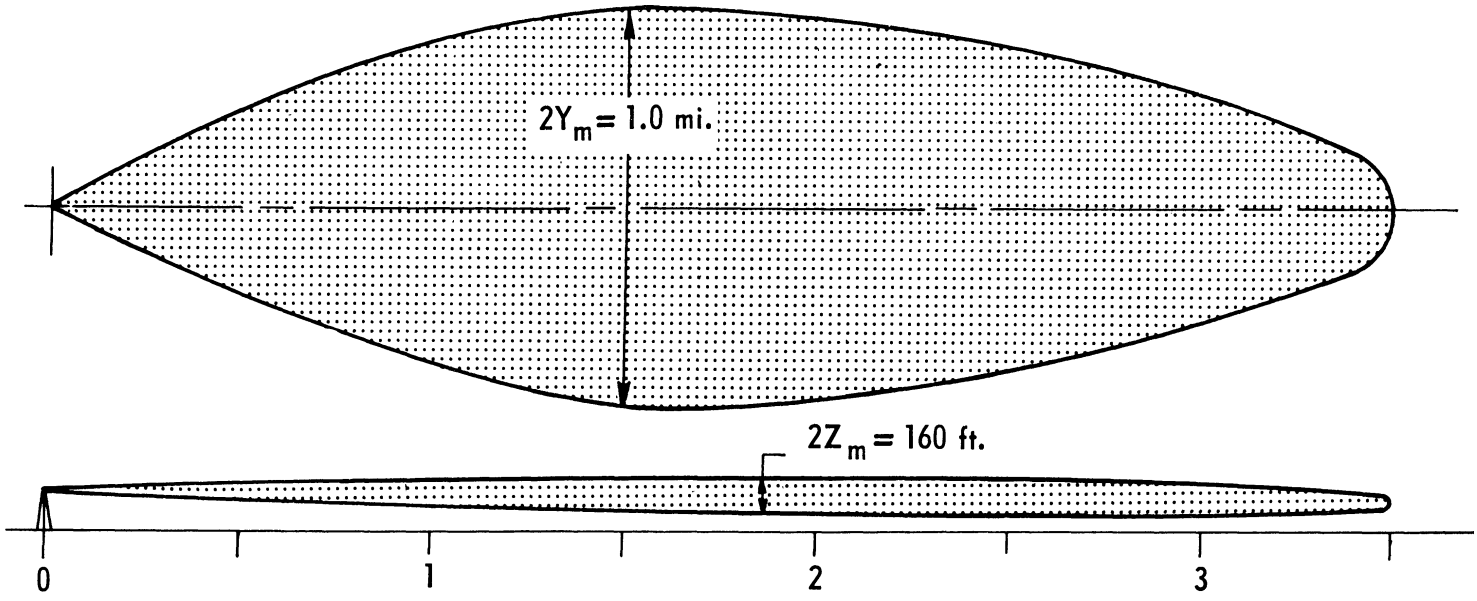

Run 15. Figures 13a and 13c show a wide, fanning plume. Tower data indicate a crosswind shear of about 20° in the layer between 256 and 128 feet, a wind speed of 9 mph, and good horizontal and vertical turbulence (see Table II). Figure 13b shows rather restricted diffusion in sharp contrast to the indication of good vertical turbulence at the tower. This lack of correlation suggests that, under inversion conditions (as indicated by the temperature profile), the mechanical turbulence generated over the trees is rapidly damped out as the plume heads out over the water. It is interesting to note that, just as in Run 8 (Figure 11), the vertical extent of the visible plume was quite shallow, yet marked fanning occurred. This suggests that the crosswind shear may be confined to a rather shallow layer of perhaps 50 feet or less.

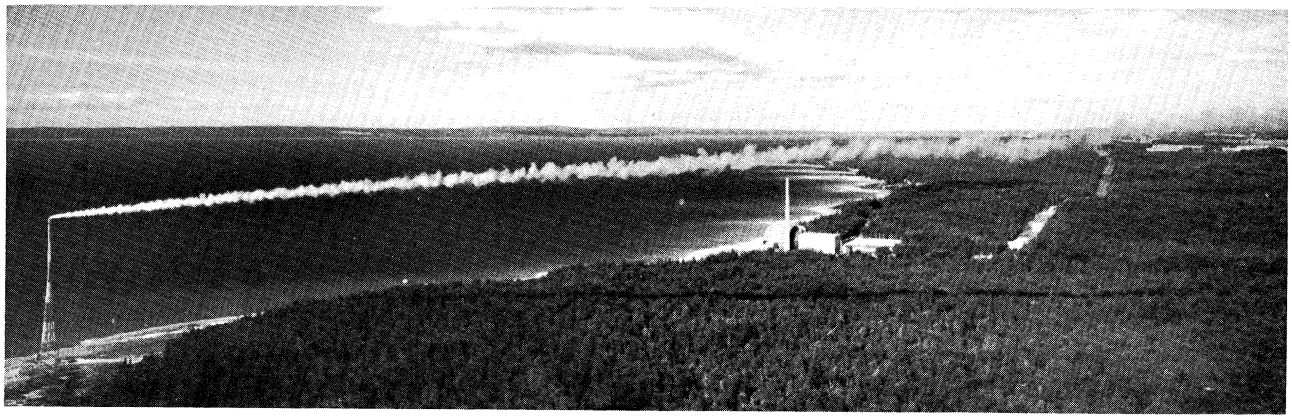

(a)

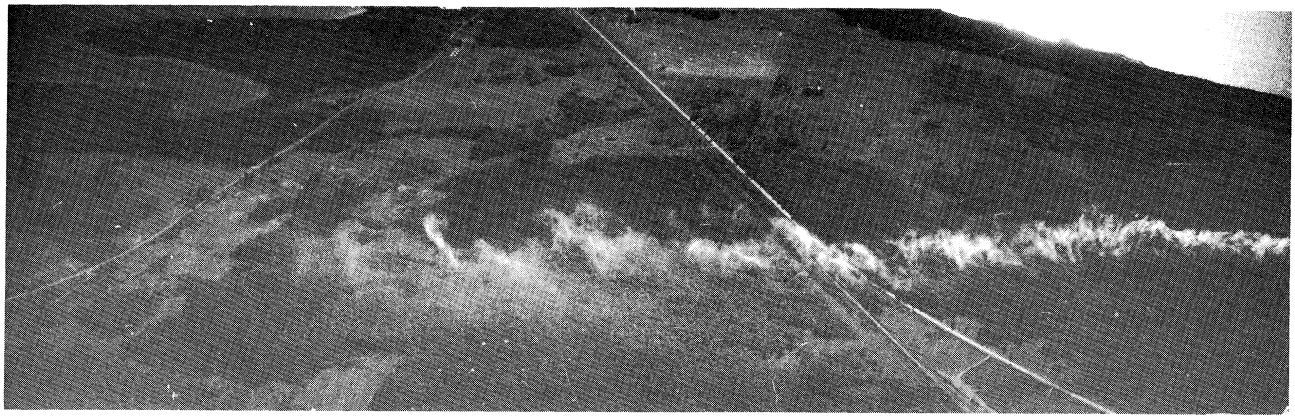

(b)

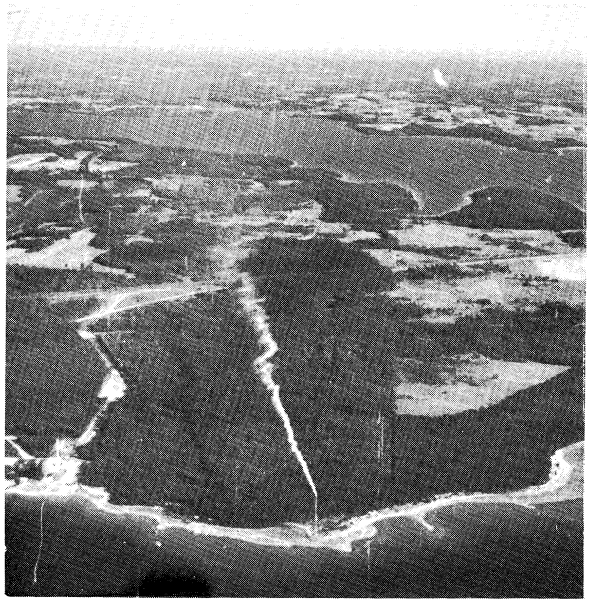

(c)

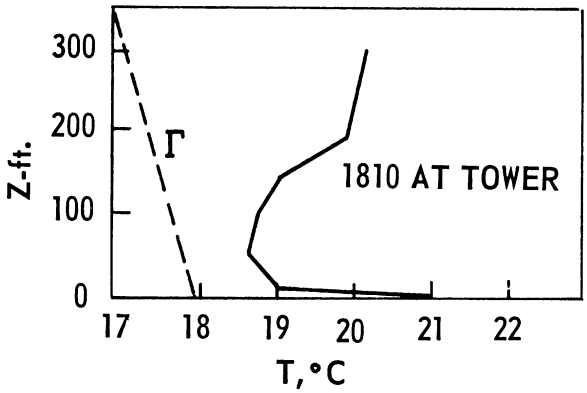

(d)

Figure 14: Representative Smoke Plume Photographs, Run 18.

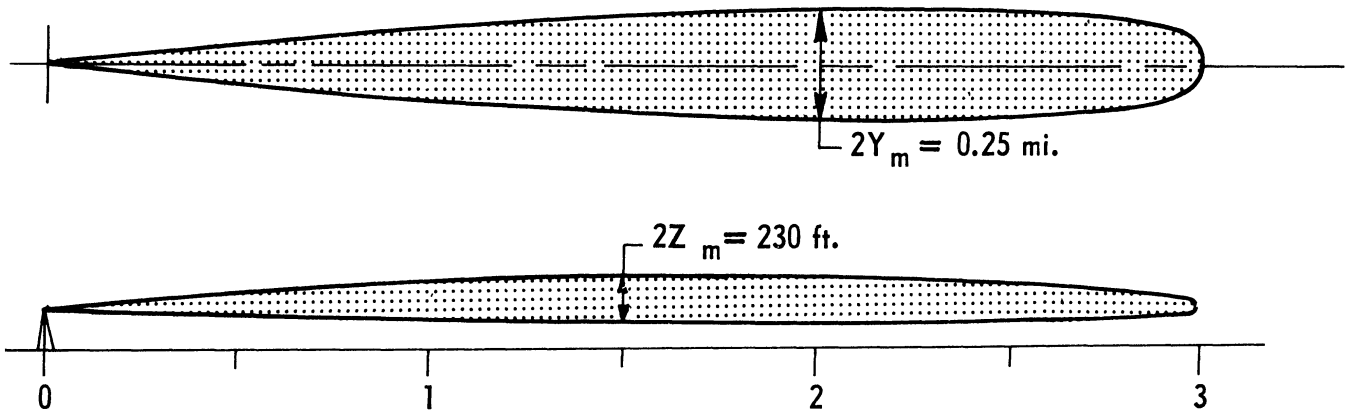

Run 18. The atmospheric conditions for Run 18 were almost exactly the same as for Run 6, with one significant difference. (See Table II.) The wind direction shear between the 256 and 128 foot levels on the tower was 15° for Run 18 and 5° for Run 6. A comparison of the photos for (compare Figure 9a to Figure 14c) the two runs provides an interesting opportunity to see the effects of crosswind shear on the diffusion of the smoke plume. The photos (compare Figure 9c to Figure 14b) show that the fine structure of the smoke eddies in each plume is quite similar. There are, however, striking differences in the widths and visible lengths of the plumes. For example, at 2 miles from the tower the Run 6 plume is 0.1 mile wide and the Run 18 plume is 0.25 mile wide. The Run 6 plume has a total visible length of about 5 miles, while the Run 18 plume has a visible length of about 3 miles. As far as the instruments and visual observation could determine, during both runs atmospheric conditions were very similar with the only significant variation being the difference in the crosswind shear. The difference in the lengths of the plumes suggests that shear increases diffusion thereby making the center line concentration in the plume fall off more rapidly and causing the plume to have a shorter visible length. Figure 14a shows the plume to have an elevated axis near the tower. This would suggest that the air is flowing up the aerodynamic hill created by the trees.

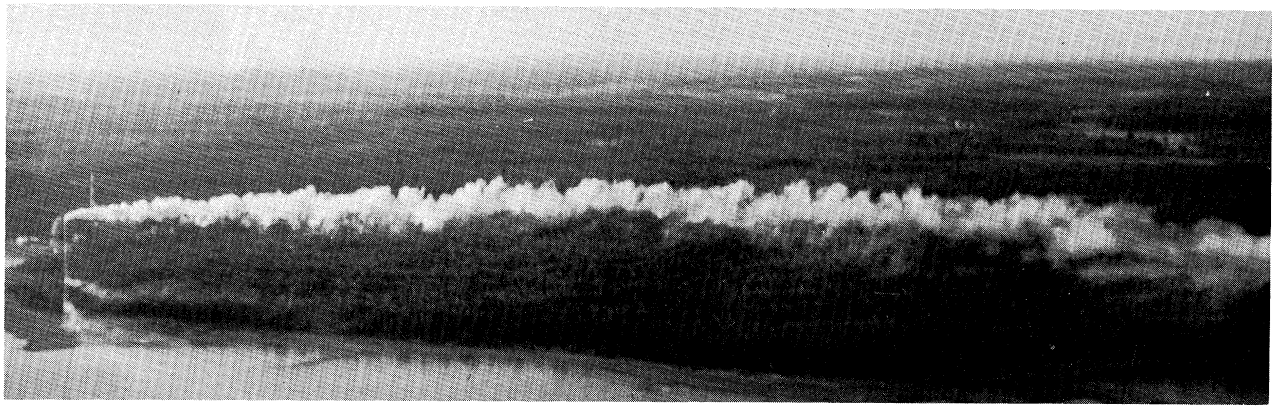

(a)

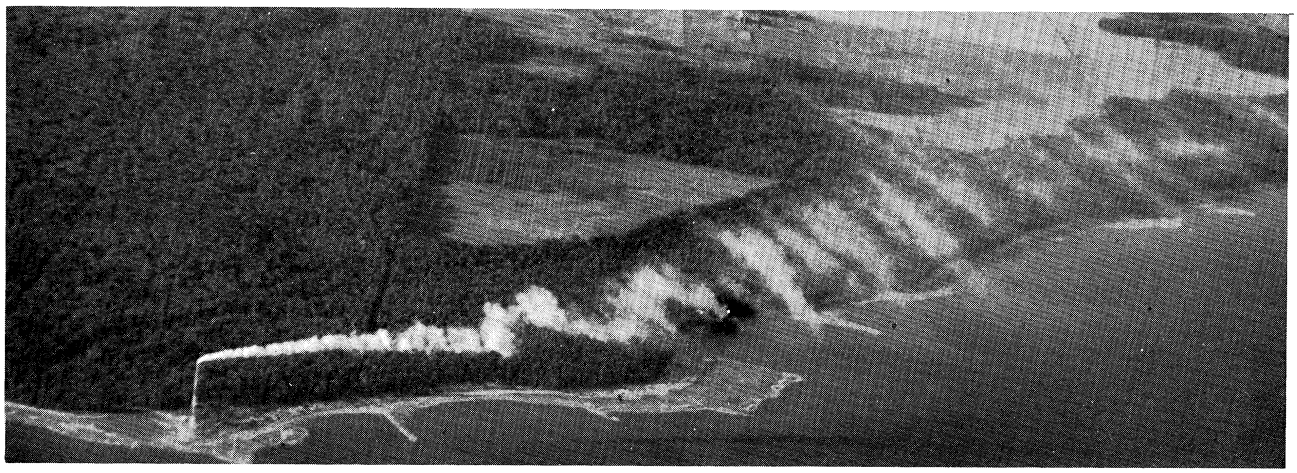

(b)

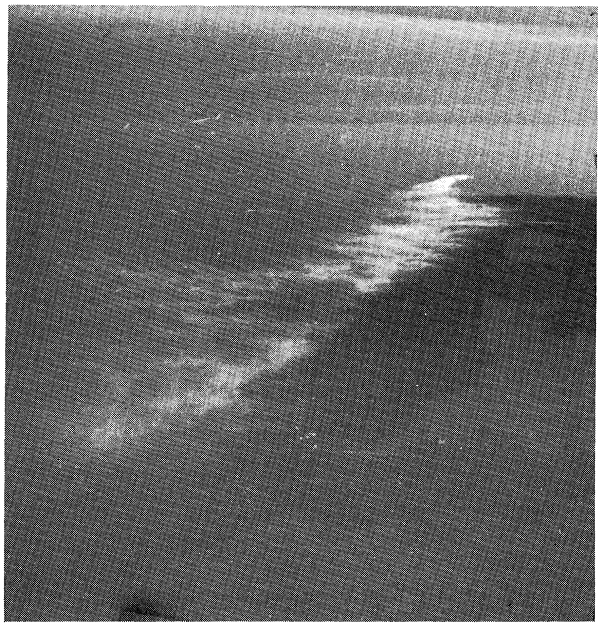

(c)

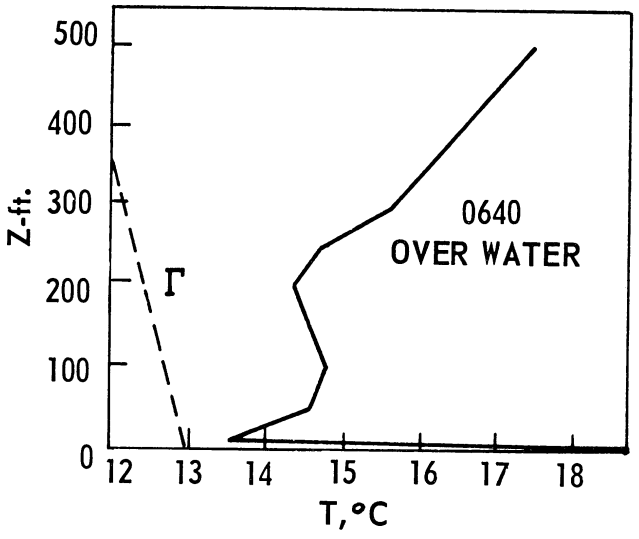

(d)

Figure 15: Representative Smoke Plume Photographs, Run 19.

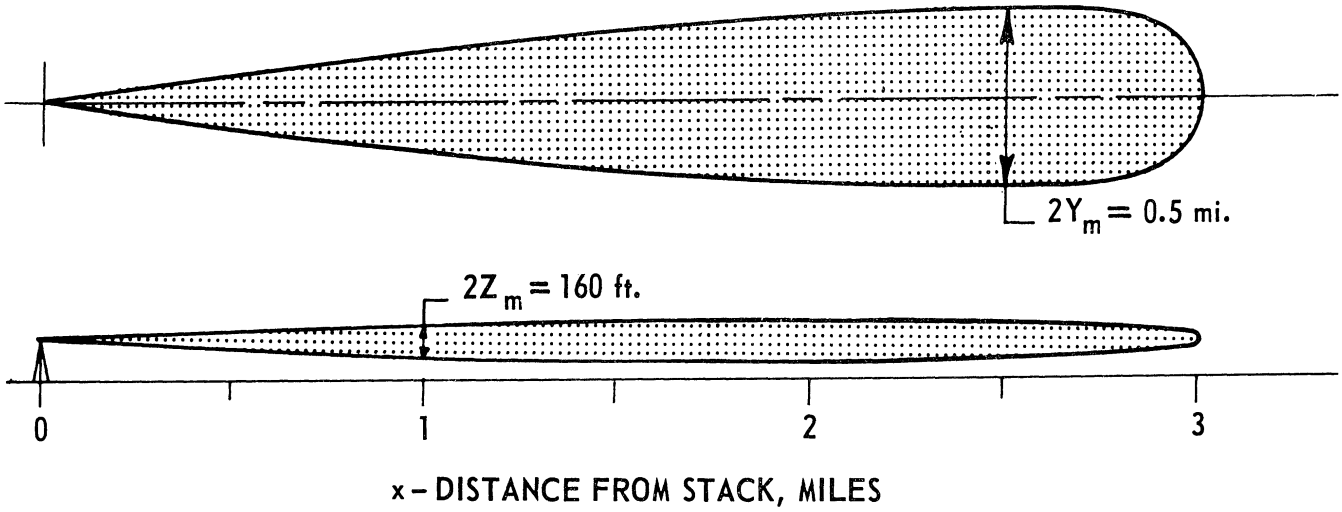

Run 19. Figures 15b and 15c again show the effects of crosswind shear on the characteristics of the visible plume. For the first quarter mile from the tower, the plume appears to be diffusing quite slowly. Then, there is an abrupt change in the diffusion characteristics. The plume begins to fan markedly. The tower data show a wind direction shear of 30° in the layer between 256 and 128 feet and a wind speed of 4 mph. The temperature profile (Figure 15d) indicates a rather strong inversion from 200 feet up; a slight lapse condition in the 100-200 foot layer; and an inversion from 100 feet down to near the water. The plume behavior can be readily explained by a consideration of the temperature profile. The smoke plume was released into stable air at the 256 foot level. The diffusion is slow because of the stability of the air and the very low wind speed (about 3 mph). The plume grows slowly and mostly in a downward direction. When the lower edge of the plume reaches the 200 foot level, vertical and horizontal diffusion increase markedly because of the slight lapse in the 100-200 foot layer. The horizontal diffusion is further enhanced by the crosswind shear which spreads the plume out. Under such calm conditions one would expect a much denser plume (hence higher concentrations) if there were no wind direction shear present. It should be noted in Figures 15b and 15c that the plume is channeled along the shoreline so as to follow each feature of the topography.

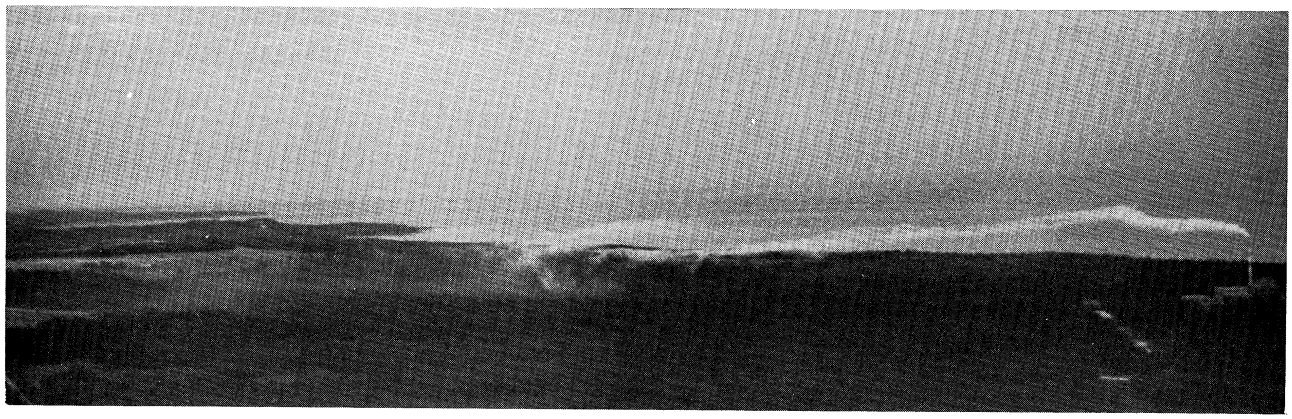

(a)

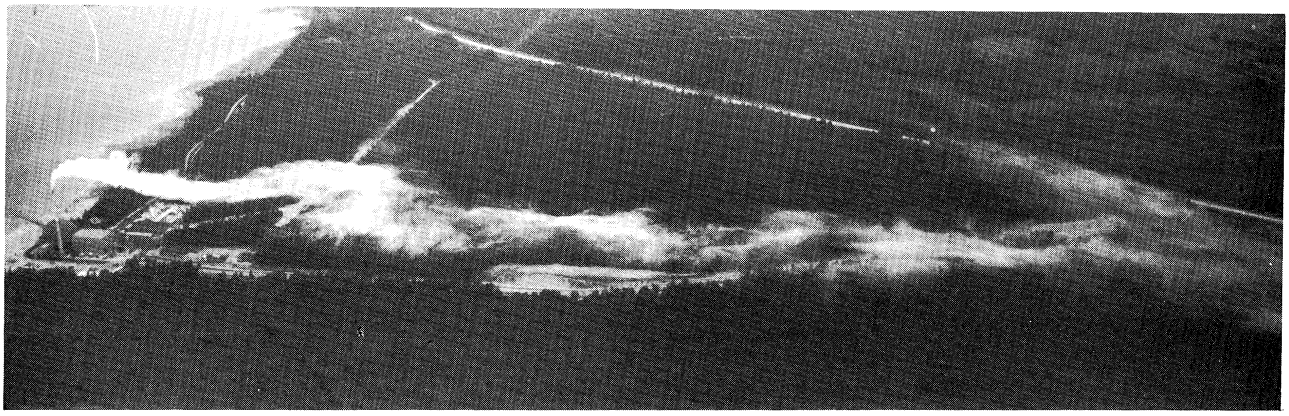

(b)

(c)

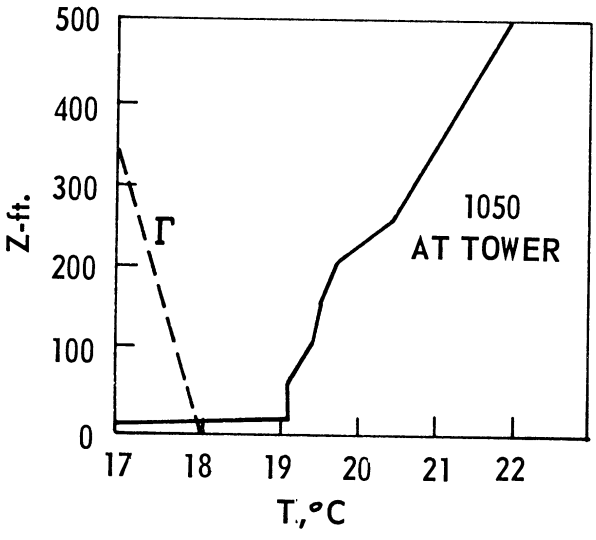

(d)

Figure 16: Representative Smoke Plume Photographs, Run 11.

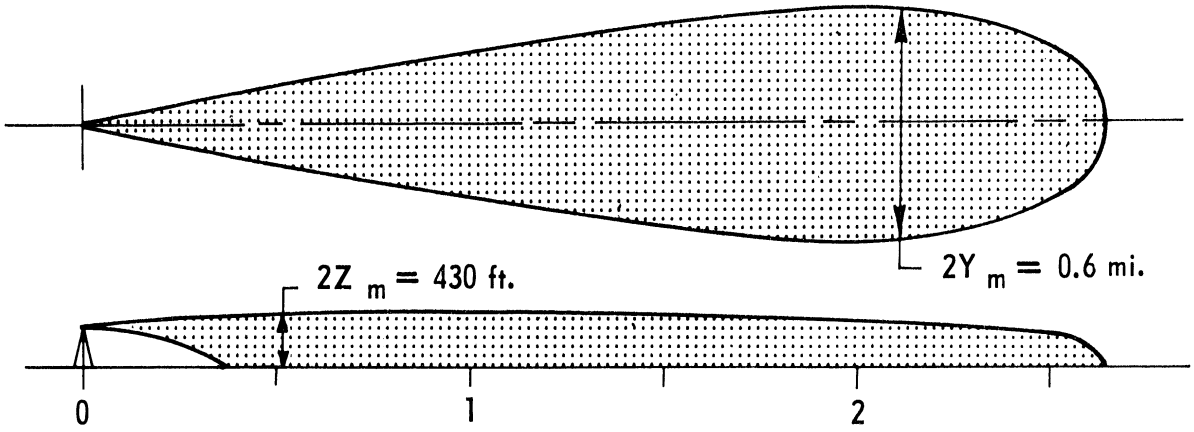

Run 11. During this run the smoke plume was released from the plant stack. A very unusual plume was produced. The temperature profile (Figure 16d) shows a fairly strong inversion at the tower. The wind was very light, about 1 mph and the day was overcast with some haze. Under these conditions one would expect very little vertical diffusion in the plume. However, Figure 16a shows unmistakable signs of three distinct vertical diffusion regimes. Close to the stack, the plume is coning in a fashion typical of a stable atmosphere with a low wind speed. Next, there appears a region in which there is very little vertical diffusion. After about a half-mile, the plume shows considerable vertical diffusion. A study of Figures 16a, 16b and 16c suggests that the first regime would be typical of diffusion over the water. The second regime would be a transition diffusion regime which has been seen frequently in the smoke plume runs. Here it is compressed into a space of less than one-half mile because of the very low wind speed. The third regime is the normal overland diffusion regime. The photographic evidence from this run shows the rapid transition from a very slowly diffusing regime, to a rather rapidly diffusing regime even under quite stable atmospheric conditions with a very light wind.

(a)

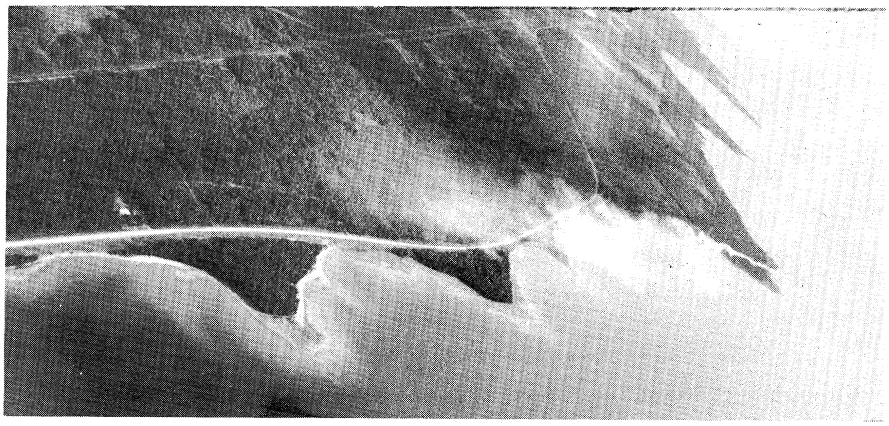

(b)

(c)

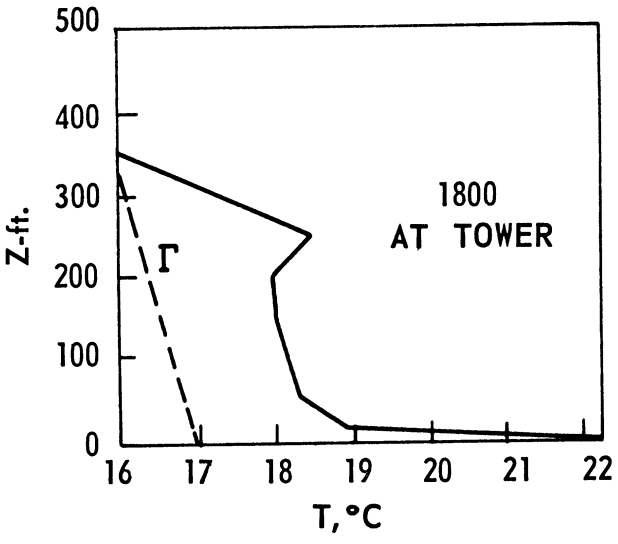

(d)

Figure 17: Representative Smoke Plume Photographs, Run 14.

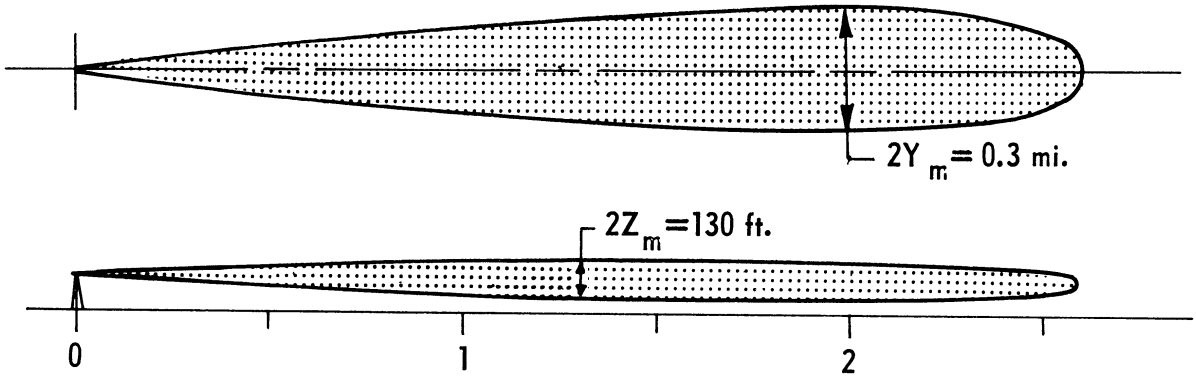

Run 14. The temperature profile for this run indicates a fairly strong inversion in a layer from 200 feet up past the 256 foot level of the tower to an undetermined height; a slight lapse down to about 50 feet; and a strong lapse from 50 feet to the water's surface. The water temperature near the tower is recorded as 21.7° C on this day, whereas for the period preceding this day and following it, the water temperature recorded was near 18° C. It appears that the steady westerly wind with fair weather had piled warm water up near the shore in Little Traverse Bay and that the 18° C temperature would be more representative of the lake surface farther from shore.

The plume was discharged into a stable layer with a wind speed of 9 mph and initially diffused rather slowly; see Figure 17a. At about 1/4 to 1/2 mile from the tower, the plume appears to be rapidly dispersed by intermediate size eddies suggestive of thermal convection. This phenomenon could be explained by considering the temperature and trajectory of the air passing the tower. The air passed over Lake Michigan and the lower layers were cooled to approximately the temperature of the lake surface, probably around 18° C. As the air approached Big Rock Point from the west it began to be heated by the warmer, shallow water close to shore. By the time the air was from 1/4 to 1/2 mile from the tower, the heated, lower air was quite unstable and hence any turbulence generated at the surface would be amplified and cause the plume to diffuse quite rapidly. Again note that in Figure 17c the plume appears to be channeled along the shoreline.

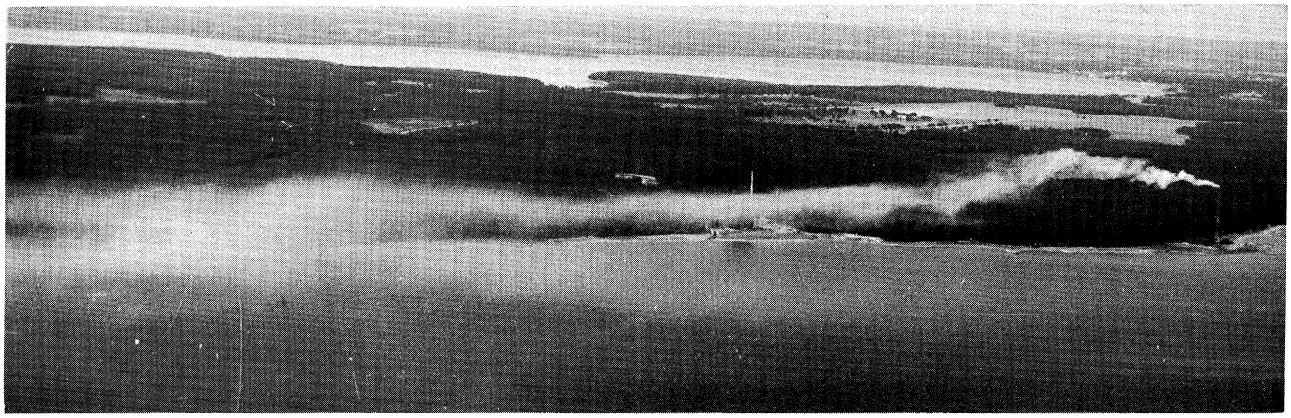

(a)

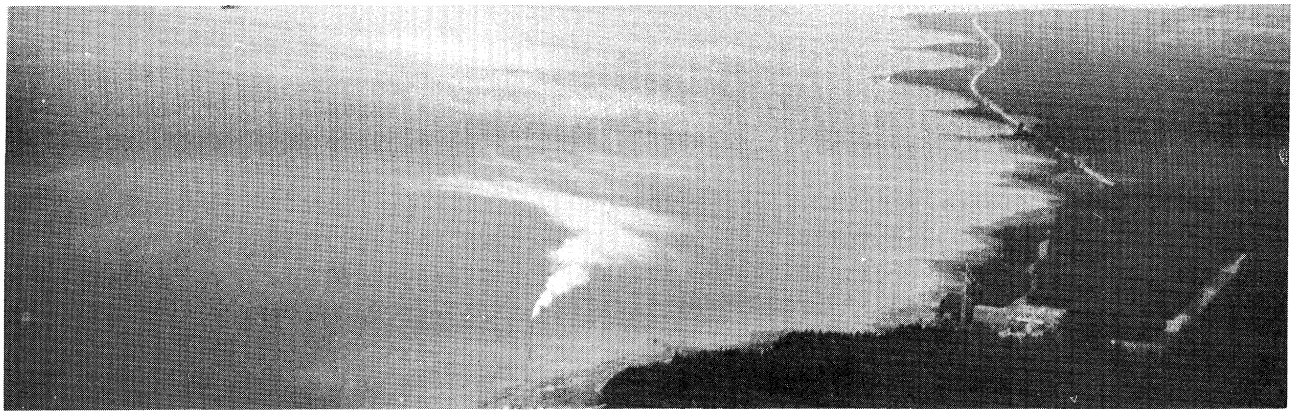

(b)

(c)

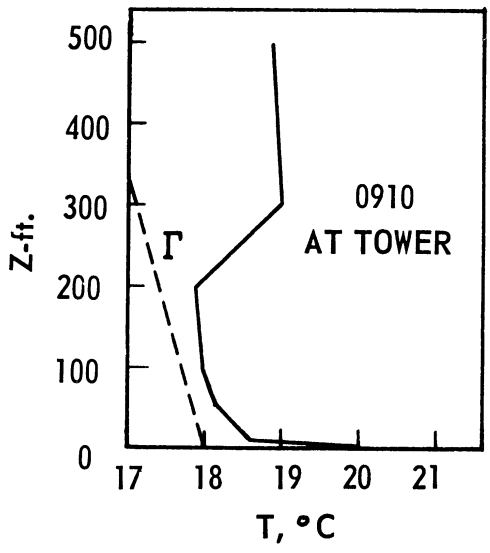

(d)

Figure 18: Representative Smoke Plume Photographs, Run 25.

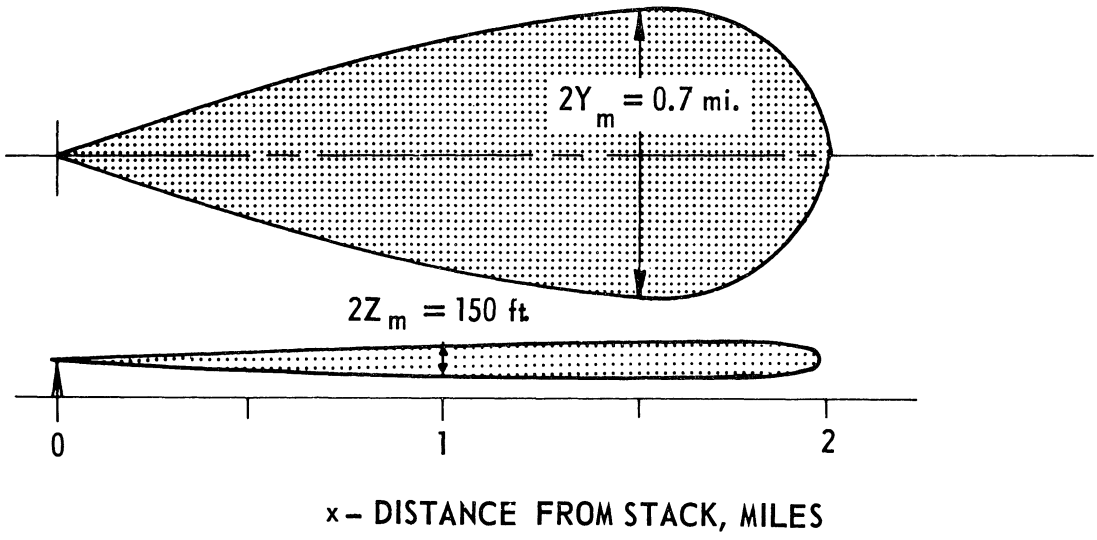

Run 25. This run exhibited the most marked case of wind direction shear of the summer 1962 series. The wind direction shear between the 256 and 128 foot levels on the tower was 45°. Figures 18a, 18b and 18c show the effects of the shear on the plume contours. The effect of the shear is so great that the plume becomes quite disjointed within one half mile and has a visible length of only 2 miles. There is some evidence of plume meander, but the quick dispersion of the plume by shear indicates that this was not the major diffusing factor. The wind speed for this run was quite low, about 3 mph. This is quite important because of the very unstable air layer close to the water. A higher wind speed would have created turbulence at the surface which would have readily reached the plume to disperse it.

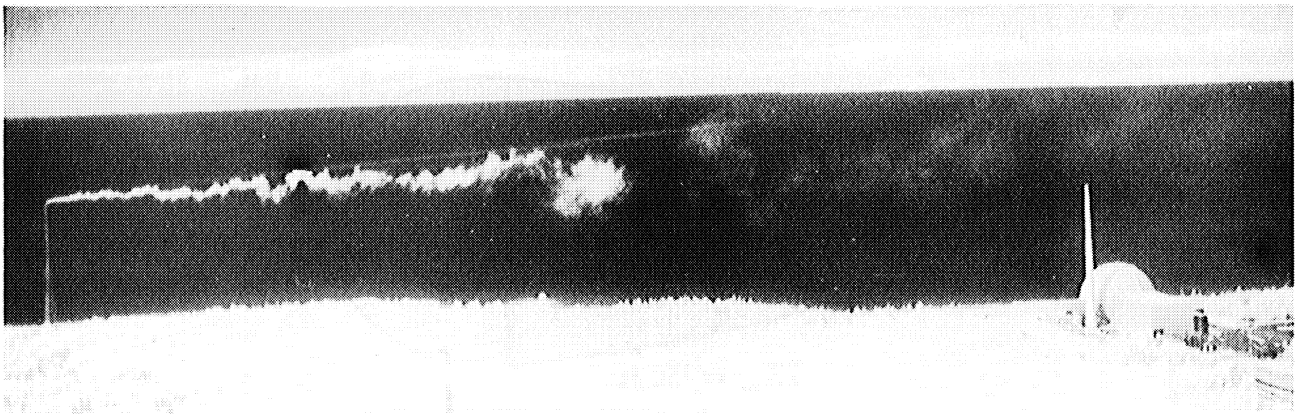

(a)

(b)

(c)

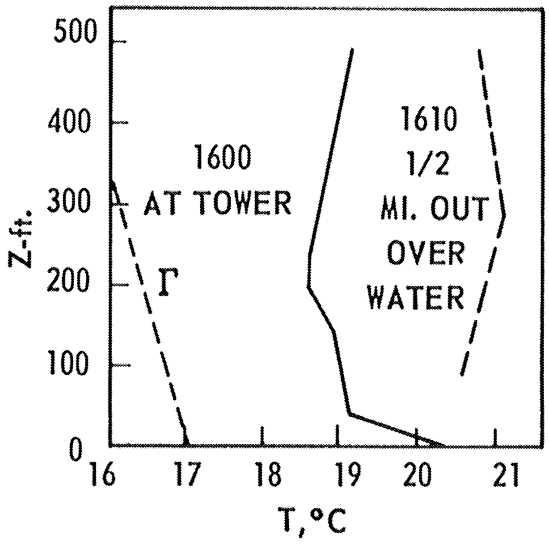

(d)

Figure 19: Representative Smoke Plume Photographs, Run 16.

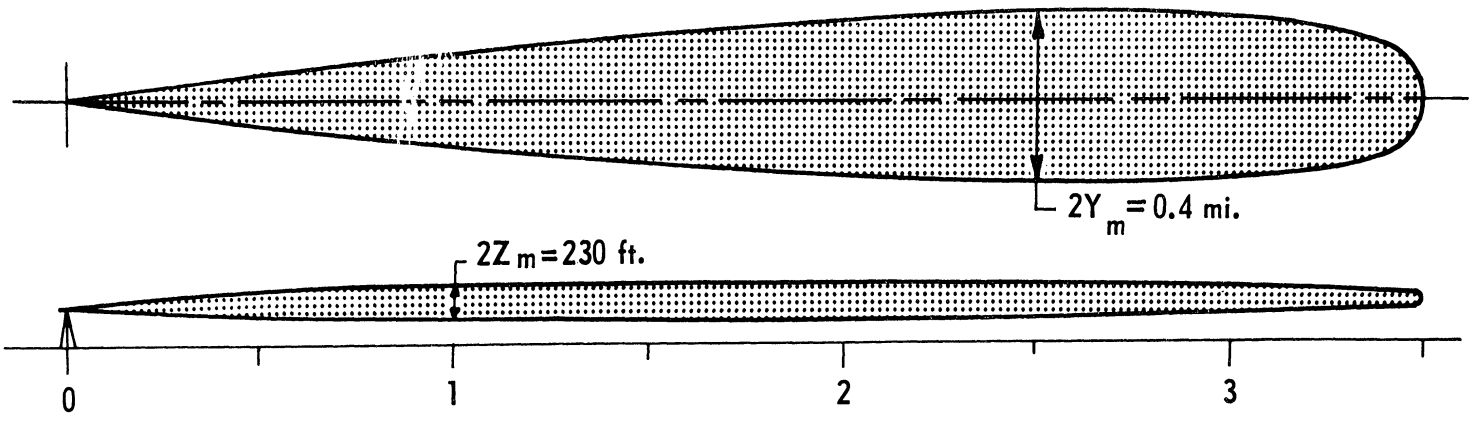

3. Near Neutral Lapse Conditions

Run 16. The wind speed was 10 mph. The temperature profile at the tower shows a near neutral lapse condition from 200 feet down to about 50 feet. The temperature profile overwater shows a slight inversion below about 300 feet and a slight lapse condition above about 300 feet. Figure 19 shows the effects of these two profiles on the visible plume. Close to the tower the diffusion appears to be moderately rapid. As the plume reaches farther over the water, the diffusion appears to be diminished somewhat. This dimunition of diffusion may be explained by noting the transition in the atmosphere from a near neutral to a slight inversion condition over the water. The result is a longer visible plume than would normally be expected for diffusion under near neutral lapse conditions. Figure 19a shows evidence of vertical turbulence reaching the plume about a quarter of a mile from the tower. Considering the unstable air layer in the lower levels, it appears that the mechanical turbulence generated by the rough surface at the tower is the cause of the enhanced vertical diffusion.

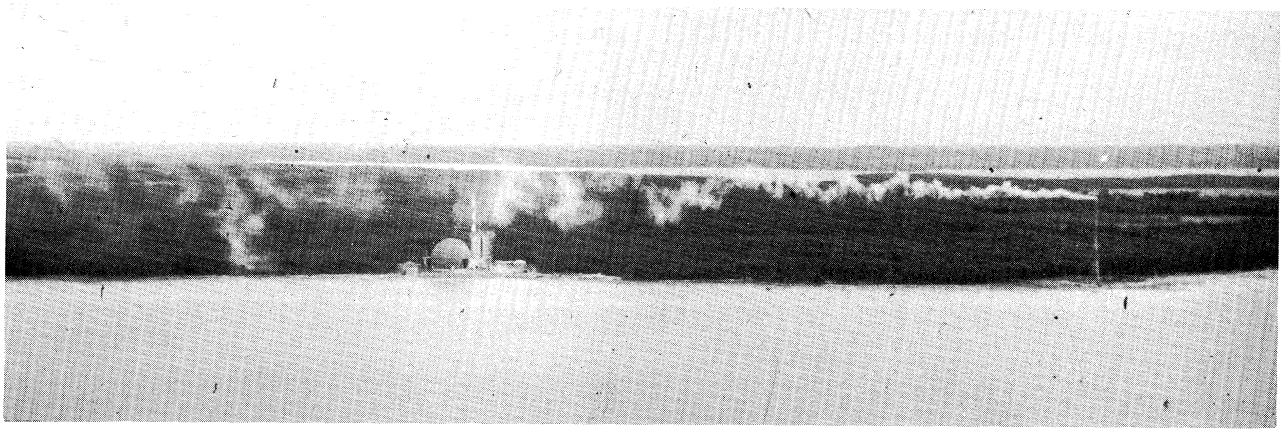

(a)

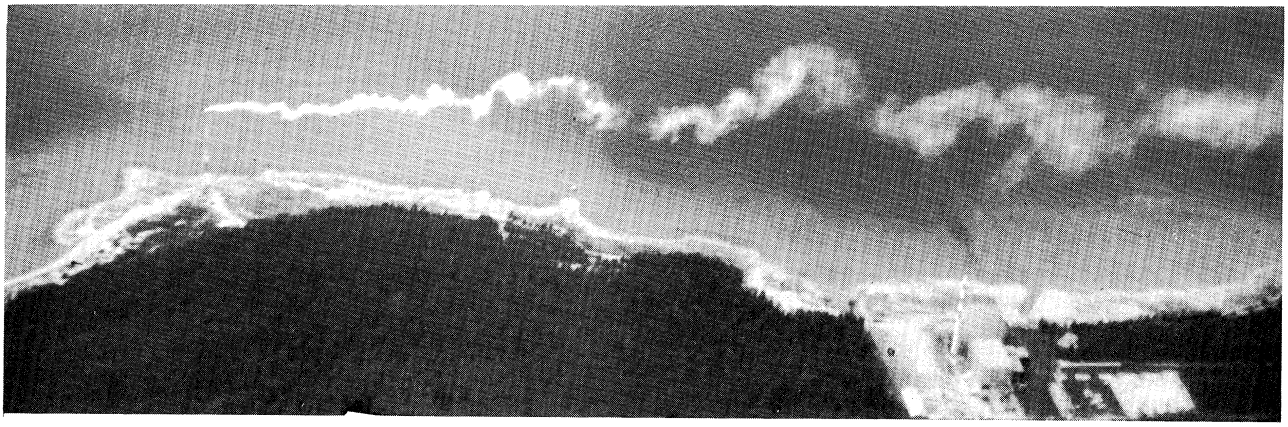

(b)

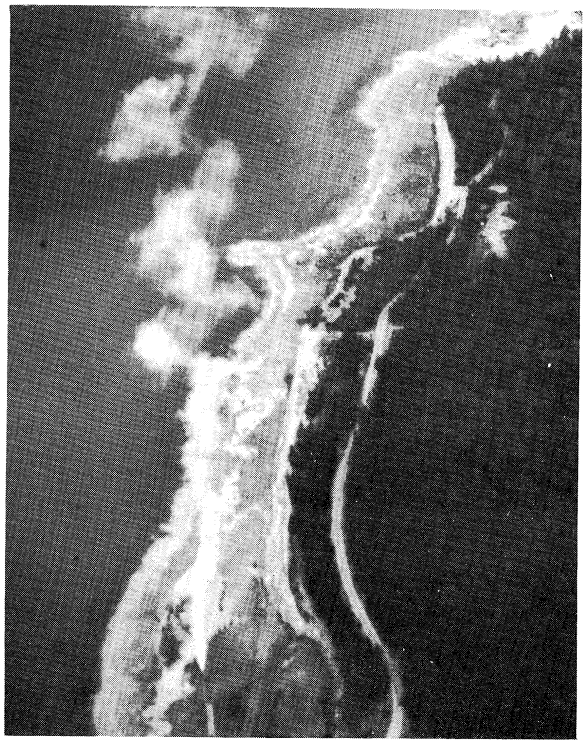

(c)

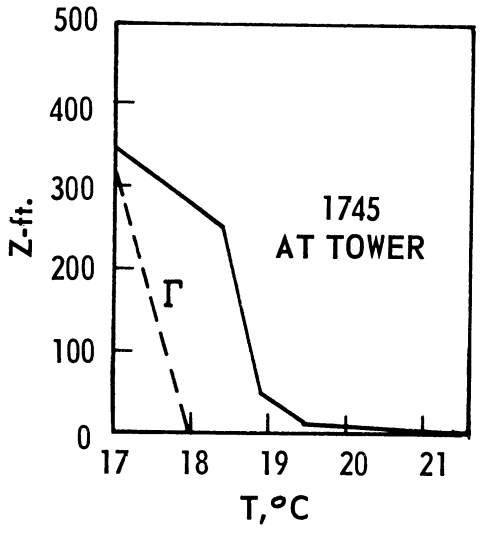

(d)

Figure 20: Representative Smoke Plume Photographs, Run 22.

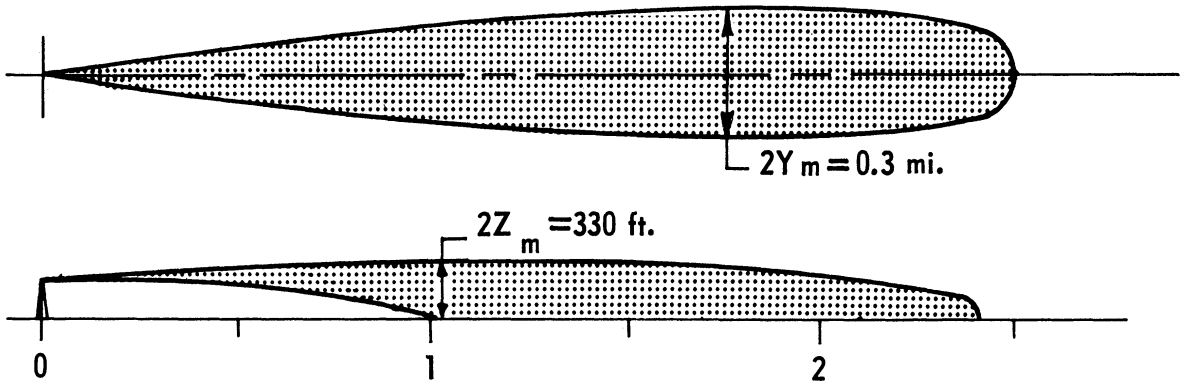

Run 22. The day was overcast; the wind speed was 8 mph. The temperature profile indicates a fairly unstable lapse condition above 256 feet; a slight lapse (near neutral) condition between 256 feet and 50 feet; and a very unstable lapse condition below 50 feet. Figure 20 indicates rapid diffusion of the plume. These photos show a plume which appears to be looping somewhat, a condition not to be expected with smooth flow over the water and near neutral lapse conditions in the layer between 256 and 50 feet. This behavior may be explained by noting that the air over the water was heated from below thus creating an unstable system, even though the sun was not shining. The visible plume, therefore, was dissipated quite rapidly. This again points out the effect of the water at the shoreline and in Little Traverse Bay being warmer than the air itself.

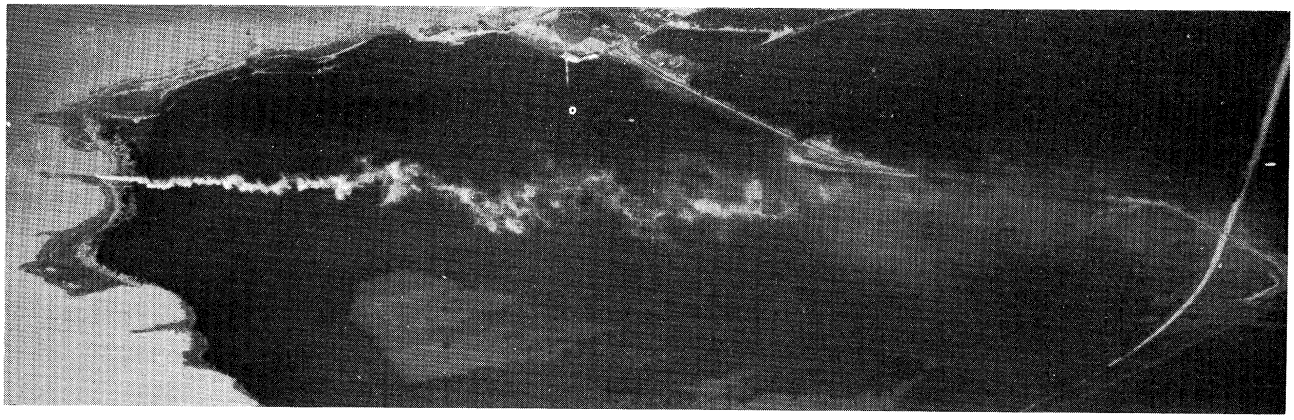

(a)

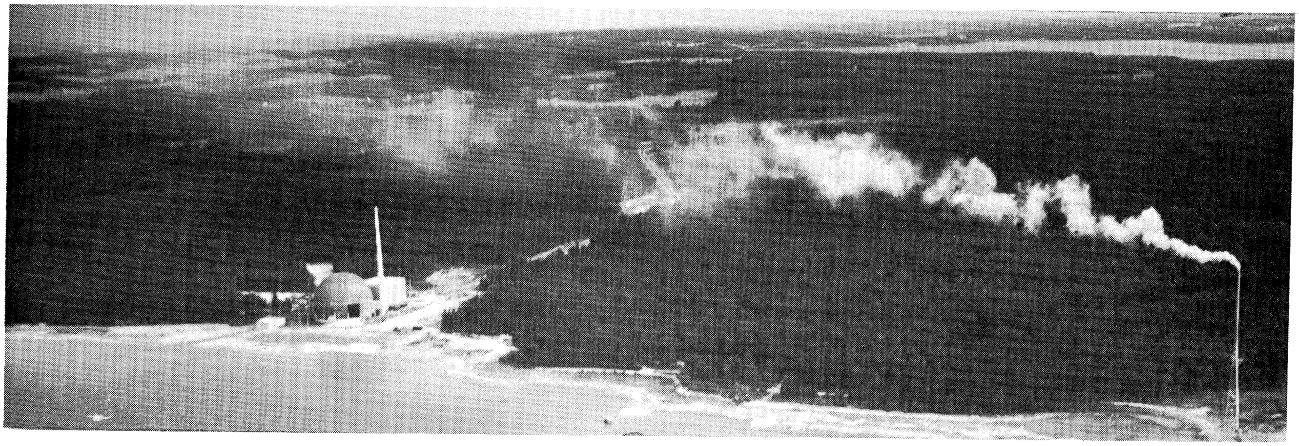

(b)

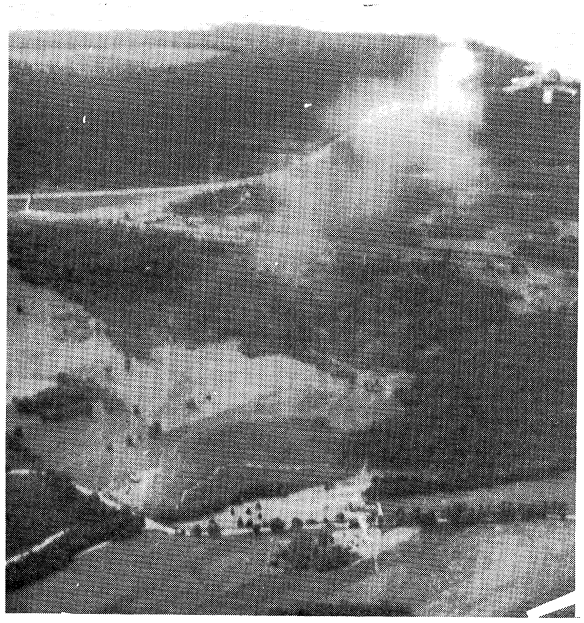

(c)

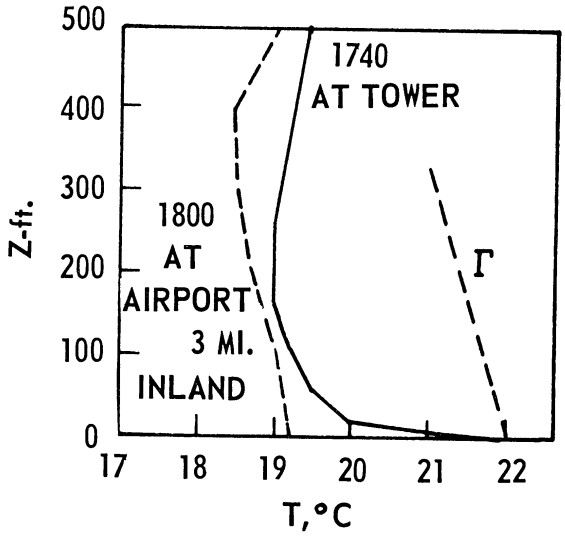

(d)

Figure 21: Representative Smoke Plume Photographs, Run 20.

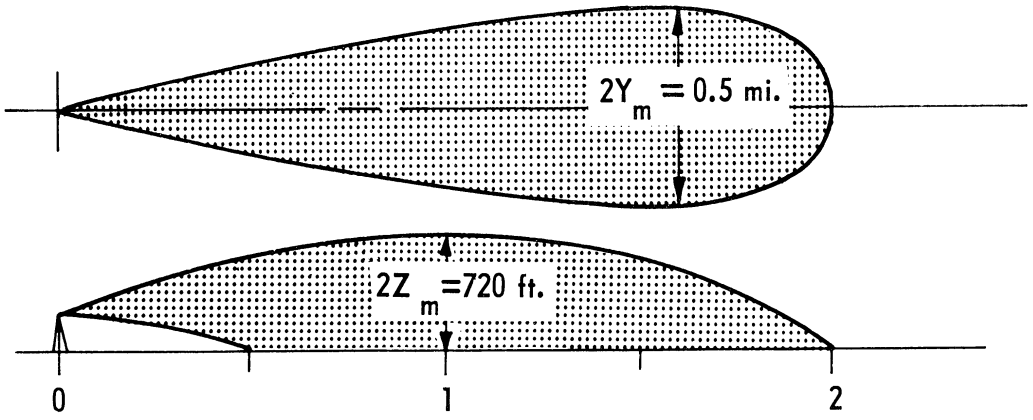

x DISTANCE FROM STACK, MILES

Run 20. The day was completely overcast, the wind speed 5 mph and the temperature profile shows a neutral atmosphere overland. Over the water, the temperature profile shows a lapse condition below 150 feet; an isothermal layer from 150 to 256 feet; and a slight inversion above 256 feet. Figures 21a, 21b and 21c show evidence of good horizontal-vertical mixing. The maximum plume height was noted to be 650 feet at about 0.8 mile from the tower; see Figure 21b. The good vertical diffusion appears to be a result of the convection created over the lake by the heating of the lower layers of air by the warm lake water. It appears that this convective turbulence persists at least two miles inland.

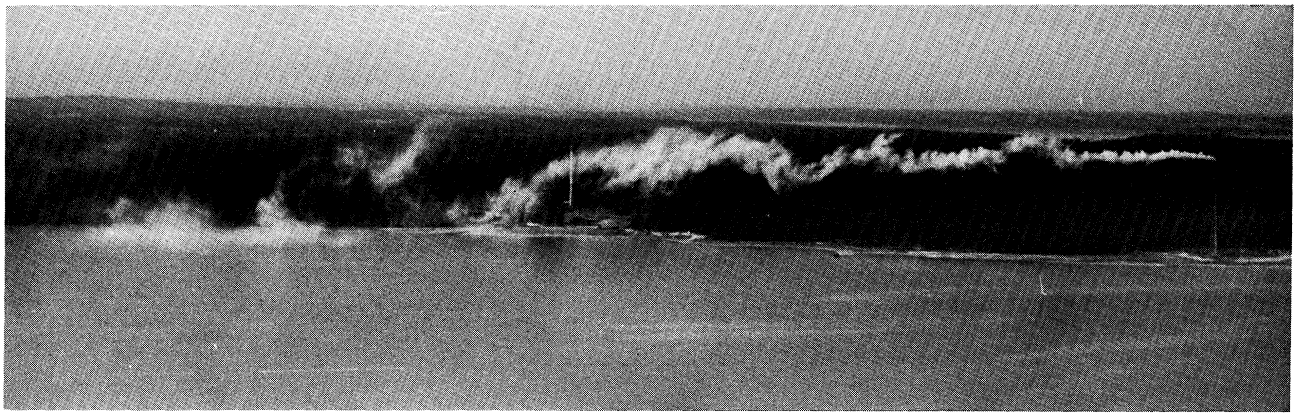

(a)

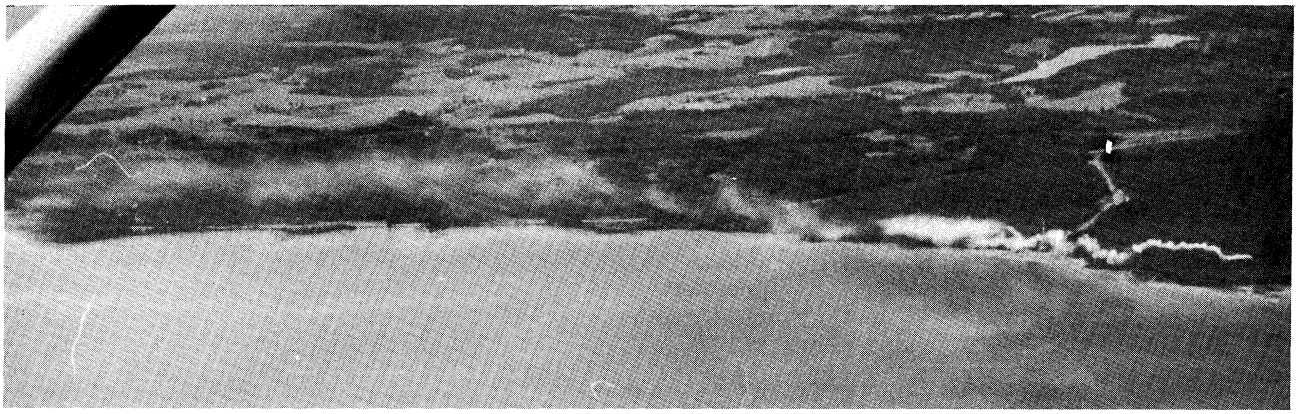

(b)

(c)

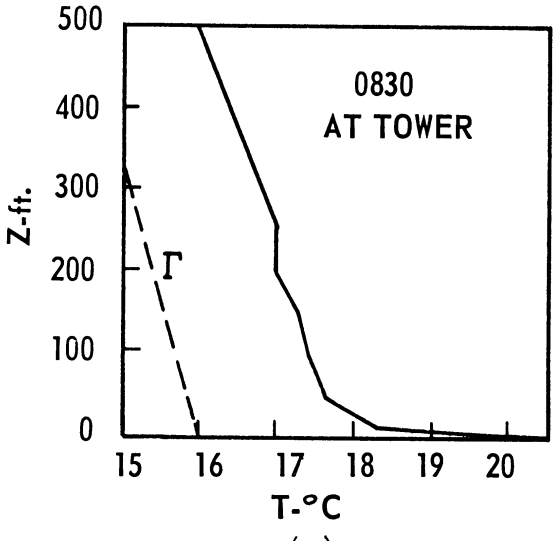

(d)

Run 22: Representative Smoke Plume Photographs, Run 21.

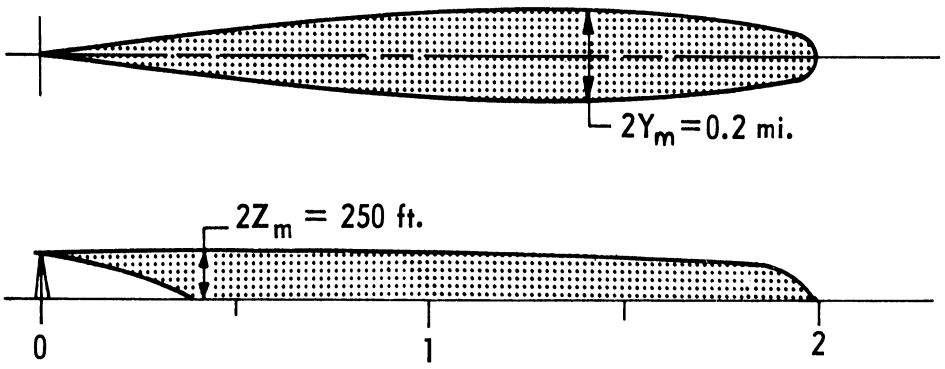

Run 21. The morning was hazy and overcast, the wind speed 4 mph. The temperature profile shows a strong lapse in the lowest 50 feet, a neutral condition from 50 to 256 feet and a fairly strong lapse above 256 feet. The plume appears to be trapped in the lowest 250 feet of the atmosphere. See Figure 22a. The shape of the visible plume in Figure 22c suggests that turbulence generated by the rough surface at the tower soon rises to the height of the smoke plume and is responsible for the rather vigorous mixing over the water. The vertical diffusion which is restricted to the lower 250 feet indicates that there is considerable mixing in this layer.

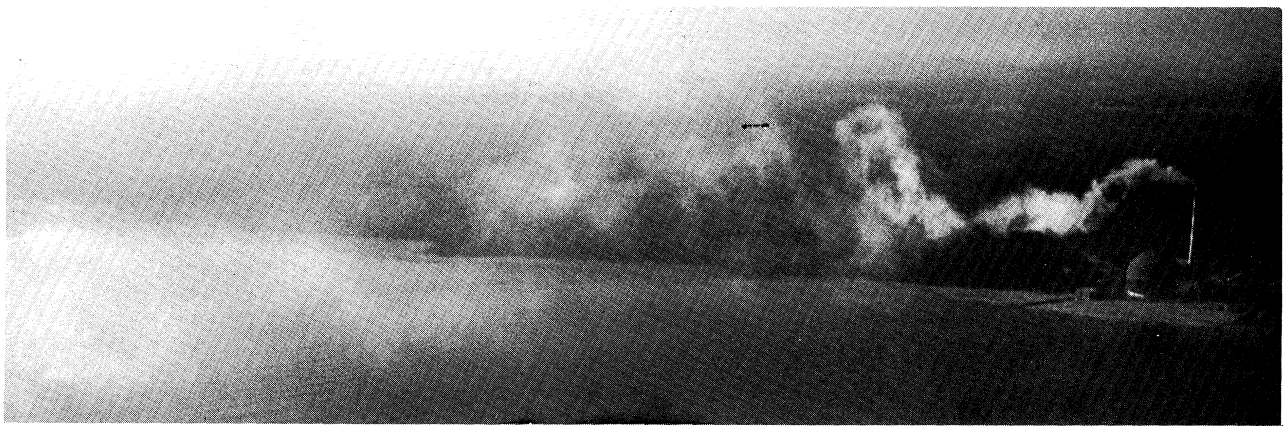

(a)

(b)

(c)

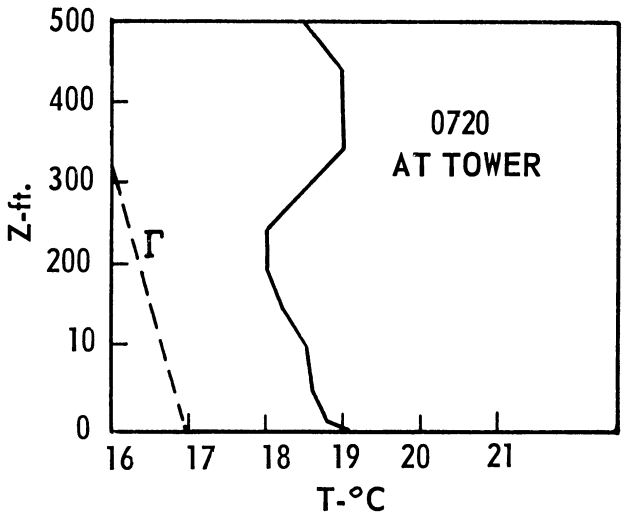

(d)

Figure 23: Representative Smoke Plume Photographs, Run 12.

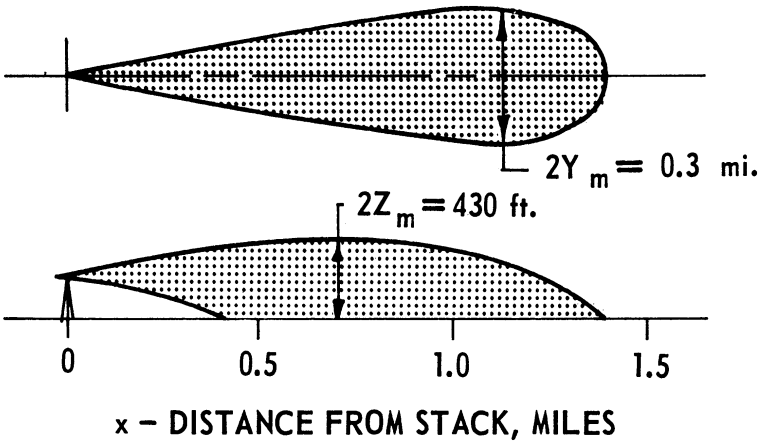

Run 12. The morning was quite hazy and there was a great deal of glare. Figures 23a, 23b and 23c show a rather vigorously diffusing, coning plume being released from the plant stack. Although the temperature profile shows an inversion above 256 feet at the tower, the vertical diffusion was rather good as evidenced by the fact that the maximum plume height was 400 feet at about 3/4 of a mile; see Figure 23e. Considering that the wind speed was only 6 mph and the lapse condition indicated an inversion above 256 feet, the diffusion must be considered excellent. The conclusion to be drawn from the photographic evidence is that the turbulence generated over land does not become damped out over the water until at least a few miles off shore.

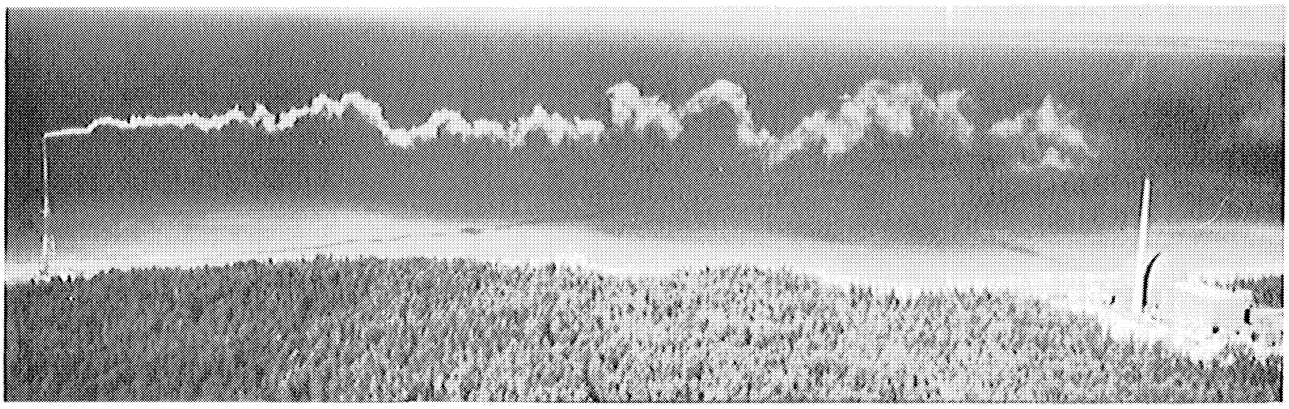

(a)

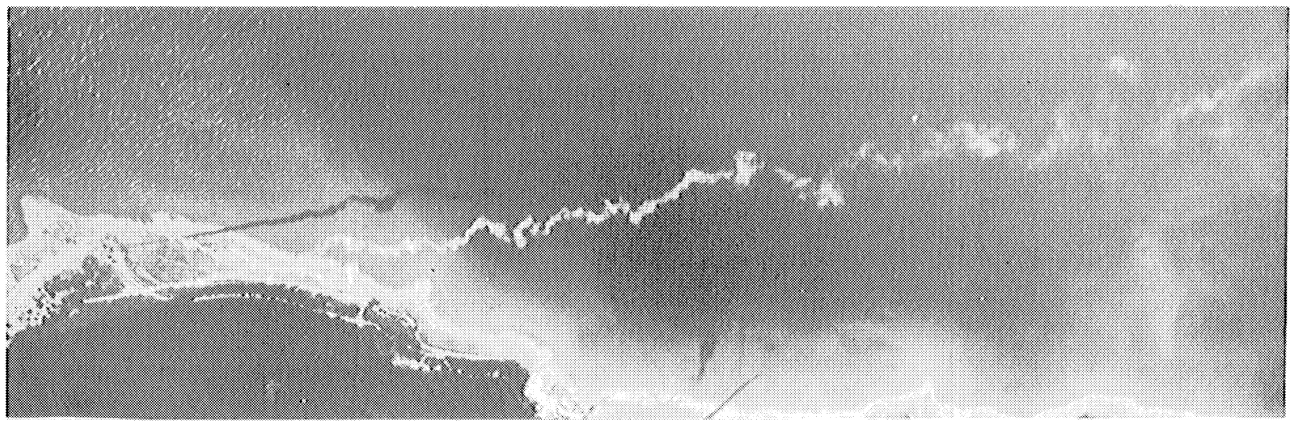

(b)

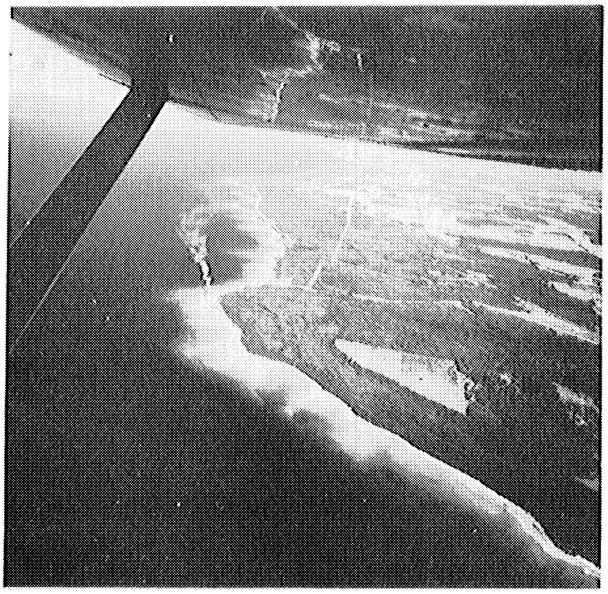

(c)

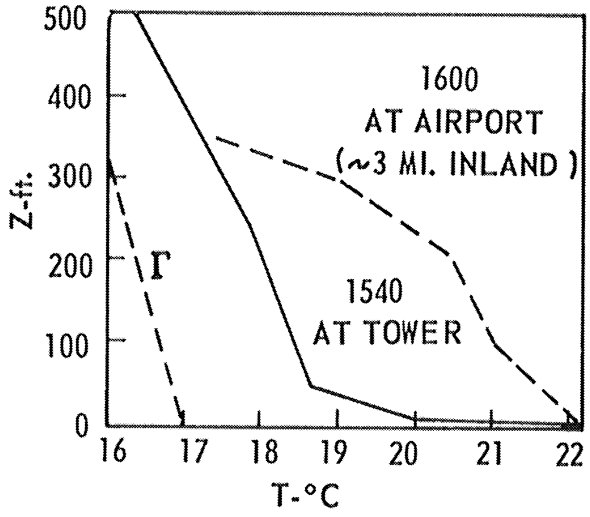

(d)

Figure 24: Representative Smoke Plume Photographs, Run 24.

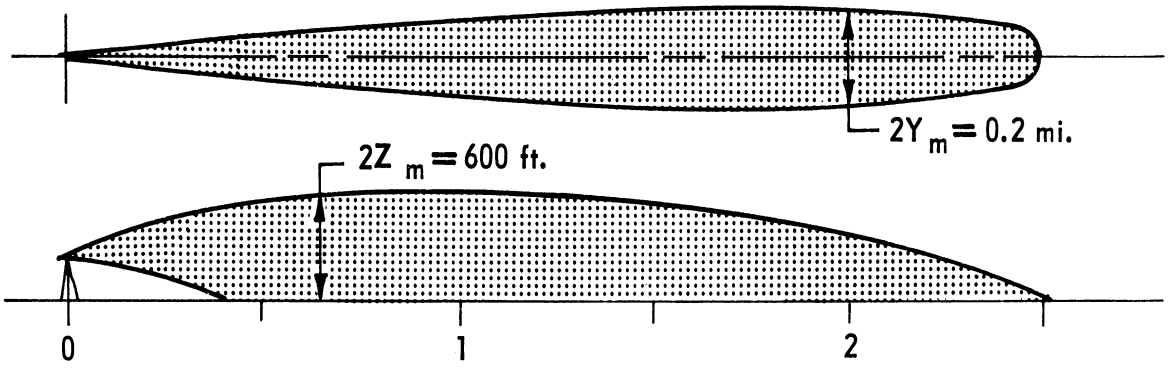

4. Unstable Lapse Conditions

Run 24. The temperature profile shows a very strong lapse in the layer from the water up to 50 feet and a somewhat weaker, but nevertheless, quite strong lapse above 50 feet. The wind speed was 12 mph. Figures 24a, 24b and 24c show the effects of the lapse conditions on the visible plume. The plume shape definitely shows a looping plume over the shallow water near the shoreline. The looping plume is undoubtedly a result of the lower layer of air being heated by the warm water trapped in Little Traverse Bay by the westerly winds. Diffusion is rapid and the visible extent of the plume is only 2-1/2 miles.

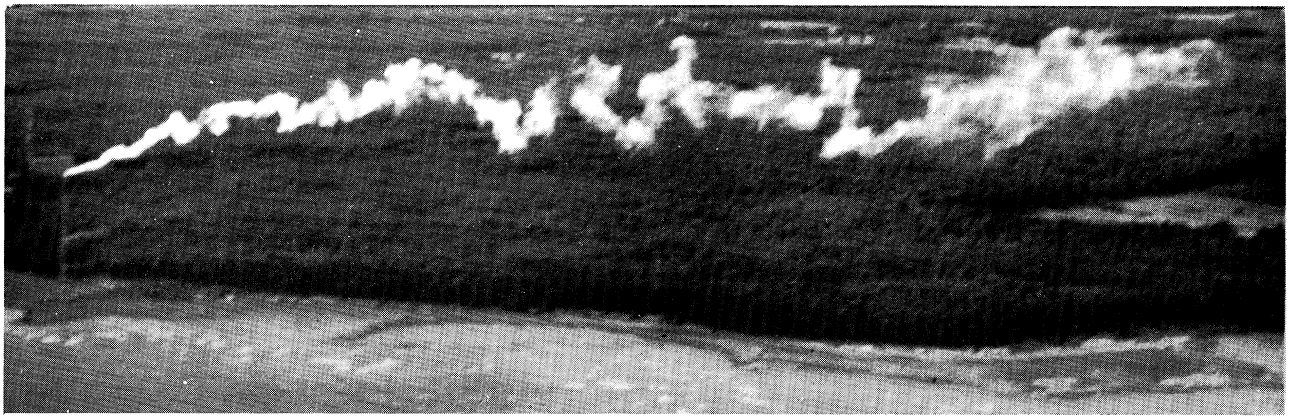

(a)

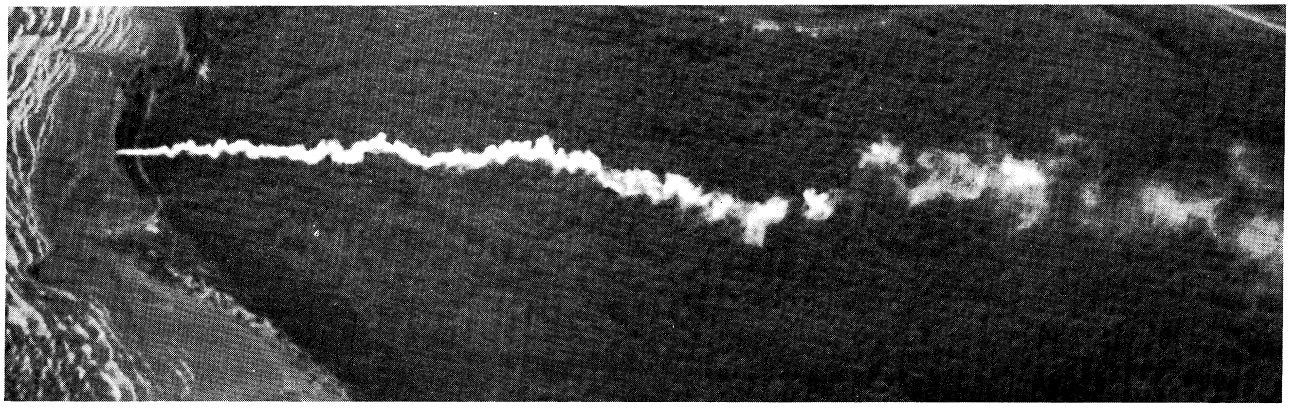

(b)

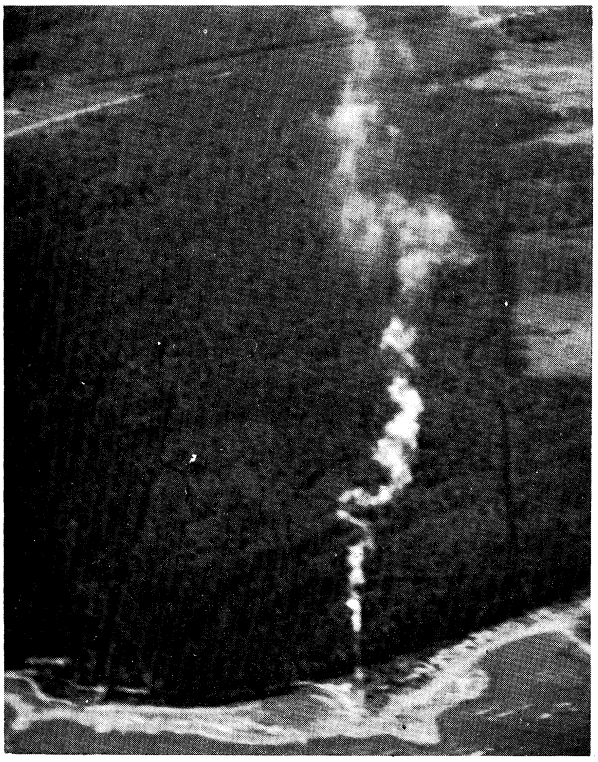

(c)

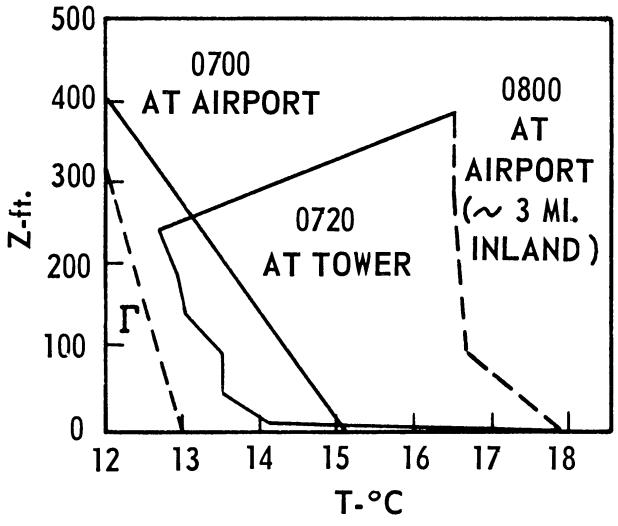

(d)

Figure 25: Representative Smoke Plume Photographs, Run 17.

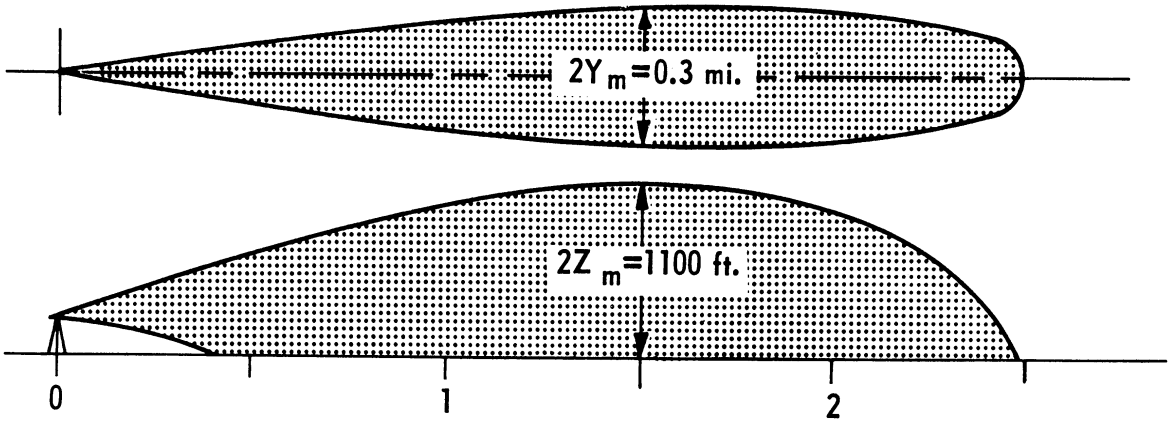

Run 17. Figures 25a, 25b and 25c show a moderately looping plume with great vertical development. The tower turbulence data do not indicate either marked vertical or horizontal motions; see Table II. This discrepancy is undoubtedly due to the smooth flow over the water where there is neither mechanical nor convective turbulence. By the time the air has traveled a short distance past the tower, it has become quite turbulent because of the very unstable layer of air close to the surface. The sizes of the eddies acting on the plume suggest mechanical turbulence caused by the rough surface, i.e., the trees. The lofting of the plume indicates a very unstable atmosphere. The temperature profiles show an unstable lapse condition both at the tower and inland. This would indicate that, under unstable conditions, the mechanical turbulence generated by the trees would reach up to the height of the plume and beyond. For a comparison refer to Figures 9 and 14. In the photos from both these runs, there is some evidence of mechanical turbulence, but in both cases because of inversion conditions, the structure of the turbulence reaching up to the plume is only the smaller eddies.

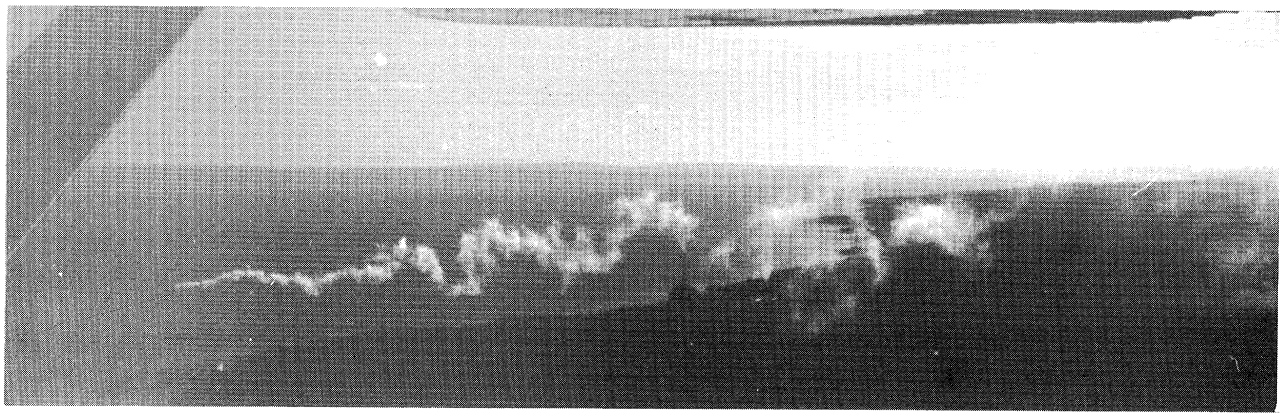

(a)

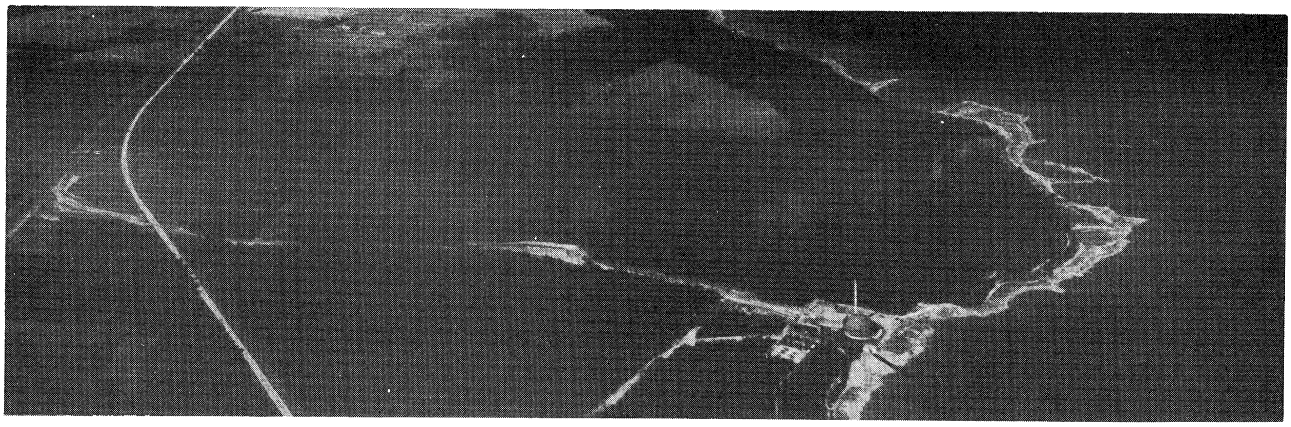

(b)

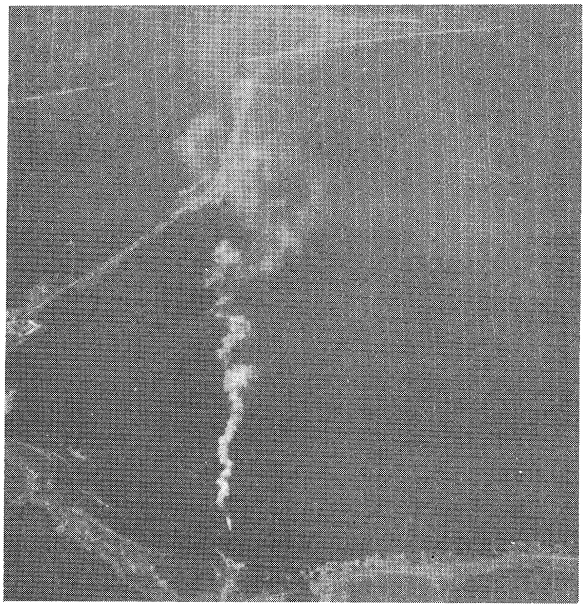

(c)

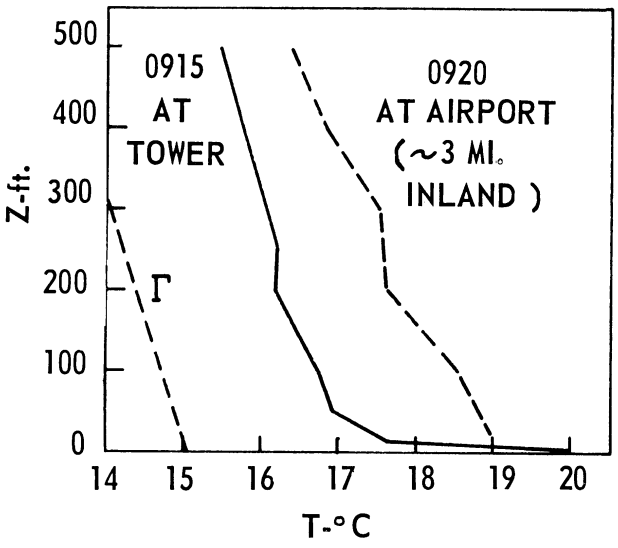

(d)

Figure 26: Representative Smoke Plume Photographs, Run 23.

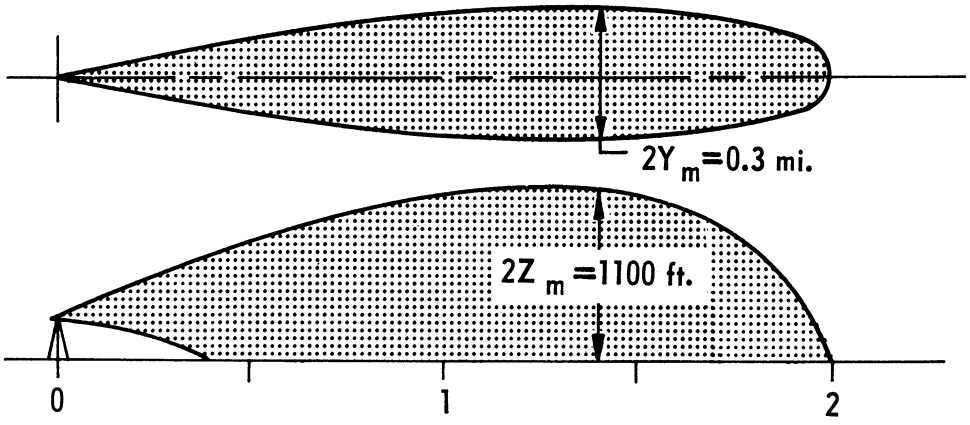

x - DISTANCE FROM STACK, MILES

Run 23. Figures 26a, 26b, 26c and 26e show a vigorously looping plume with great vertical development. The tower turbulence data indicate moderate horizontal turbulence, fair vertical turbulence and a wind speed of 8 mph. The temperature profile shows a fairly strong lapse condition in the atmosphere both over the water and over the land. Again the effect of the very unstable layer of air close to the surface as the plume comes off the water is evident. The turbulence generated by the trees rapidly reaches up to the plume and beyond.

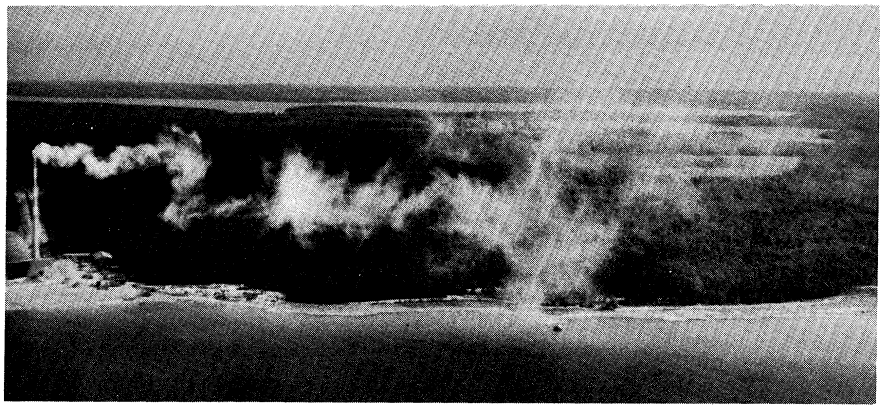

(a)

(b)

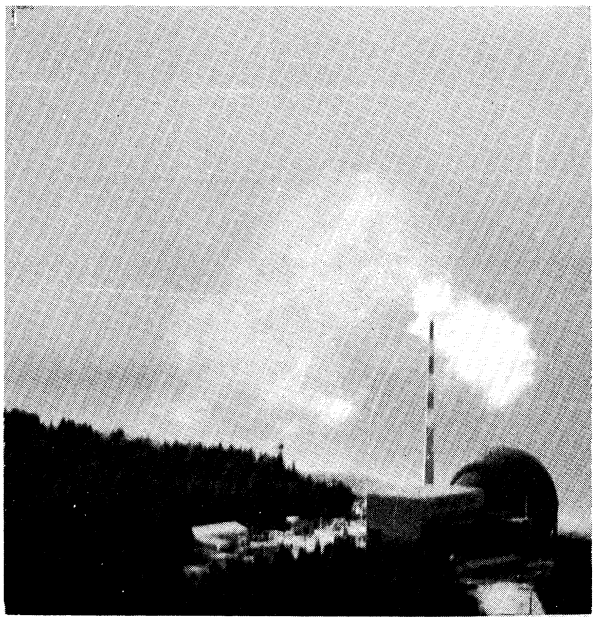

(c)

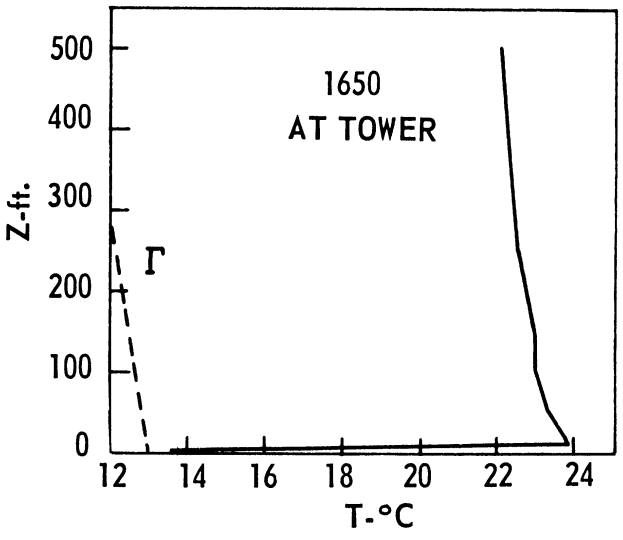

(d)

Figure 27: Representative Smoke Plume Photographs, Run 9.

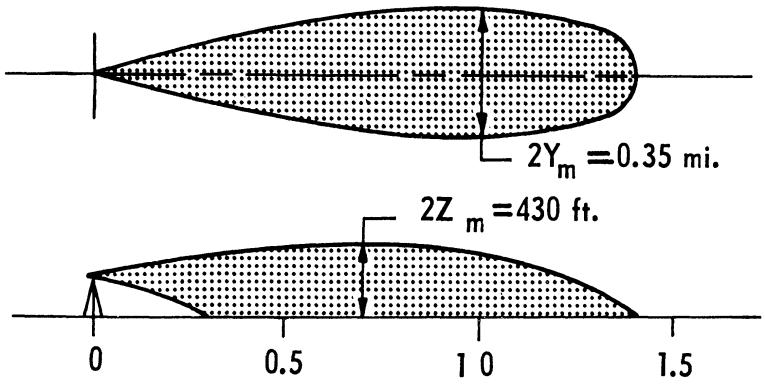

x - DISTANCE FROM STACK, MILES

Run 9. The temperature profile shows a lapse rate in the atmosphere slightly greater than dry adiabatic. The wind speed was 11 mph. Figures 27a, 27b and 27c show a rather vigorously looping plume. It is noteworthy that the length of the visible plume is only about 1.3 miles. This short length indicates that the good turbulence developed over the land does not die out over the water until a few miles from the shore. It should be noted that the temperature difference between the air at 10 feet overland and the water is 10° C. With such a great temperature difference, an inversion should build up rapidly from the water's surface. However, under unstable conditions overland, this run indicates that the plume will have diffused substantially before the inversion builds up.

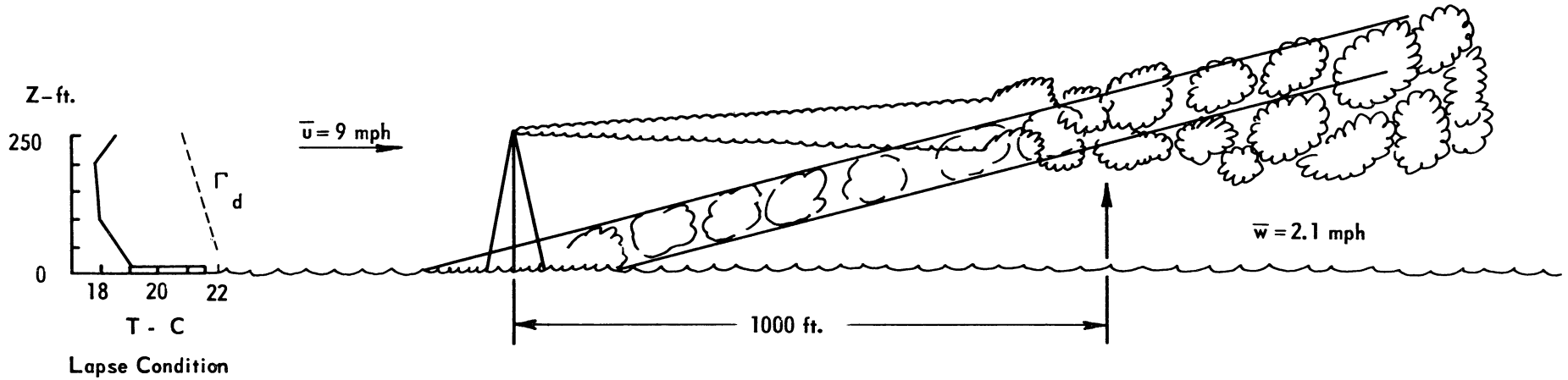

Assume: $z^2 = 4\,Kt$ Describes the unstable system.

where, z = height of the turbulence = 250 feet = 7600 cm
K = Fickian diffusion coefficient
t = travel time for eddy to reach $z = x/\bar{u}$
x = distance downwind eddy reaches z = 1000 feet
$\bar{u}$ = horizontal speed of eddy = 9 mph = 13 fps

$t = x/\bar{u} = 100/13 = 77$ s

$$K = \frac{(7600)^2}{(4)(77)} = 1.9 \times 10^5 \quad cm^2/s$$

which is a reasonable value of K in such an unstable system.

Figure 28. Unstable meteorological system at Big Rock Point. Air coming off the cooler lake is heated from below by warmer water at the shoreline. Mechanical turbulence is caused by the air flowing over the rough surface of the point of land on which the tower is located. Data from Run 14.

C. Conclusions From Photographic Data

1. Crosswind shear enhances the atmospheric diffusion of smoke plumes when the vertical diffusion brings the plume down into the shear layers. Under identical atmospheric conditions, a visible plume acted upon by shear is wider and shorter than a plume not affected by shear. This results in reduced center line concentrations for the distances in the plume after it has grown enough vertically to penetrate into the shear layer.

2. With winds from the sector 270 degrees through 360 degrees, lake water is trapped in Little Traverse Bay and heated in the shallows along the shore. When these winds persist for a few days with fair weather, the temperature of the water along the shore of the bay rises sharply. It is not unusual for the water at the shore to warm up 3° C in one day. This warm water, when warmer than the air, acts as a source of heat to the air moving over it. If the temperature difference between the trapped water and the air is great enough, an unstable meteorological system is set up. Any turbulence induced by the transition from flow over a smooth surface to flow over the rough beach is accentuated in this unstable system. Turbulent eddies then quickly rise to the height of the plume and diffusion is enhanced considerably. Figure 28 illustrates the phenomenon with data from Run 14. Figure 17a is a photograph of a plume diffusing under these conditions. A calculation which assumes that the buildup of turbulence from the rough surface of the point of land protruding out into the otherwise all water trajectory, follows the parabolic law is shown on Figure 28. K calculated from the data is about 10^5 cm^2/s which is a reasonable value under these conditions. This calculation tends to confirm the validity of the conclusion that the turbulence affecting the plume is generated at the rough beach where there is the transition from smooth overwater flow to rough flow at the beach.

3. Slightly unstable air moving from the warm land over the cooler water maintains its turbulent character long enough to markedly diffuse the plume released at the shore. However, air that is near neutral overland and moves out over the cooler water loses its neutral character within a few miles of shore. It appears that the inversion builds up more rapidly from the cooler water when the air flowing from the warmer land is near neutral rather than unstable.

4. Stable air coming off the water changes in character to near neutral or unstable within a few miles from the shoreline when the ground is warmer than the water, depending on the wind speed. Even when there is a fairly strong inversion at the shoreline, the photographic evidence shows that turbulence builds up from the ground within 3 miles of the shore. See Figures 10, 14, 16 and 17. All show a marked change of regime within a few miles of the shore.

5. Under certain restrictive atmospheric conditions, plumes may travel long distances from the site with little dilution. For example, the longest plume of the 1962 series occurred with plume flow over the lake, an inversion aloft which trapped the plume in a shallow layer above the water and a moderate wind speed. Nevertheless, for diffusion of a plume overland or along the shore, various atmospheric mechanisms such as crosswind shear act to enhance atmospheric diffusion, especially under stable atmospheric conditions. It must be remembered that any plume which flows out over the water must eventually encounter a shoreline. Because the plume will be deeper and wider, the special atmospheric diffusion mechanisms operating at a shoreline will have a very great effect on the diffusion of the plume overland. It is for this reason that the slow diffusion of a plume overwater should definitely not be considered a disadvantage at shoreline sites.

REFERENCES

1. Hewson, E. W., and Gill, G. C., Progress Report No. 1, Meteorological Study of Natural Ventilation in the Atmosphere, Big Rock Point Nuclear Plant, Charlevoix, Michigan, The University of Michigan Report No. 04015-1-P, November 1961.

2. Hewson, E. W., Gill, G. C., and Walke, G. J., Progress Report No. 2, Meteorological Study of Natural Ventilation in the Atmosphere, Big Rock Point Nuclear Plant, Charlevoix, Michigan. The University of Michigan Report No. 04015-2-P, March 1962.

3. Gifford, F., Smoke Plumes as Quantitative Air Pollution Indices, International Journal of Air Pollution, Vol. 2, 1959.

4. Frenkiel, F. N., and Katz, I., Studies of Small-Scale Turbulent Diffusion in the Atmosphere, Journal of Meteorology, Vol. 13, 1956.

5. Stewart, N. G., Gale, H. J., and Crooks, R. M., The Atmospheric Diffusion of Gases Discharged From the Chimney of the Harwell Reactor BEPO, International Journal of Air Pollution Vol. I, 1958.

6. Pasquill, F., The Estimation of the Dispersion of Windborne Material, The Meteorological Magazine, Vol. 90, No. 1063, February 1961.

7. Trorey, L. G., Handbook of Aerial Mapping and Photogrammetry, London: Cambridge University Press, 1950.

8. Atomic Energy and Meteorology, A Report by the Atomic Energy Commission, Report No. AECU-3066, July 1955.

9. Brock, F. V., and Hewson, E. W., Analog Computing Techniques Applied to Atmospheric Diffusion: Continuous Point Source, Journal of Applied Meteorology, Vol. 2, No. 1, February 1963.

10. Pasquill, F., Atmospheric Diffusion, New York: D. Van Nostrand Co. 1962, Pages 203-205.

APPENDIX I

Data From Smoke Plume Photographs

Figure	Run	Date and Time	Film and Filter	Height Ft	f-Stop and 1/Speed	Film Speed and Light Meter Reading	Lens mm
8a	13	12 July 0745	Slow IFR + 25A	3000	11 @ 60	ASA-50,	28
8b		0720	Pan X + 25A	300	5.6 @ 125	5.6 @ 125	50
8c		0744	Slow IFR + 25A	2400	11 @ 60		28
9a	6	26 June 1805	Kodachrome II	6000	8 @ 125	ASA-50,	50
9b		1820	Pan X + 25A	3000	8 @ 100	8 @ 250	35
9c		1815	Pan X + 25A	3500	4 @ 100		35
10	6	26 June 1810	Pan X + 25A	6000	8 @ 100	ASA-50, 8 @ 250	35
11	8	28 June 1805	Pan X + 25A	250	4 @ 100	ASA-50, 5.6 @ 100	50
12a	8	28 June 1758	Pan X + 25A	350	5.6 @ 100	ASA-50,	50
12b		1802	Pan X + 25A	350	5.6 @ 100	5.6 @ 100	50
12c		1820	Fast IFR + 25A	3000	5.6 @ 125		28
13a	15	13 July 0727	Pan X + 25A	300	8 @ 125	ASA-50,	35
13b		0708	Pan X + 25A	500	8 @ 125	5.6 @ 125	35
13c		0725	Pan X + 25A	3000	8 @ 125		35
14a	18	15 July 1747	Pan X + 25A	300	5.6 @ 125	ASA-50,	28
14b		1819	Pan X + 25A	3000	8 @ 125	11 @ 125	28
14c		1804	Pan X + 25A	3000	5.6 @ 125		28
15a	19	16 July 0610	Kodachrome II	500	4 @ 100	ASA-50,	50
15b		0620	Kodachrome II	3000	4 @ 100	8 @ 125	50
15c		0624	Pan X + 25A	3000	8 @ 125		21
16a	11	5 July 1035	Pan X + 25A	500	5.6 @ 500	ASA-50,	35
16b		1040	Pan X + 25A	1500	5.6 @ 250	5.6 @ 250	35
16c		1050	Pan X + 25A	2000	11 @ 125		35
17a	14	12 July 1800	Pan X + 25A	3000	4 @ 125	ASA-50,	50
17b		1803	Pan X + 25A	3000	5.6 @ 125	5.6 @ 125	50
17c		1810	Pan X + 25A	3000	4 @ 125		50
18a	25	19 July 0940	Pan X + 25A	500	5.6 @ 100	ASA-25,	50
18b		0932	Pan X + 25A	2000	8 @ 100	5.6 @ 125	50
18c		0910	Fast IFR + 88A	3000	5.6 @ 125		28

Figure	Run	Date and Time	Film and Filter	Height Ft	f-Stop and 1/Speed	Film Speed and Light Meter Reading	Lens mm
19a	16	13 July 1550	Fast IFR + 88A	300	11 @ 125	ASA-50,	28
19b		1604	Pan X + 25A	3000	11 @ 125	8 @ 100	35
19c		1606	Pan X + 25A	3000	11 @ 125		35
20a	22	17 July 1740	Kodachrome II	300	4 @ 100	ASA-25,	50
20b		1750	Kodachrome II	1500	5.6 @ 100	4 @ 100	50
20c		1760	Kodachrome II	2800	4 @ 100		50
21a	20	16 July 1740	Pan X + 25A	3000	8 @ 125	ASA-50,	35
21b		1747	Pan X + 25A	500	5.6 @ 125	5.6 @ 100	35
21c		1742	Pan X + 25A	3000	5.6 @ 125		35
22a	21	17 July 0815	Pan X + 25A	250	16 @ 125	ASA-100,	21
22b		0830	Pan X + 25A	2200	16 @ 125	16 @ 125	21
22c		0828	Pan X + 25A	2200	16 @ 125		21
23a	12	11 July 0720	Pan X + 25A	300	8 @ 125	ASA-25,	50
23b		0719	Pan X + 25A	500	4.9 @ 125	5.6 @ 100	50
23c		0722	Fast IFR + 88A	500	22 @ 60		28
24a	24	18 July 1525	Pan X + 25A	500	4 @ 125	ASA-50,	21
24b		1550	Pan X + 25A	3000	8 @ 125	8 @ 125	21
24c		1535	Pan X + 25A	3000	4 @ 125		21
25a	17	14 July 0703	Kodachrome II	500	5.6 @ 100	ASA-50,	50
25b		0711	Kodachrome II	3000	5.6 @ 100	8 @ 100	50
25c		0717	Kodachrome II	3000	5.6 @ 100		50
26a	23	18 July 0840	Pan X + 25A	500	16 @ 125	ASA-100,	21
26b		0852	Pan X + 25A	3000	11 @ 125	16 @ 125	21
26c		0905	Pan X + 25A	3000	16 @ 125		21
27a	9	2 July 1700	Pan X + 25A	300	8 @ 100	ASA-50,	50
27b		1713	Pan X + 25A	3000	5.6 @ 100	8 @ 100	50
27c		1705	Pan X + 25A	300	8 @ 100		50

APPENDIX II

Photography Techniques for Smoke Plume Studies Utilizing Aerial Photography

The ability to derive meaningful measurements from photographs of smoke plumes largely depends on the quality of the photographs being analyzed. High-quality aerial photographs of smoke plumes can only be obtained by the careful use of good equipment. It is the purpose of this Appendix to relate the results of a great deal of experimentation in arriving at the optimum combination of photographic techniques and equipment.

The basic problem encountered in the analysis of the photographs of smoke plumes was the difficulty in determining the visible edges of the plume. In some instances when the plume was photographed from the side, the upper edge of the plume would be completely lost in haze or cloud. Then again, when the plume was photographed from above, the plume boundaries on occasion would be lost in the light-colored sand of the beach or in the surf. These problems were compounded by the necessity of getting as much of the plume in each photograph as possible for the purpose of determining the maximum plume width or height. Even with a wide-angle lens, the camera would need to be about a mile away to get enough of a typical plume in a side-view photograph to accurately determine the maximum plume height. On side-view photographs taken at this distance, the upper edge of the plume often could not be determined accurately because of clouds in the background, haze or glare. This problem could not be solved so a compromise technique for locating the upper edge of the plume was used. This technique consisted, in part, of flying at the height of the top of the plume, about one-fourth of a mile from the plume and taking careful note of the time and the airplane height and location for each picture taken. The maximum height of the plume as determined by visual observations was noted on the data sheet and a photograph was taken at this location to double-check the visual fix. The maximum plume height could be fairly readily determined by moving the airplane up or down until the upper edge of the plume was coincident

with the horizon. Because the airplane was so close to the plume it could be assumed that when the upper edge of the plume was coincident with the horizon, the upper edge of the plume was at the same height as the airplane. The altimeter reading in the airplane therefore gave the maximum plume height.

The problem of determining the maximum width and length of the visible plume was solved in a different manner. Except when the plume flowed directly over the lake surf or the light colored beach, the edges of the plume could be readily determined from photographs taken at about 3000 feet. An attempt was made to take photographs of the plume vertically downward so there would need to be no rectification of the photographs, i.e., the plume dimensions could be determined directly from the photographs without using grids or other devices. Unfortunately, it proved to be extremely difficult to get good quality vertical photographs because of the instability of the light airplane used. As a compromise, it was found that satisfactory results could be obtained by using high (or horizon) oblique photographs, i.e., photographs taken with the optical axis of the camera tilted so as to include the visible horizon. If the depression angle, i.e., the angle the optical axis makes with the horizontal, is kept constant for all the photographs taken, and if the height of the airplane is constant, one perspective grid may be used to analyze all the photographs. A depression angle of about 30 degrees was found to yield good results. As an aid in maintaining the 30 degree depression angle while taking photographs, a line can be drawn with India ink on the front glass of the camera view finder at the proper position to tilt the optical axis of the camera 30 degrees from the horizontal. Then by lining up the line on the viewfinder with the horizon, the photographer can be sure of having a depression angle of about 30 degrees. Appendix III contains information on the construction and use of perspective grid overlays in analyzing smoke plume photographs.

The problem of losing the plume in the lake surf was solved by the use of an infrared film and a Wratten No. 88 filter. On photographs taken with infrared film, the lake showed up almost jet black. The white smoke plume stands out quite well against this very

dark background. Other background problems were reduced by the use of Kodachrome II color film. The color photographs, in general, proved to be superior to the black and white photographs. This may be directly attributed to the constant high quality of careful film processing. The processing of the black and white films (both standard and infrared films) proved to be troublesome. The quality of both the developing and the printing of the black and white films proved to be quite variable. This led the group to conclude that it probably would be better to take all the plume photographs on color film wherever possible.

Table II-1 lists the specifications of the camera equipment used during the experimental runs. All gave good results. The movies of smoke plumes taken proved to be very interesting but of limited use in analyzing the behavior of the smoke plumes in the types of analyses used in this report.

Table II-2 lists the types of film and filters used with short comments as to how they worked out.

TABLE II-1
PHOTOGRAPHIC EQUIPMENT

Camera	Size	Type	Lens Focal Length
Baldina	35 mm	Still	50 mm
Leica	35 mm	Still	28 mm and 21 mm
Electric Speed Graphic	35 mm	Still	35 mm
Bell and Howell	16 mm	Movie	Variable - Turret

TABLE II-2
FIIMS AND FILTERS

Film	ASA Rated Film Speed	Filter Type	Film Speed With Filter for Best Results	Comments
Kodachrome II	Daylight ASA-25	None	ASA-32	Slight Underexposure Gave Best Results.
Kodak Pan-X	ASA-40	Wratten 25A	ASA-50)	Underexposure Gave Best Results. Problem in Obtaining Uniform Film Processing and Printing.
Kodak Plus-X	ASA-160	Wratten 25A	ASA-100)	
Kodak High Speed Infrared	Daylight ASA-80	Wratten 88A	ASA-25	Excellent Results for Photos Against Clear Sky or Water Background. Sensitive to Glare.
Kodak (Slow) Infrared (IR 135)	Tungsten ASA-20	Wratten 25A	ASA-2	Difficult To Use To Obtain Properly Exposed Photos. Very Glare Sensitive.

APPENDIX III

CONSTRUCTION OF PERSPECTIVE GRIDS FOR PHOTOGRAPHIC ANALYSIS [7]

The use of perspective grids is primarily suited to country having little relief, and requires that the depression angle and height of aircraft be determinate. Referring to Figure III-1, the method consists of constructing a perspective grid, such as would be produced by photographing a rectangular grid which might be imagined to exist on the ground. In practice, transparencies of a number of grids should be constructed for a particular lens to cover the range of height and depression angle required. Assume that an oblique photograph was taken at a height of H = 3000 feet with a 35 mm camera with a lens focal length of 28 mm. The photo was enlarged to a standard 5-1/4 inch print. Converting to an equivalent lens focal length, f = (28)(5-1/4)/(35) = 4.25 inches. Calculate and draw the proper perspective grid, the size of the grid squares being 400 m. The proofs of the formulae used in the following example are not given but can be found in reference [7].

GRID CONSTRUCTION

1. First, locate the principal point, p, which will be the exact center of the photograph, then draw the principal vertical, i.e., the line through p at right angles to the apparent horizon on the photograph.

2. Calculate the angle d' the depression angle of the optical axis from the apparent horizon. The depression angle is defined as the inclination of the camera line of sight from the horizontal. On Figure III-1 ph' measured 1.45 inches. Therefore, if d' = psh'

Tan psh' = 1.45/4.25 = .346, psh' = 19° 5'

Because of the effects of curvature and refraction, the visible horizon is below the true horizon. The angular difference between the true and the apparent horizon is called the dip of the horizon. It has been shown that the dip of the horizon in minutes is very nearly equal to the square root of the height ($\sqrt{H}$), when H is in feet. Therefore,

Dip = $\sqrt{3000}$ = 55', psh = d = 20°

3. Calculate hh', the distance between the true and the apparent horizons.

$hh' = ph - ph' = f \tan d - ph'$

$= 4.25 \tan 20 - 1.45 = 0.20$ inch

Mark h; draw the true horizon through h parallel to the apparent horizon.

4. All lines on the photograph parallel to ph vanish at h. We wish to draw the perspective projection of a series of such lines 400 m. (1312 ft) apart; these will vanish at h. The distance hD, in inches, is equal to H sec d/grid unit in feet. Through D draw a line parallel to the true horizon. On it mark off divisions of 1 in., as shown in Figure III-1; join these points to h. The resultant fan is the projection of a series of lines 400 m apart on the ground, and parallel to the principal line NP:

$hD = 3000 \sec 20/1312 = 2.43$ inches

5. If a series of equally spaced parallels be cut by a line at 45°, and lines at right angles to these parallels be drawn from the intersections with diagonals as shown, the result is a series of squares. Now all lines at 45° to ph vanish at the same point; if we can calculate this point we can draw the projection of the diagonal, and so construct the projection of the squares. The distance in question is $hv_1 = hv_2$:

$hv_1 = f \sec d = 4.25 \sec 20 = 4.50$ inches

Mark the point v_1 and draw v_1p produced. Now a series of lines at right angles to the principal vertical, through the points intersected by the 45° line pv_1, gives the required grid. v_1 and v_2 should both be used to provide a check on drafting.

6. It is not necessary to carry the grid much past the principal point because the squares become so foreshortened that plotting from the background of the photograph is inaccurate. In dividing the line through D into 1 inch intervals, it is not necessary to carry the divisions out very far. The division for the upper part of the grid may be obtained by extending, on any parallel farther up the picture, the few equal divisions which will have been obtained on it by rays from D. These additional points are joined to h in the same way as were the divisions from D. This point will be clear when an

actual grid is drawn. Similarly, remembering that all 45° lines parallel to pv_1 vanish at v_1, an additional diagonal may be drawn to v_1 from the corner of any grid square. This diagonal will locate the parallels for the bottom of the picture. The only reason for drawing the diagonal through the principal point in the first place is to make p come at the corner of a grid square.

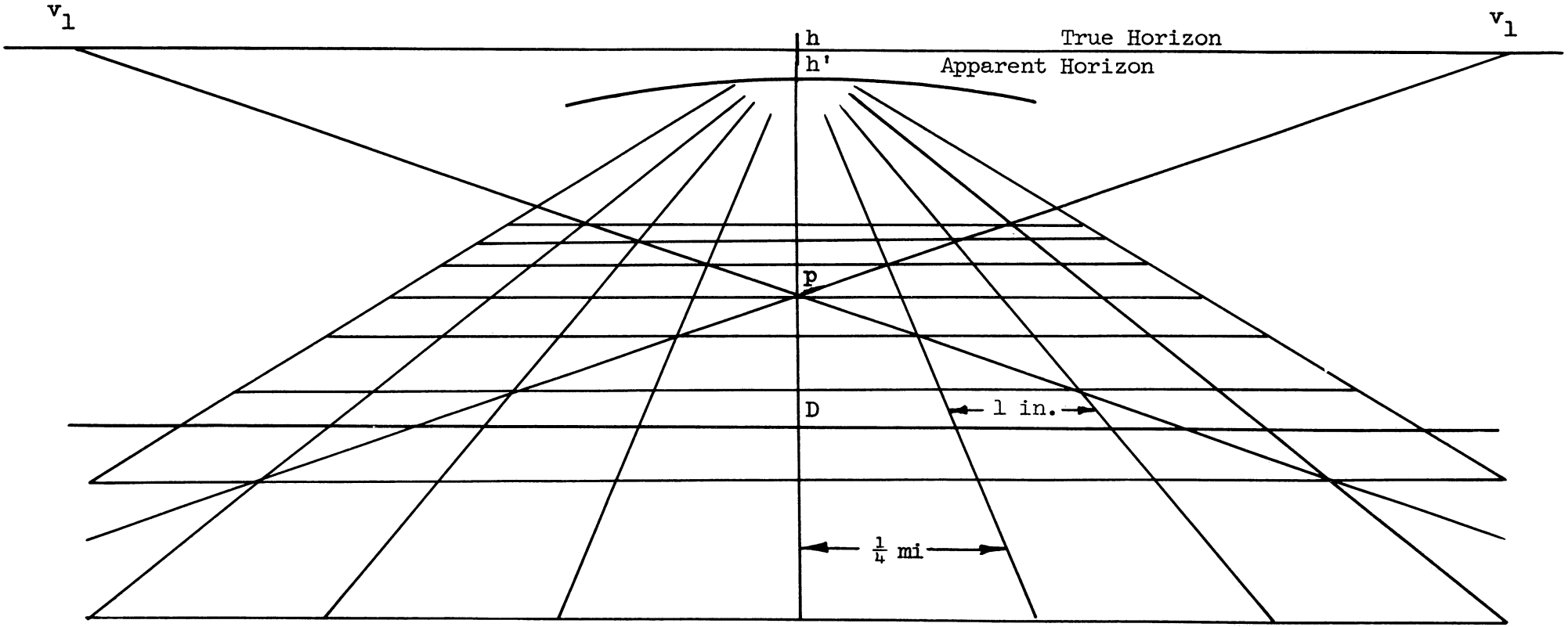

Figure III-1. Construction of a perspective grid to be used for rectification of oblique photographs taken during a smoke plume photography run. Height of camera = 3000 feet, depression angle = 20^{o}, camera lens focal length = 4.25 inches.

APPENDIX IV

Application of Meteorological Data To Estimate Average Dose Levels

A. Background

The net results of any meteorological study for an industrial application should be both passive and active in nature. First, the meteorological survey should demonstrate that the site chosen has adequate natural ventilation so that potential atmospheric contamination problems would on the average be at a minimum. These results may be considered passive in nature. The active results from a meteorological survey would revolve about the concept of using the very advantageous atmospheric dispersion conditions when necessary in the operation of the plant.

In the operation of a boiling water reactor, radiogases are emitted from a stack on a routine basis. Just as meteorological conditions will vary in time, so will the emission rate of the radiogases. The interplay of the variable emission rate of the radiogases and the dispersion capability of the atmosphere will determine what the off-site radiation dosages will be. Since the licensing regulations stipulate that the radiation dosages may be averaged over a whole year, it would be advantageous to the plant operator to be able to readily estimate radiation doses at various points downwind from the plant. Holland's nomogram as presented in "Meteorology and Atomic Energy," Page 108, provides a ready tool to estimate external gamma dosage. The following sections recommend parameters to be used with the nomogram for quick estimates.

B. Meteorological Parameters

The use of meteorological parameters derived from meteorological studies at the site will permit the nomogram to be adapted to the peculiar conditions at the Big Rock Point site. This use of these parameters with the nomogram permits the rapid calculation of radiation dose to a receptor on the ground using actual parameters derived from instrument readings at the site. Instructions for using the nomogram are printed in the reference itself. The parameters to be used in the calculations are:

1. Wind Direction
2. Lapse Condition
3. Wind Direction Shear
4. Radioactivity Released From the Stack or an Estimate of the Radioactivity Released
5. Wind Speed

C. Derivation of the External Gamma Dosage Parameters

The basic details of the development of the Holland nomogram are contained in "Meteorology and Atomic Energy." The reader is referred to this source for complete details. Only the adaptation of parameters to be used in the Holland nomogram for Big Rock Point conditions will be discussed here.

1. Wind Direction. The direction from which the wind blows determines the distance from the stack to the point on the ground for which the radiation dose is calculated. For example, wind from 240° has an all water trajectory for approximately 9 miles before a plume would be overland. Therefore, the radiation dose is calculated for a distance 9 miles from the stack. On the nomogram, four distances from the stack are to be used in the dose calculations.

Category 1. Dose calculated for a distance 80 m from the base of the stack. This calculation estimates the radiation dosage to personnel working close to the plant buildings.

Category 2. Dose calculated for a distance 900 m downwind from the base of the stack. This calculation estimates the radiation dosage to the closest point outside the site boundary.

Category 3. Dose calculated for a distance 14.4 km (9 miles) downwind from the base of the stack. This calculation estimates the radiation dosage to the nearest point of land across Little Traverse Bay.

Category 4. Dose calculated for a distance 60 km (36 miles) downwind from the base of the stack. This calculation estimates the radiation dosage to the nearest point of land across Lake Michigan.

It has been said that Sutton's equation underestimates the downwind concentrations for long distances from the source. This is said to be especially true overwater. The data collected to date indicate that, for a shoreline site such as Big Rock Point, shear forces acting over the

water enhance the diffusion. The data would suggest that diffusion overwater from the Big Rock Point site might be estimated adequately by Sutton's equation.

2. Lapse Condition. Four lapse condition categories were chosen for analyzing the data. The category is determined by the difference between the air temperature at the 250 foot and 50 foot levels on the tower. This temperature difference determines the degree of atmospheric stability in the region of greatest interest. This region is the air layer between the top of the stack and the ground. Table IV-1 lists the lapse conditions, the corresponding temperature differences and the stability parameter, n, to be used in Sutton's equation.

Table IV-1
Lapse Condition Categories

Lapse Condition	Temperature Difference $(T_{256} - T_{50}) = \Delta T$	Sutton Stability Parameter, n
Unstable	$\leq$-0.6 Deg C	0.20
Near Neutral	-0.6 Deg C to 0 Deg C	0.25
Stable	0.1 Deg C to 3.0 Deg C	0.33
Very Stable	$>$ 3.0 Deg C	0.50

3. Diffusion Coefficients. Holland's nomogram was derived assuming isotropic turbulence, i.e., $C_y = C_z$. As the smoke study has shown, under most conditions C_y is greater than C_z. To correct for nonisotropy, the Holland nomogram was adapted to use $C = C_y C_z$. Since the mean free path of the gamma radiation is about 100 m in air, the dose calculations should not be significantly affected by the above approximation. Table IV-2 lists the Sutton diffusion coefficients to be used on the nomogram.

Table IV-2
Diffusion Coefficients

Lapse Condition	n	C_y	C_z	$C_y C_z$
Very Stable	0.50	0.40	0.03	0.11
Very Stable - With S $\geq 15^\circ$	0.50	0.80	0.03	0.16
Stable	0.33	0.40	0.05	0.14
Stable - With S $\geq 15^\circ$	0.33	0.80	0.05	0.20
Near Neutral	0.25	0.40	0.10	0.20
Near Neutral - With S $\geq 15^\circ$	0.25	0.80	0.10	0.28
Unstable	0.20	0.40	0.20	0.28

It will be noted that provisions in the above table have been made to account for the effect of wind direction shear on diffusion. In the table S is the wind direction shear between the 250 foot and 128 foot levels on the tower. As shown in the main body of this report, wind direction shear has a substantial effect on the diffusion of a plume in the first 5 or 10 miles from the stack.

APPENDIX V

The Construction of a Nomogram to Calculate Sutton's Diffusion Coefficients From Wind Direction Traces or Smoke Plume Measurements.

The Physical Problem

The steady state concentration from a continuously emitting point source at the origin of the x, y and z-axes is usually expressed mathematically by the familiar Gaussian diffusion equation:

$$X_{(x,y,z)} = \frac{Q}{2\pi\bar{u}\left[\sigma_y^2\ \sigma_z^2\right]^{\frac{1}{2}}} \quad \exp - \frac{y^2}{2\sigma_y^2} \quad \exp - \frac{z^2}{2\sigma_z^2} \quad \ldots\ldots\ldots (1)$$

where, X = concentration of material at point (x,y,z), (M/L^3)
Q = emission rate of the source, (M/T)
$\bar{u}$ = mean wind speed along x-axis, (L/T)
σ_y^2, σ_z^2 = horizontal and vertical variances of the plume concentration distribution, (L^2), which are a function of the dispersion time T.

This expression for the concentration directly utilizes physical measurements, the variances, of the plume. Although this is the basic diffusion equation, most people in air pollution are more familiar with a variant of this equation known as the Sutton equation. The only difference between the two equations is in the expression for the plume variances. In Sutton's equation:

$$\sigma^2 = 1/2C^2\ x^{2-n} \quad \ldots\ldots\ldots\ldots\ldots\ldots\ldots\ldots\ldots\ldots\ldots\ldots\ldots\ldots (2)$$

where, C = a generalized diffusion coefficient, $(L^{n/2})$
x = distance downwind, (L)
n = a dimensionless parameter which depends upon atmospheric stability

Because of the greater familiarity of the Sutton equation, it is more convenient to express experimental results in this form. The problem is to convert the experimental results to the proper form.

In the experimental results, the square root of the variance, σ_d, has the units of degrees, whereas, equation (1) requires σ to be in units of length. The conversion to the proper units and thence to the Sutton form is done in the following manner:

Taking the square root of equation (2) and solving for C

$$C = \sqrt{2}\ \sigma\ x^{\frac{n-2}{2}} \qquad \ldots\ldots\ldots\ldots\ldots\ldots\ldots\ldots\ldots\ldots\ (3)$$

but, $\sigma = \sigma_r\ x$ $\ldots\ldots\ldots\ldots\ldots\ldots\ldots\ldots\ldots\ldots\ (4)$

where, σ_r is in radians,

and, $\sigma_r = (\frac{2\pi}{360})\ \sigma_d$ $\ldots\ldots\ldots\ldots\ldots\ldots\ldots\ldots\ldots\ldots\ (5)$

where, σ_d is in degrees

Substituting equation (5) into equation (4), then substituting equation (4) in equation (3), the following expression for C is found:

$$C = 0.0247\ \sigma_d\ x^{n/2} \qquad \ldots\ldots\ldots\ldots\ldots\ldots\ldots\ldots\ldots\ldots\ (6)$$

This is the basic equation for calculating C from experimental results; σ_d can be determined in any number of ways. If it is assumed that wind direction fluctuations are normally distributed, then dividing the range of the wind direction trace by 4.3 will yield an estimate of σ_d; or the width of a smoke plume at x, expressed in degrees divided by 4.3 will also yield an estimate of σ_d.

The Nomogram

The nomogram was set up in the following manner:

First Step - Basic Equation - $C = 0.0247\ \sigma_d\ x^{n/2}$

Ranges of Variables: C = .01 to 1

σ_d = 1 to 100

n = 0 to 1

x = 1 to 100,000

1. Set $C/(.0247)\sigma_d = A$, therefore, $A = x^{n/2}$. Solve by construction of a Z-chart.
2. Take log of both sides: $\log A = n/2 \log x$.
3. Set, $\log A = f_1(u)$; $\log x = f_2(v)$; $n/2 = f_3(w)$.
4. Solve for the various moduli for h = 5 in. for all vertical scales.

$$m_1 = \frac{h_1}{\text{Range } f_1(u)} = \frac{5 \text{ in.}}{2 \text{ cycles}} = 2.5 \text{ in./cycle}$$

$$m_2 = \frac{5 \text{ in.}}{5 \text{ cycles}} = 1.0 \text{ in./cycle}$$

5. Choose two 5 inch vertical lines connected by a diagonal. Lay off on the right-hand line a scale, $x = m_2 f_2(v)$ and on the left-hand line, $A = m_1 f_1(u)$.
6. Select an anchor point on the midpoint the x-scale. Therefore l = distance from origin of x-scale = 2.5 in. Calculate an auxiliary modulus, $N = lm_1/m_2$.
7. Plot an auxiliary scale on the reference line $n' = N f_3(w)$ starting at the origin for successive values of w.
8. Transfer the n'-scale to the n-scale by projecting lines drawn through the anchor point on the x-scale and the values on the n'-scale to the n-scale. Mark the values and the Z-nomogram portion is done.

Second Step

1. Let $1/0.0247\ C = \sigma_d\ A$.
2. Take log of both sides, $\log C - \log(.0247) = \log \sigma_d + \log A$.
3. Set $\log \sigma_d = f_1(u)$, $\log A = f_2(v)$;

$$\log C = f_3(w).$$

4. Calculate the various moduli

$$m_1 = \frac{5 \text{ in.}}{2 \text{ cycles}} = 2.5 \text{ in./cycle}$$

$$m_2 = \frac{5 \text{ in.}}{2 \text{ cycles}} = 2.5 \text{ in./cycle}$$

$$m_3 = \frac{m_1 m_2}{m_1 + m_2} = \frac{(2.5)(2.5)}{(2.5+2.5)} = 1.25 \text{ in./cycle.}$$

5. Choose two lines an appropriate distance apart, say 4 inches. Draw the third line dividing the distance between the first two by the ratio $\frac{4\ m_1}{m_1 + m_2} = 2$ in.
6. Lay off the scales on the σ_d scale by using $\sigma_d = m_1 f(u)$.
7. Calculate an anchorage point for the C-scale by inserting values of σ_d and A into the equation, $.0247\ C = \sigma_d\ A$ connect the values of A and σ_d and mark the point on the C-scale. The value of C at this point is $(\sigma_d\ A)/.0247$. Complete the C-scale by calculating $C = m_3 f_3(w) = 1.25$ (log C). Mark on C-scale starting at the anchorage point.

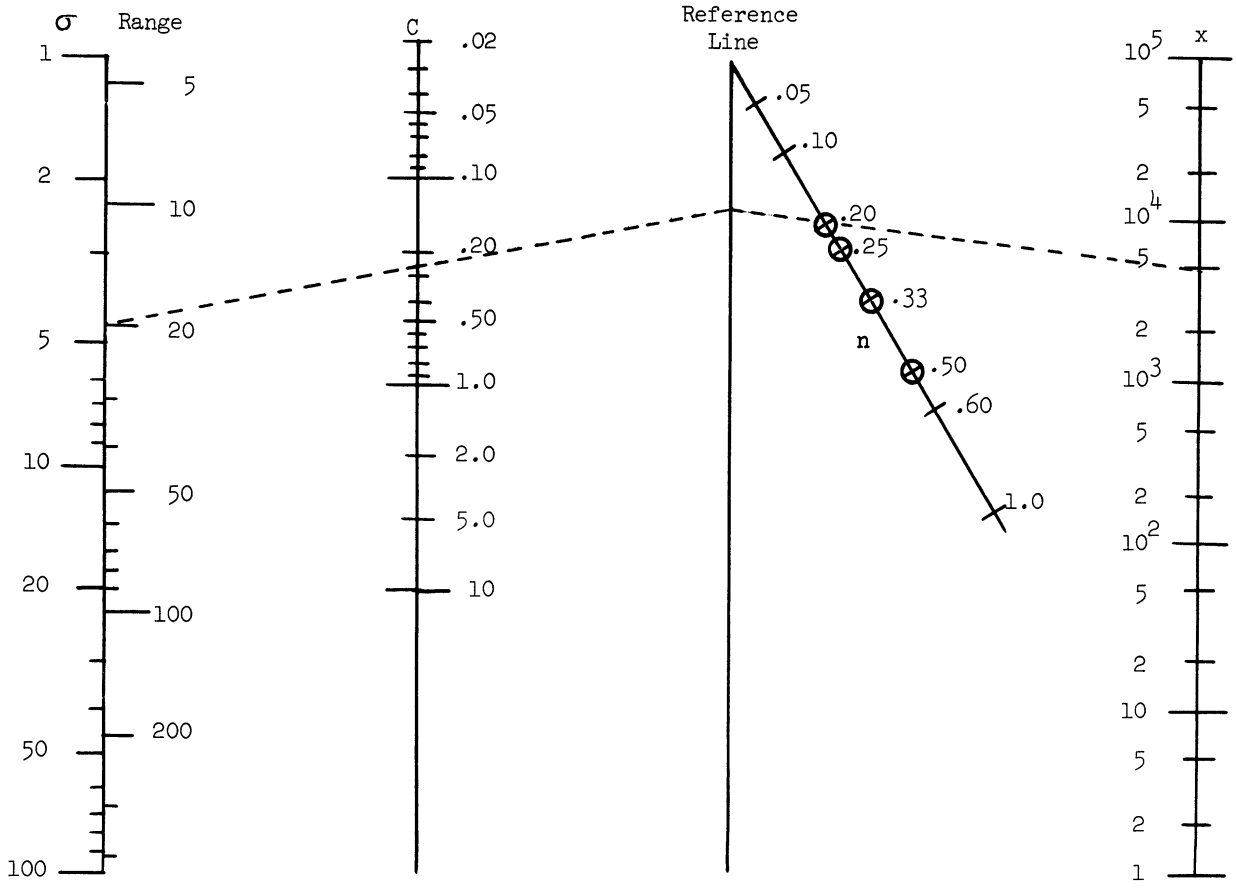

NOMOGRAM FOR CALCULATING THE SUTTON DIFFUSION COEFFICIENT FROM DATA COLLECTED DURING A SMOKE PLUME PHOTOGRAPHY EXPERIMENT.

Given: x, n, σ or Range. Find: C.

where, C = Sutton's diffusion coefficient averaged over x, $(\text{meters})^{n/2}$.

x = distance downwind where C is desired, meters, here $x = x_t$, length of visible plume

n = Sutton's stability parameter, dimensionless.

σ = standard deviation of the wind trace, degrees, or

Range = range of the wind direction trace, or, the width of the visible smoke plume at x, degrees.

Procedure: Assume x_t = 3 mi = 4800 m, n = 0.20, Range = 20°

1. Mark x, n, σ (or Range) on the appropriate scales.

2. Draw a line through x and n, intersecting the Reference Line.

3. Draw a line through the point on the Reference Line and or Range, mark the intersection with the C-scale. This is the value of C desired, C = 0.28.

G. J. Walke